



**ADDIS ABABA UNIVERSITY  
SCHOOL OF GRADUATE STUDIES  
DEPARTMENT OF CHEMISTRY**

**GRADUATE PROJECT (Chem.774)**

**9,9-Disubstituted Fluorene-Based Polymers:  
Preparation and Characterization**

By  
Ayalew Hussen

Advisor: Wendimagegn Mammo (Professor)

A Graduate Project Submitted in Partial Fulfillment of the  
Requirements for the Degree of Master of Science in Chemistry

July 2009

## Declaration

I, the undersigned, declare that this MSc project is my original work and has not been presented for any degree in any other university and that all sources of materials used for this project have been duly acknowledged.

Name: **Ayalew Hussen**

Signature: \_\_\_\_\_

This MSc. project has been submitted for examination with my approval as a university advisor.

Name: **Wendimagegn Mammo (Professor)**

Signature: \_\_\_\_\_

Date and place of submission: Department of Chemistry  
Addis Ababa University

July 2009

## **Acknowledgements**

Words cannot express my thanks to my project advisor, Professor Wendimagegn Mammo, whose patience and sacrifice as well as his time and money are invested in shouldering the responsibility of making my wish real in addition to his continuous, unreserved, professional and technical support. I regret that I cannot thank him enough. He has been my shield and my light all through this journey. He endured me more than the usual material hardships this kind of work and study entails. It is in the deepest sense of gratitude I dedicated this work to him, who sacrificed more than somebody might expect.

I equally wish to put on record of my profound and heart-felt thanks to Professor Ermias Dagne and Dr. Ashebir Fiseha whose help have been at my disposal during the time of hardship I faced in the process of the work. Had it not been for their urgent help next to the Almighty God, this work would not have been completed on time. My profound gratitude also goes to Dr. Shimelis Admassie for characterizing the synthesized polymers by running CV and UV-vis spectroscopy.

I can never forgive myself if I fail to thank Dr. Teferi Yeshitela and his family whose initiation and support to fulfill my aspiration have never been departed from me, especially at the time I faced health problem.

Many other people have also helped me in making my academic career smooth and successful. I regret that I cannot name all of them here. To mention a few, my laboratory mates, Fiseha, Dessalegn and Zewdu, my parents and relatives, and all chemistry post graduate students, who were great help for the completion of the project.

Addis Ababa University is gratefully acknowledged for covering all the medical and related expenses during the time I was injured by laboratory accident. The department of chemistry at Addis Ababa University is also acknowledged for providing the laboratory space and the necessary chemicals to conduct the research work.

## Table of Contents

Acknowledgements.....	a
List of Schemes .....	iv
List of Tables .....	v
List of Figures .....	v
List of Abbreviations .....	vi
Abstract .....	vii
1. Introduction .....	1
2. Review of Related Literature .....	4
2.1. Synthesis of Fluorene-Based Monomers .....	5
2.2. Synthesis of Fluorene-Based Polymers.....	10
2.3. Copolymerization: Tuning the Opto-Electronic Properties by Manipulating the Structures.....	14
2.4. Optical and Electronic Properties of Polyfluorenes.....	16
3. Objective of the Project Work .....	18
4. Results and Discussion .....	19
4.1. Synthesis of Fluorene-Based Monomers .....	19
4.2. Synthesis of Alternating Monomeric Sub-units.....	30
4.3. Synthesis of Alternating Copolymers .....	39
4.3.1. Synthesis and Characterization.....	40
4.3.2. Optical Properties.....	43
4.3.3. Electrochemical Properties.....	46
5. Conclusion .....	48
6. Experimental Section.....	50
6.1. Materials and Methods .....	50

6.2. Monomer Synthesis .....	50
6.2.1. Synthesis of 2,7-dibromofluorene ( <b>6</b> ).....	50
6.2.2. Synthesis of 2,7-dibromo-9,9-didodecylfluorene ( <b>24</b> ) .....	51
6.2.3. Synthesis of 9,9-didodecylfluorene-2,7-dicarbaldehyde ( <b>25</b> ).....	52
6.2.4. Synthesis of 1,4-bis(hexyloxy)benzene ( <b>29</b> ).....	52
6.2.5. Synthesis of 1,4-bis(chloromethyl)-2,5-bis(hexyloxy)benzene ( <b>30</b> ).....	53
6.2.6. Synthesis of 1,4-bis(cyanomethyl)-2,5-bis(hexyloxy)-benzene ( <b>31</b> ).....	54
6.2.7. Synthesis of 2,5-dihexyloxy-1,4-bis{2-(4'-bromothieryl)-2-cyanovinyl}- benzene ( <b>32</b> ).....	54
6.3.8. Synthesis of 2,7-bis (4,4,5,5-tetramethyl-1,3-2-dioxaborolane)-9,9- didodecyl fluorene ( <b>7</b> ).....	55
6.3. Polymer Synthesis.....	56
6.3.1. Synthesis of poly[9,9-dioctyl-9H-fluorene-2,7-diyl-alt-2,5-dihexyloxy-1,4- bis(2-thienyl-2-cyanovinyl)benzene] ( <b>40</b> ) .....	56
6.3.2. Synthesis of poly(9,9-didodecyl-9H-fluorene-2,7-diyl-alt-9,9-dibenzyl-9H- fluoren-2,7-diyl) ( <b>41</b> ) .....	57
6.3.3. Synthesis of poly[(9,9-didodecyl-9H-fluorene-2,7-diyl)(1-cyanoethene- 1,2-diyl)(2,5- bis(hexyloxy)phenylene)(2-cyanoethene-1,2-diyl)] ( <b>42</b> ).....	57
6.3.4. Synthesis of poly[9,9-didodecyl-9H-fluorene-2,7-diyl-alt-2,5-dihexyloxy- 1,4-bis(2-thienyl-2-cyanovinyl)benzene] ( <b>43</b> ) .....	57
7. References .....	58
8. Appendices.....	61

## List of Schemes

<b>Scheme 1:</b> Different approaches for the bromination of fluorene and fluorene derivatives .....	6
<b>Scheme 2:</b> Alkylation of fluorene by nucleophilic substitution reaction.....	8
<b>Scheme 3:</b> Alkylation of fluorene or 2,7-dibromofluorene by phase transfer catalysis reaction.....	8
<b>Scheme 4:</b> Synthesis of boronic acid (a), and boronate ester (b) for Suzuki-coupling reaction .....	9
<b>Scheme 5:</b> Synthesis of 9,9-dialkyl-2,7-dicarbaldehydefluorene.....	9
<b>Scheme 6:</b> Synthetic routes for various fluorene-based monomers.....	10
<b>Scheme 7:</b> Schematics of synthetic methods of PFs: (a) Yamamoto route; (b) Stille, and (c) Suzuki route (R = alkyl).....	11
<b>Scheme 8:</b> Synthesis of functional polyfluorenes <i>via</i> a modified one-pot Suzuki-Miyaura condensation polymerization.....	12
<b>Scheme 9:</b> The synthesis of poly(9,9-dioctylfluorene) by applying Grignard metathesis polymerization method.....	13
<b>Scheme 10:</b> Synthesis of polyfluorene based polymer through Knoevenagel polycondensation.....	16
<b>Scheme 11:</b> Proposed mechanism for the generation of keto defect sites.....	17
<b>Scheme 12:</b> Syntheses of fluorene-based monomers.....	20
<b>Scheme 13:</b> The mechanism of the phase transfer catalysis reaction.....	26
<b>Scheme 14:</b> Synthetic scheme for the alternating monomeric sub-units.....	31
<b>Scheme 15:</b> Synthesis of <b>40</b> , <b>41</b> and <b>43</b> through a modified Suzuki polymerization reaction.....	41
<b>Scheme 16:</b> Synthesis of <b>42</b> <i>via</i> Knoevenagel polycondensation route .....	42

## List of Tables

<b>Table 1:</b> $^1\text{H-NMR}$ (400MHz, $\text{CDCl}_3$ ) data ( $\delta_{\text{ppm}}$ ) of compounds <b>6</b> and <b>24</b> .....	21
<b>Table 2:</b> $^{13}\text{C-NMR}$ (100.6 MHz, $\text{CDCl}_3$ ) data ( $\delta_{\text{ppm}}$ ) for compounds <b>6</b> , <b>24</b> , <b>25</b> and <b>7</b> ....	24
<b>Table 3:</b> $^1\text{H-NMR}$ (400MHz, $\text{CDCl}_3$ ) data ( $\delta_{\text{ppm}}$ ) of compounds <b>25</b> and <b>7</b> .....	29
<b>Table 4:</b> HMQC data for compound <b>32</b> .....	37
<b>Table 5:</b> $^1\text{H-NMR}$ (400 MHz, $\text{CDCl}_3$ ) data ( $\delta_{\text{ppm}}$ ) of compounds <b>29-32</b> .....	38
<b>Table 6:</b> $^{13}\text{C-NMR}$ (100.6 MHz, $\text{CDCl}_3$ ) data ( $\delta_{\text{ppm}}$ ) for compounds <b>29-32</b> .....	39

## List of Figures

<b>Figure 1:</b> Examples of aromatic conjugated polymers.....	2
<b>Figure 2:</b> Chemical structures and synthetic route for PF-based alternating copolymers. ....	15
<b>Figure 3:</b> Structures of byproduct compounds identified during the alkylation of 2,7-dibromofluorene.....	27
<b>Figure 4:</b> UV-vis absorption spectra of <b>40</b> in thin films and in chloroform solution.....	45
<b>Figure 5:</b> UV-vis absorption spectra of <b>41</b> in thin films.....	45
<b>Figure 6:</b> $\text{CHCl}_3$ solution UV-Vis absorption spectrum for <b>43</b> .....	45
<b>Figure 7:</b> Cyclic voltammogram for copolymer <b>40</b> .....	48
<b>Figure 8:</b> Cyclic voltammogram for copolymer <b>41</b> .....	48
<b>Figure 9:</b> Cyclic voltammogram of copolymer <b>43</b> films on glassy carbon plates.....	48

## List of Abbreviations

DMF: N,N-Dimethylformamide

DMSO: Dimethyl sulfoxide

NMR: Nuclear magnetic resonance

HOMO: Highest Occupied Molecular Orbital

LUMO: Lowest Unoccupied Molecular Orbital

$\delta$ : Chemical shift

*J*: Coupling constant

s: Singlet

d: Doublet

t: Triplet

brd: Broad doublet

brs: Broad singlet

m: Multiplet

dd: Doublet of doublets

ppm: Parts per million

NBS: *N*-Bromosuccinimide

PLED: Polymer light emitting diodes

PL: Photoluminescence

EL: Electroluminescence

HAc: Acetic acid

THF: Tetrahydrofuran

LED: Light emitting diodes

# **9,9-Disubstituted Fluorene-Based Polymers: Preparation and Characterization**

**By**

**Ayalew Hussien**

**Advisor: Wendimagegn Mammo (Professor)**

## **Abstract**

*A family of conjugated polymers based on 9,9-disubstituted fluorenes and cyanovinylenes were reported. The polymers were synthesized by employing a slightly modified Suzuki coupling polymerization reaction and condensation polymerization utilizing the Knoevenagel reaction. The resulting polymers showed good solubility in chloroform. The energetic positions of the band edges were determined by cyclic voltammetry. The synthesized polymers were characterized by using spectroscopic techniques such as UV-Vis and <sup>1</sup>H- NMR. The presented polymers exhibited emission of blue to red colors.*

## 1. Introduction

The term polymer is derived from the Greek's 'poly' and 'mers' meaning many parts. Some prefer the term macromolecule or large molecule. A polymer is thus a substance composed of molecules with large molecular mass consisting of repeating units connected by covalent chemical bonds. In some cases the repeating unit is linear. In other cases, the chains are branched or interconnected to form three-dimensional networks. The small molecules that combine with each other to form polymer molecules are termed as monomers.

The basic concepts of polymer science apply equally to natural and synthetic polymers and to inorganic and organic polymers, and as such are important in medicine, nutrition, engineering, biology, physics, mathematics, computers, environment, space, ecology, health, etc. Polymers are involved in all of the major new technologies including synthetic blood and skin; computer chips, CDs, liquid crystals, and circuit boards-information visualization, storage and retrieval; energy creation, storage, and transmission (portable electrical power (batteries), efficient, light, and low-emission transportation; high temperature superconductors, targeting and control of drug delivery, and other replacement parts; transportation; space craft; solar and nuclear energy; and photonics (optical fibers) [1].

Electrically conducting polymers are composed of conjugated polymer chains with  $\pi$ -electrons delocalized along the backbone. In the neutral, or undoped form, the polymers are either insulating or semiconducting. The polymers are converted to the electrically conductive, or doped, form *via* oxidation or reduction reactions that create delocalized charge carriers [2].

In addition to making processable polymers, another important synthetic challenge for electroactive conducting polymers is to prepare polymers with small band-gaps. The relatively large band-gaps in common conducting polymers are generally attributed to bond alternation [4]. For device applications, it is especially important to control the

electronic band structure of the polymer to achieve a band gap of the desired magnitude and frontier orbitals, HOMO (highest occupied molecular orbital) and LUMO (lowest unoccupied molecular orbital) (or band edges), of the proper energies.

One of the greatest advantages of organic polymers compared with inorganic materials is their flexibility: they can be chemically modified and easily shaped according to the requirements of a particular device [2]. Their versatility and compatibility, coupled with ease of fabrication and light weight, make them useful materials for electronic devices [5]. The most popular application seems to be solid-state rechargeable polymer batteries. Conducting polymers may find application in nonlinear optical devices, particularly in optoelectronics, e.g., signal processing and optical communication. These applications benefit from polymer flexibility, mechanical strength, high damage threshold, and ultra-fast response, in the subpicosecond range [6].

In the last decade, highly-efficient stable light emitting conjugated polymers have drawn great attention of researchers for their potential applications both in full-color displays and even in next generation lighting source, and tremendous progress has been made in this field [7,8]. Of all large band-gap light-emitting polymers investigated so far, polyfluorene (PF) (Figure 1) and its derivatives have drawn great interests for their exceptional optoelectronic properties, such as good thermal and chemical stability, high fluorescence quantum yield, good film forming and hole-transporting properties [8]. Due to the large energy gap of polyfluorene homopolymer, it is a highly attractive class of conjugated material for applications in polymeric blue light emitting devices [9,10].

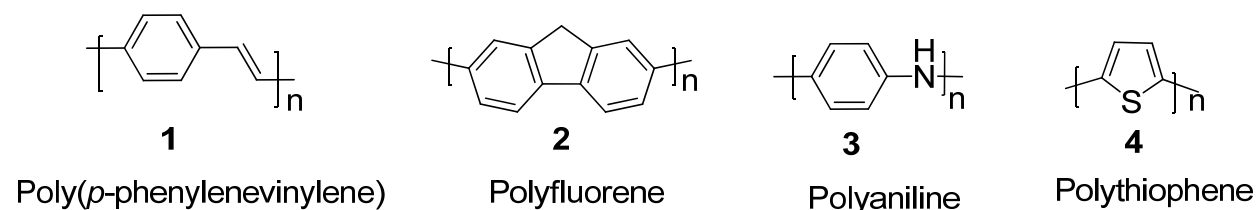


**Figure 1:** Examples of aromatic conjugated polymers.

There are a number of properties inherent to the PFs that have enabled them to generate growing interest in recent years. Important as an underlying strength is the

development of effective synthesis and purification routes to a high molecular weight material that is substantially free of impurities and chemical defects [7]. In addition, PFs have many desirable characteristics for use as the active constituents in polymer-based devices. For example, in respect of display applications, they can be chemically tuned to give electroluminescence emission across the full visible spectrum from blue to red [11]. In addition, the high photoluminescence quantum efficiency [PLQE] values and good carrier transport characteristics typical of PFs, have allowed the fabrication of efficient light emitting diodes [LEDs]: Blue emission LEDs use fluorene homopolymers and/or fluorene/arylamine copolymers and blends [12], materials that are also well suited for use as matrix polymers for green emission LEDs [11]. In addition, PFs can be readily processed from the solution on to etched silica gratings to produce low threshold, distributed feedback lasers [13].

A crucial structural difference between PFs and both PPVs and poly(*p*-phenylene)s [PPPs] is the existence of the bridging C-9 atom between the alternate pairs of phenylene rings. In this respect, PFs are intermediate between PPPs and so called ladder poly(phenylene)s [LPPs], in which each of the phenylene rings is locked into a planar conformation by bridging carbon atoms on both sides of every phenylene-phenylene bond. The addition of long alkyl (or other) substituents at the C-9 position makes PFs soluble in many organic solvents.

## 2. Review of Related Literature

A major recent development in the field of molecular electronics has been the discovery of electroluminescent conjugated polymers, that is, fluorescent polymers that emit light when excited by the flow of an electric current. These materials may now challenge the domination by inorganic materials of the commercial market in light-emitting diodes. Conjugated polymers are particularly versatile because their physical properties (color, emission efficiency) can be fine-tuned by manipulation of their chemical structures [14].

As functional materials, polymeric materials offer many advantages such as good film-forming properties, ease of design and synthesis, and reasonable cost. As a consequence, conjugated polymers with delocalized electronic structure have received great attention from both academic and industrial laboratories recently [15, 16].

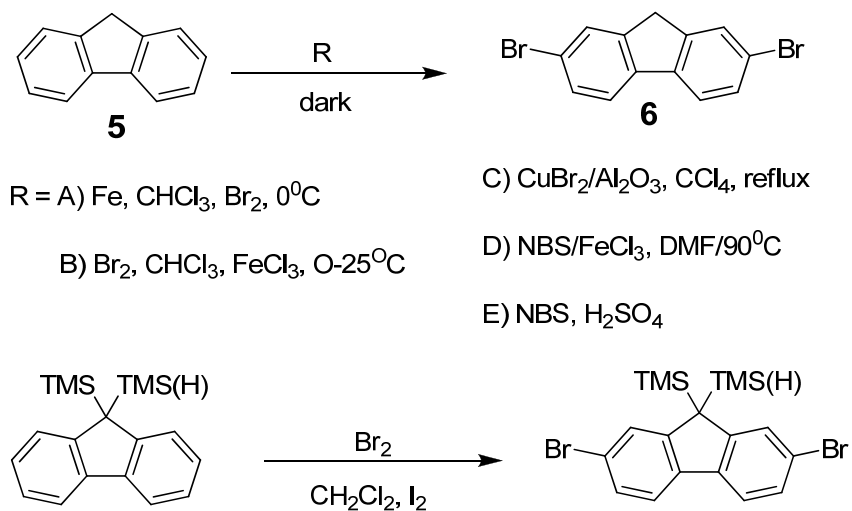
The award of the Nobel Prize for Chemistry in 2000 to Professors Alan Heeger, Alan MacDiarmid, and Hideki Shirakawa for their discovery that “doped” polyacetylene can conduct electricity changed the way that polymers were viewed and led to major advances in plastic electronics [22]. Among these was the discovery of electroluminescent polymers and their application in light-emitting devices. These devices are now becoming commercially available, representing the final step in the advance of organic electronics from a laboratory curiosity to a part of everyday life. Electroluminescence (EL) in conjugated polymers was first reported in poly(*para*-phenylenevinylene) (PPV) in 1990 [21]. Since then considerable effort has been devoted to developing conjugated materials as the active units in light-emitting devices (LEDs) for use in display applications. Recently, polyfluorenes have emerged as attractive alternatives, and they have become the subject of considerable attention. Poly-(9,9-dioctylfluorene) (PFO), for example, is a high mobility hole transport polymer from which efficient blue EL devices have been fabricated [22]. It is, therefore, appropriate to review the synthesis of such polymers and to provide a brief introduction to their applications.

## 2.1. Synthesis of Fluorene-Based Monomers

Fluorene, or 9H-fluorene, is a polycyclic aromatic hydrocarbon. It forms white crystals that exhibit a characteristic, aromatic odor similar to that of naphthalene. It has a violet fluorescence, which gave it its name. It is insoluble in water and soluble in benzene and ether. The protons in the 9-position of the fluorene ring are acidic ( $p^{Ka} = 23$  in DMSO) [17] and removal of one of them with a base, such as sodium hydroxide, leads to the stable fluorenyl anion, which is aromatic and has an intense orange color. The anion is a nucleophile and most electrophiles react with it by adding to the 9-position [25].

2,7-Dibromofluorene (**6**) plays the central role in the syntheses of several fluorene based monomers and polymers. It is a commercially available material but it can also be synthesized in laboratories by bromination of fluorene applying different bromination methodologies as depicted in Scheme 1. One method reported in the literature involves the use of N-bromosuccinimide (NBS) in sulfuric acid solution [24]. It is important that the reaction proceeds in the dark to avoid any bromination of the aliphatic part of the starting molecule. The other method reported in literatures involves the addition of  $Br_2$  to the chloroform solution of the starting fluorene based material at  $0^{\circ}C$  and further addition of catalytic amount of ferric chloride or metallic iron [25,8]. An alternative strategy involves the use pre-made copper(II) bromide on alumina as a brominating agent to be added to a solution of fluorene in carbon tetrachloride [25]. The preparation of  $CuBr_2$  on alumina involves the addition of neutral alumina to a distilled water solution of copper(II) bromide, removal of the water under reduced pressure, and drying of the resulting brown powder at  $90^{\circ}C$  below a pressure of 1mmHg for 4h [25]. NBS in DMF solvent and catalytic amount of ferric chloride was also used to brominate the 2,7-position of fluorene with a relatively high yield [26]. This method was reported to be simpler compared with the copper bromide method [25]. At room temperature, even an excess of NBS gave the monosubstituted product of 2-bromofluorene. However, by varying the temperature, most of the product resulted in 2,7-dibromofluorene. Another bromination strategy reported for the preparation of 2,7-dibromo-9-trimethylsilylfluorene from 9-trimethylsilylfluorene involves the addition of  $Br_2$  and catalytic amount of iodine

to the dichloromethane solution of the starting material and then cooling the resulting mixture to about 5<sup>0</sup>C in ice water [27]. 2,7-Dibromofluorene can also be accessed from fluorene by dissolving the reactant in 1:1 mixture of chloroform and acetic acid at 0<sup>0</sup>C and adding bromine dropwise using a pressure equalizing dropping funnel.



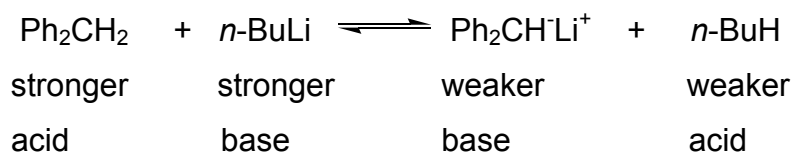
**Scheme 1:** Different approaches for the bromination of fluorene and fluorene derivatives

The electronic properties of many conjugated polymers sensitively depend on their molecular and supramolecular structure. The molecular aspects are often related to the substitution pattern at the conjugated main chain, which determines the conformation of the macromolecule, or to the presence of structural defects [28]. For a maximum  $\pi$ -conjugation along the main chain, the substituents that guarantee the solution processing of the materials should not cause an unwanted distortion of the aromatic building blocks. Regarding this point, the 9,9-disubstituted fluorene moiety represents a very favorable building block for obtaining processable, conjugated polymers.

Due to the tetrahedral  $\sigma$ -bonding orbital at the C-9 atom, the substituents tend to extend out of the backbone plane and be locally perpendicular to the chain-axis. Therefore, substitution at the C-9 position does not greatly increase the steric interactions between or cause distortion in the conjugated backbone itself, even though

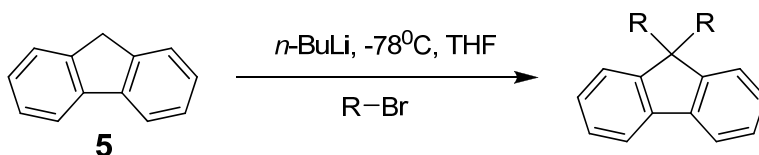
the interaction can lead to significant twisting of the main chain in PF derivatives. Furthermore, the C-9 atom provides a facile site for tuning the solubility, opto-electronic properties and interchain interactions [29]. The rigid planarized biphenyl structure bridged by a methylene group in the fluorene monomer unit leads to a wide band-gap with blue emission, so that PFs possess the unique ability to emit color spanning the entire visible spectrum with high efficiency and low operating voltage [29].

The synthesis of 9,9-disubstituted fluorene-based polymers begins with the preparation of the corresponding monomeric sub-unit. The most commonly used reactions are nucleophilic substitutions using alkyllithium reagents (Scheme 2), and phase transfer catalysis reactions as shown in Scheme 3. The former uses a strong base like *n*-butyllithium (*n*-BuLi) in dry THF at -78<sup>o</sup>C to deprotonate the acidic protons from the benzylic positions to form 9-fluoryllithium, which is a resonance stabilized anion, and consequently, the resulting aryllithium acts as a nucleophile to undergo nucleophilic substitution reaction with an alkyl halide [25,30]. For reactions involving a proton transfer, the equilibrium should lie on the side of the weaker acid and the weaker base. In this case, the reaction works because the organolithium that is formed (9-fluoryllithium, which can be protonated to give fluorene, p<sup>Ka</sup> about 23) [17] is less basic (more stable) than the organolithium we started with (*n*-BuLi, which can be protonated to give *n*-butane, P<sup>Ka</sup> about 50). In other words, the reaction proceeds in the direction of forming the more stable (weaker) acid (butane), *i.e*, the one derived from the more basic compound (*n*-BuLi) and the basicity of the organolithium decreases.



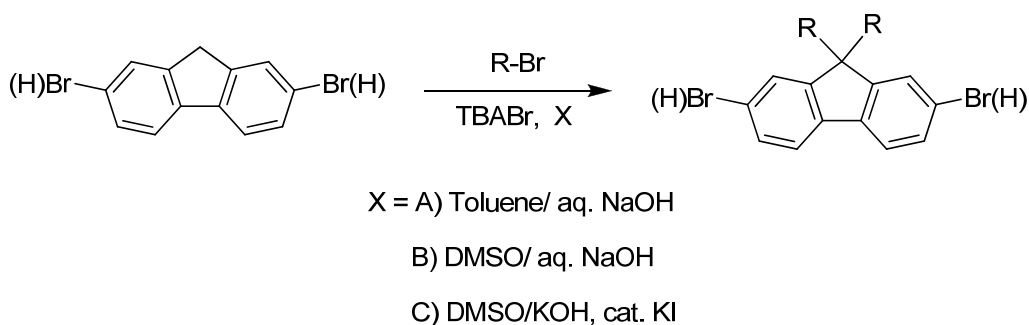
This route can be used only for the alkylation of fluorene but not for 2,7-dibromofluorene due to the very fast nature of the halogen-lithium exchange as compared to the hydrogen-lithium exchange reaction. In order to prepare 2,7-dibromo-9,9-dialkylated

fluorene, one needs to do the alkylation first on fluorene and then subsequent bromination of the resulting 9,9-dialkylated fluorene [25].



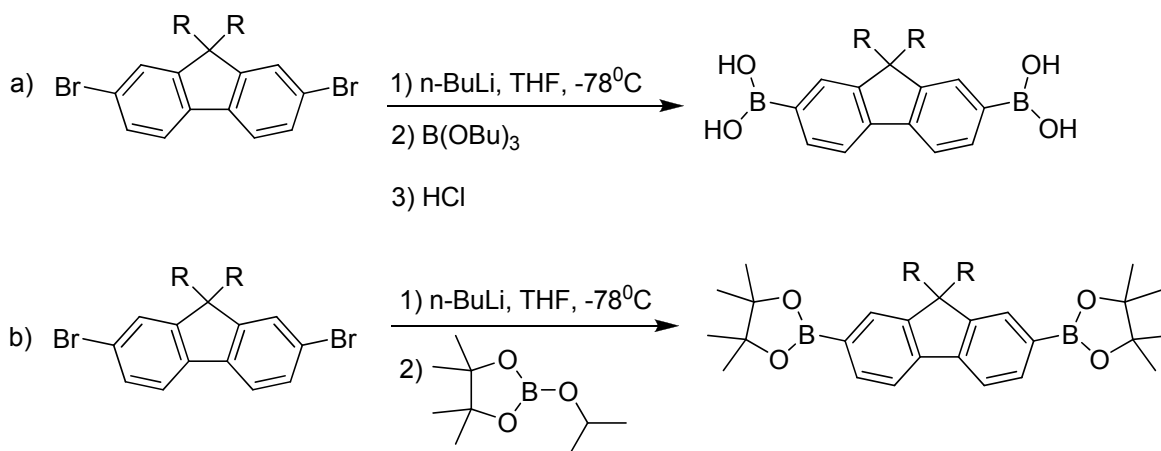
**Scheme 2:** Alkylation of fluorene by nucleophilic substitution reaction.

An alternative reaction pathway that has been reported in literatures for the synthesis of 9,9-dialkyl substituted fluorenes and fluorene derivatives is the phase transfer catalysis reaction. The reaction involves the use of a two phase system like equal volumes of toluene and aqueous NaOH solution [26], DMSO and aqueous NaOH [31,33], and tetraalkylammonium bromide as phase transfer catalyst (Scheme 3). The use of aqueous KOH solution instead of aqueous NaOH in DMSO in the presence of catalytic amount of KI for the synthesis of 9,9-dialkylated fluorene by phase transfer catalysis reaction has also been reported [32]. The advantage of the phase transfer reaction over the nucleophilic substitution reaction is that it can be implemented on a 2,7-dihalogenated fluorene and it avoids the risk of halogenating the side chain and unwanted reactions on functional groups of the side chain.



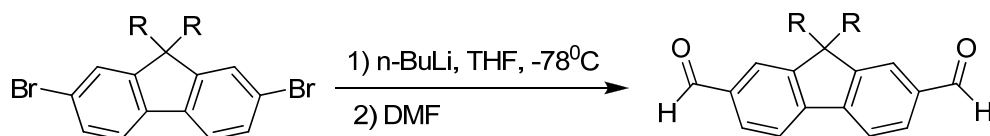
**Scheme 3:** Alkylation of fluorene or 2,7-dibromofluorene by phase transfer catalysis reaction. (TBABr = *tert*-butylammonium bromide)

9,9-Dialkyl-2,7-dibromofluorene itself can be used as a monomer for the synthesis of its homopolymer or different copolymers by reacting it with other appropriate difunctional materials. But it can also be used as an interesting precursor for the syntheses of very useful fluorene-based monomers. For example, it can be used for the synthesis of the corresponding diboronic acids or boronate esters, which can be polymerized through the Suzuki-type polymerization route with dihaloaryls. The synthesis of 2,7-bis(4,4,5,5-tetramethyl-1,3,2-dioxaborolan-2-yl)-9,9-dialkylfluorene involves the use of *n*-BuLi in dry THF at  $-78^{\circ}\text{C}$  to undergo halogen-metal exchange and subsequent treatment of the resulting aryllithium with 2-isopropoxy-4,4,5,5-tetramethyl-1,3,2-dioxaborolane [25] as shown in Scheme 4.



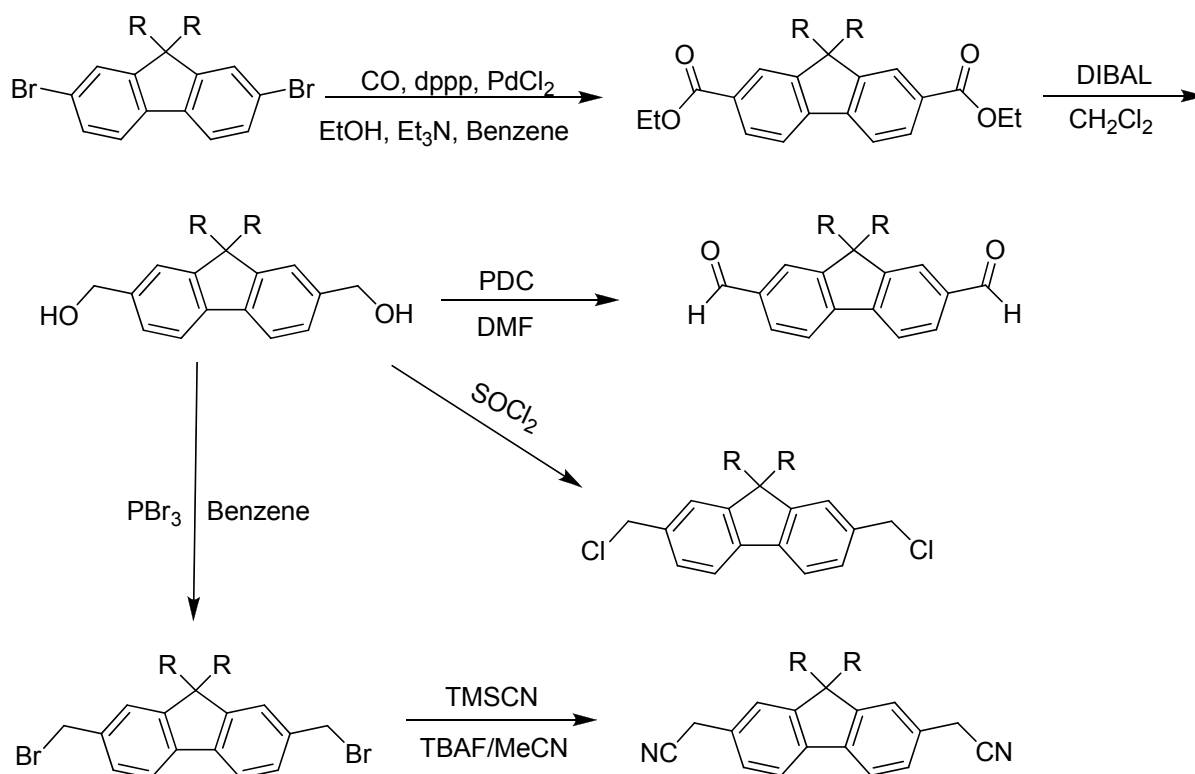
**Scheme 4:** Synthesis of boronic acid (a), and boronate ester (b) for Suzuki-coupling reaction.

Halogen-metal exchange between 2,7-dibromofluorene derivative followed by reaction with DMF can also be used to prepare a very important monomer, 9,9-dialkyl-2,7-dicarbaldehydefluorene (Scheme 5), that can be polymerized with a bis(nitrile) through Knoevenagel condensation polymerization route.



**Scheme 5:** Synthesis of 9,9-dialkyl-2,7-dicarbaldehydefluorene.

The synthesis of this 2,7-dicarbaldehydefluorene derivative from the corresponding 2,7-dibromo material by applying a different route has also been reported in literatures [31]. But this path (Scheme 6) takes several steps to reach to the desired monomer and is not economically attractive as compared to the above reaction. The syntheses of different fluorene-based monomers starting from 2,7-dibromo-9,9-dialkylfluorene is also depicted in Scheme 6.

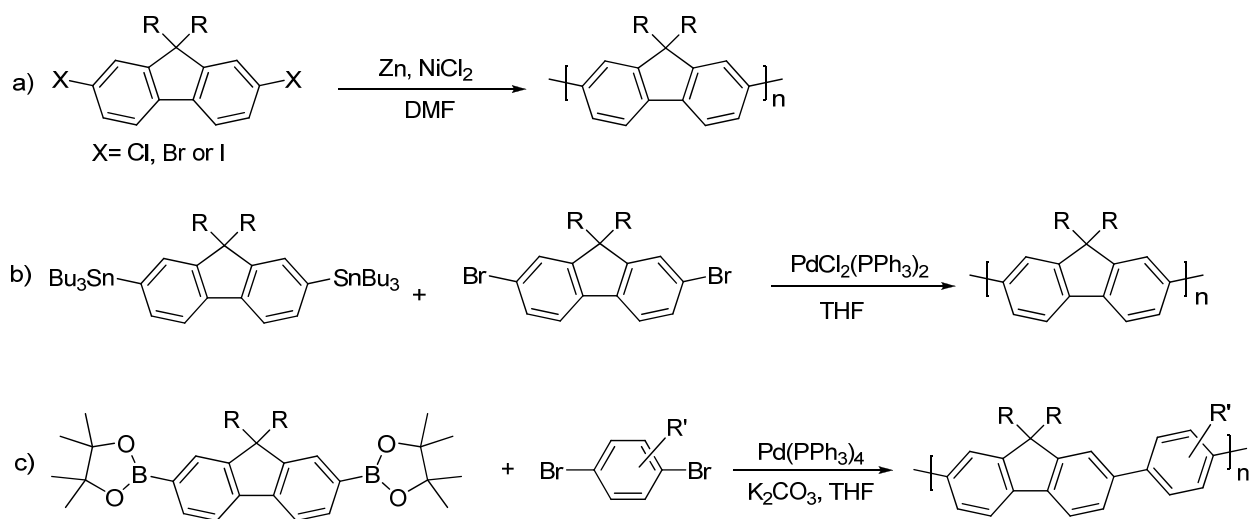


**Scheme 6:** Synthetic routes for various fluorene-based monomers.

## 2.2. Synthesis of Fluorene-Based Polymers

A number of polyfluorene (PF) polymers and their derivatives have been studied since poly(9,9-di-*n*-hexylfluorene) (PDHF) was first reported as a blue light emitting polymer [34]. The interest in these polymers arose because they show highly efficient photoluminescence (PL) and electroluminescence (EL), excellent thermal and oxidative

stability, and good solubility in common organic solvents [11,30]. First attempts to synthesize soluble, processable poly(2,7-fluorene)s (PFs) *via* an attachment of solubilizing substituents in 9-position of the fluorene core were published in 1989 by Yoshino and co-workers [34]. They coupled 9,9-dihexylfluorene oxidatively with  $\text{FeCl}_3$  and obtained low molecular weight poly(9,9-dihexylfluorene). That oxidative coupling was not strictly regioselective, as structural defects were created besides regular 2,7-linkages [35,28]. The enormous progress in the availability of efficient and strictly regioselective transition metal catalyzed aryl-aryl couplings has paved the way for the synthesis of high molecular weight, structurally well-defined PF derivatives. As such, typical metal-mediated aryl cross-couplings (Yamamoto, Stille, and Suzuki reactions) [29] (Scheme 7) are continuously being refined for yield, extent of conversion, and catalyst loading. In particular, the Suzuki and Stille reactions require aryl dihalide and dimetalated (boron and tin, respectively) co-monomers in theoretical perfect stoichiometric balance to achieve high molecular weights.

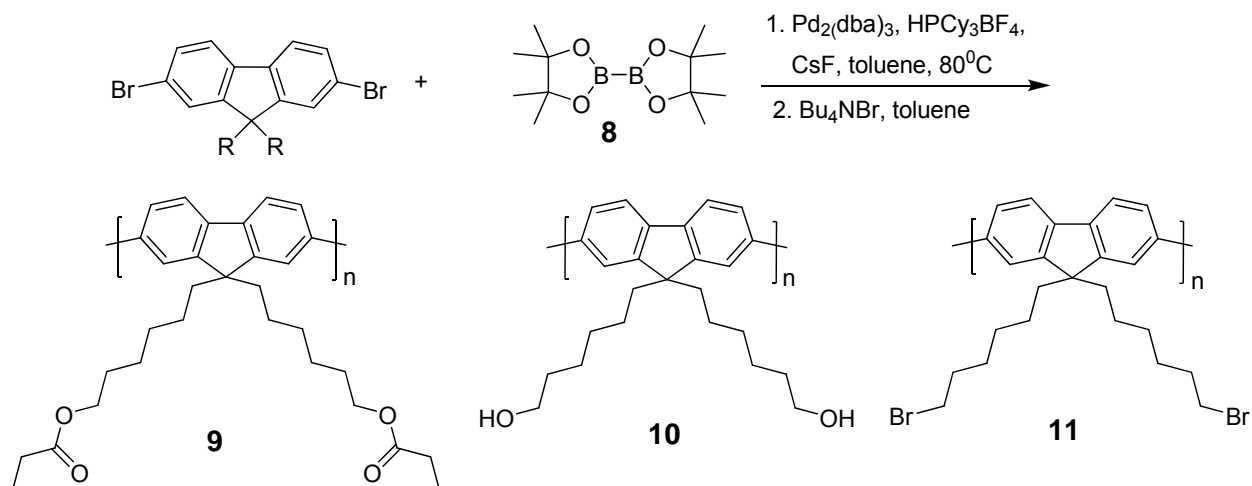


**Scheme 7:** Schematics of synthetic methods of PFs: (a) Yamamoto route; (b) Stille route, and (c) Suzuki route (R= -alkyl).

The PF homo- and copolymers studied in the literature were most often synthesized *via* the Yamamoto route in the previous times [11]. There was also a study on materials synthesized by the Dow Chemical Company using the Suzuki route [34], which appears

now to be the preferred route for the synthesis of PFs for use in commercially focused display development. The Yamamoto aryl-aryl coupling [28] involves a Ni-catalyzed reaction between dihalogen (typically bromine) substituted aryl monomers and occurs under harsher conditions than the Pd-catalyzed Suzuki coupling of diboronyl- and dibromo-substituted aryl monomers [29]. Copolymers synthesized *via* the Yamamoto route necessarily have statistical chain structures and it is then unclear what fraction of starting monomers end up in the soluble fraction that is subsequently used for experimentation [36].

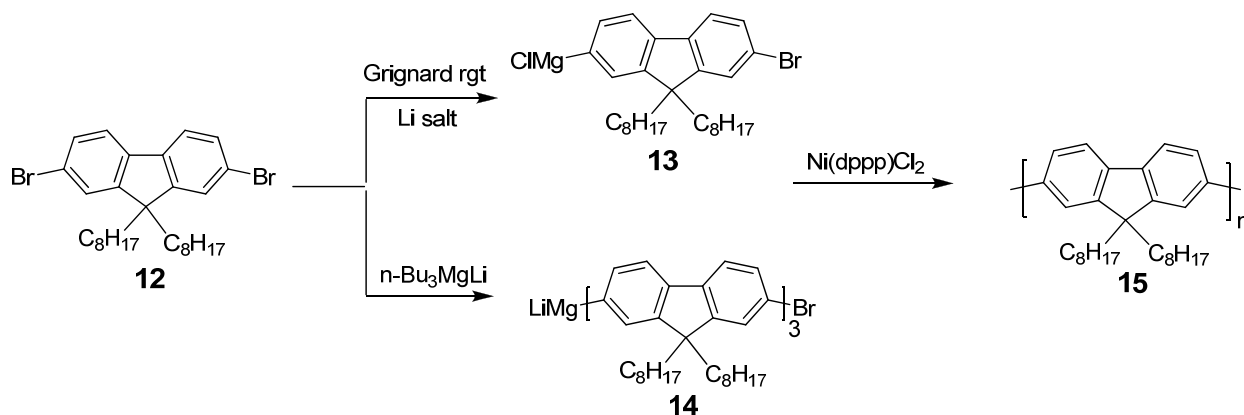
Recently, synthesis of functional polyfluorenes *via* a modified Suzuki-Miyaura polycondensation reaction was reported by the Ryan group [36]. This group effectively demonstrated that the Suzuki polymerization could be run by the replacement of a Brønsted base with cesium fluoride (Scheme 8). The work reported shows the synthesis of polymers with pendant group functionality (specifically haloalkyl, ester, and alcohol) that were previously synthetically inaccessible. The fluoride-mediated Suzuki polymerization of fluorenes reported by this group suggests that the fluoride ion can effectively coordinate to, and activate, an aryl boronic ester for subsequent transmetalation with palladium.



**Scheme 8:** Synthesis of functional polyfluorenes *via* a modified one-pot Suzuki-Miyaura condensation polymerization.

It is well-known that toluene is a good solvent for the Suzuki synthesis of poly(9,9-dioctylfluorene) (PFO) under normal conditions, but the solubility of CsF in toluene is low. However, when a small amount of tetrabutylammonium bromide (TBAB) in degassed toluene was added to the reaction, high yield and molecular weight polymers were formed [36] indicating that a phase transfer catalyst in the toluene system was necessary for the polymerization to proceed at a reasonable rate.

The synthesis of PFs by applying Grignard metathesis method has also been reported by the Mihaela group [37]. PFs are less reactive in the magnesium-halogen exchange process, preventing the use of normal Grignard metathesis as polymerization method. However, it has been previously reported by Knochel and co-workers that the addition of LiCl to isopropylmagnesium chloride leads to enhanced reactivity [38]. The addition of lithium chloride to a Grignard reagent turns it into what is called a “turbo-Grignard” and breaks the polymeric aggregates formed in solution to produce a very reactive complex,  $[i\text{-PrMgCl}_2 \cdot \text{Li}^+]$ . The magnesiate character of the complex  $[i\text{-PrMgCl}_2 \cdot \text{Li}^+]$  may be responsible for the enhanced reactivity of this reagent. In addition, the LiCl additive can be replaced with other lithium, magnesium, or zinc salts. Magnesium-halogen exchange can also be performed with magnesium “ate” complexes such as  $\text{R}_3\text{MgLi}$ , where  $\text{R} = n\text{-Bu}$ ,  $t\text{-Bu}$ , or  $i\text{-Pr}$  [39, 40].



**Scheme 9:** The synthesis of poly(9,9-dioctylfluorene) by applying Grignard metathesis polymerization method. (Grignard reagent =  $i\text{-PrMgCl}$ ,  $t\text{-BuMgCl}$ )

### 2.3. Copolymerization: Tuning the Opto-Electronic Properties by Manipulating the Structures

As is very usual in polymer chemistry, the copolymerization technique is an effective synthesis strategy to modify short- or long-range organization in materials and consequently brings about some novel properties to materials. Copolymers are divided into several categories, and here our interests are only focused on one of them: alternating copolymers.

For applications in LEDs, one major problem is the imbalance of the injection and transport of holes and electrons. One approach to solve such problems is to exploit the alternating copolymers by incorporating various co-monomers [29].

Electronic and physical properties, redox behavior and emission color of the alternating copolymers can be fine tuned by tailoring the molecular structures, including attaching different functional groups onto the comonomers, changing the steric configuration in n-doped type segments or by controlling the repeat number of comonomers in one alternating unit. Huang *et al.* investigated a series of PF-based copolymers alternated with various structural units [41]. Figure 2 shows the studied compounds and their synthetic route. The attachment of electron-withdrawing ester groups leads to an obvious blue shift in the absorption spectrum, thus enhancing the displacement of the equilibrium geometry of the polymer at the excited states from its ground state but strongly reducing the fluorescence quantum yields, while the attachment of electron-donating alkoxy groups on the phenylene ring causes a red shift as reported in the literature [41]. Substitution with alkoxy groups has two effects. First, the band gap is reduced, leading to a marked red-shift in emission. Secondly, it generally enhances solubility in many organic solvents [21, 43].

The development of novel polymers that are soluble in common organic solvents and processable by industrially relevant techniques is necessary for the practical application of conjugated polymers. Such processable polymers with tailored electronic structures

also possess the possibility to be multifunctional materials that can find application in numerous device architectures.

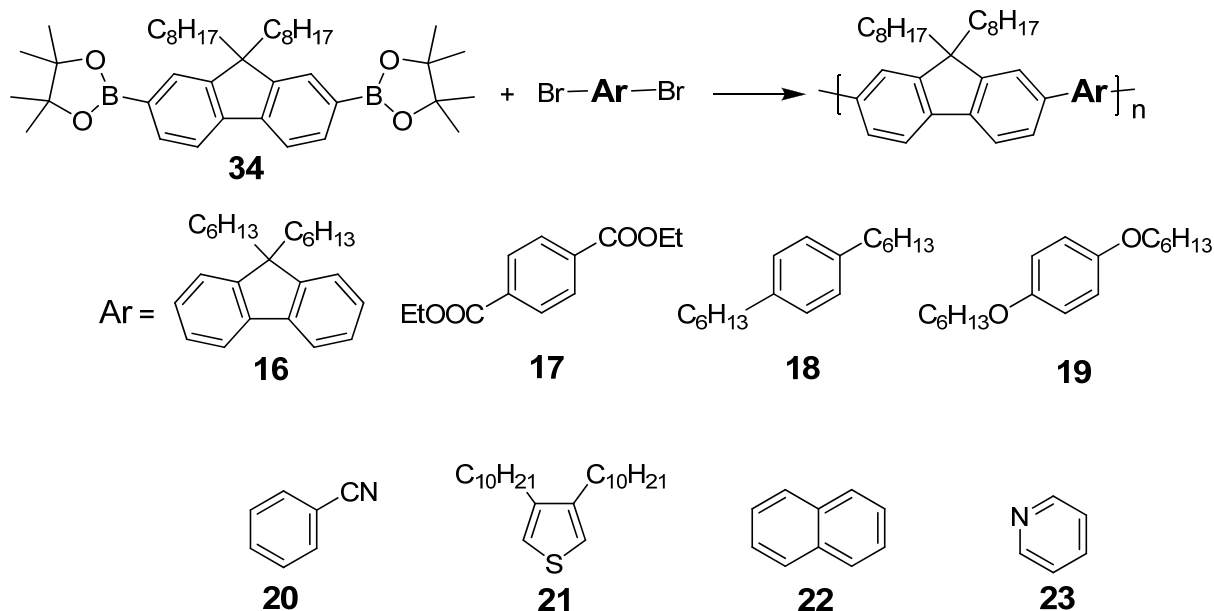
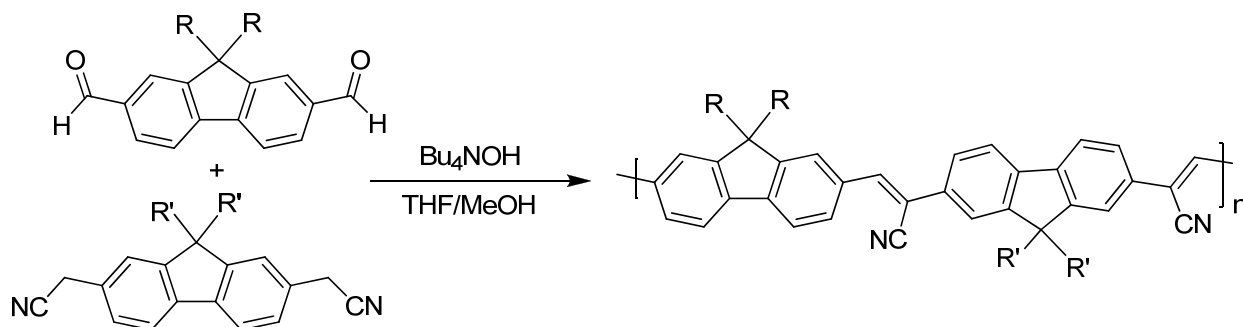


**Figure 2:** Chemical structures and synthetic route for PF-based alternating copolymers.

Reagents and conditions:  $(\text{PPh}_3)_4\text{Pd}(0)$  (1.0 mol %) toluene/2M  $\text{K}_2\text{CO}_3$  (3:2), reflux.

Copolymers of phenylene and fluorene vinylene units have been investigated. In the case of poly(phenylenevinylene), when phenylene units are replaced with fluorene units, the HOMO-LUMO gap is predicted to increase. The replacement does not change the HOMO energy level but lifts the LUMO energy level. To compensate for this effect and to reduce the bandgap, cyano (CN) groups can be introduced on the fluorene units instead of the phenylene units. The cyano groups are also known to reduce the barrier to electron injection [33]. Thus, by altering these chemical structures and modifying the polymer backbone conformation, one can easily tune the electrooptical properties for this copolymer design. Improvements in EL efficiency have also been obtained by placing the electron-withdrawing substituents on the vinylene moiety [42]. It is expected and has been confirmed by calculation that a cyano substituent (and presumably other electron withdrawing groups) on the ring or vinylene moiety should lower the HOMO

and LUMO energies and increase the electron affinity of the polymer, thus improving the efficiency of electron injection and the potential efficiency of an LED using such a polymer [4]. Such polymers can be prepared by Knoevenagel condensation between the appropriate dialdehydes and diacetonitriles (Scheme 10) [31].



**Scheme 10:** Synthesis of polyfluorene based polymer through Knoevenagel polycondensation.

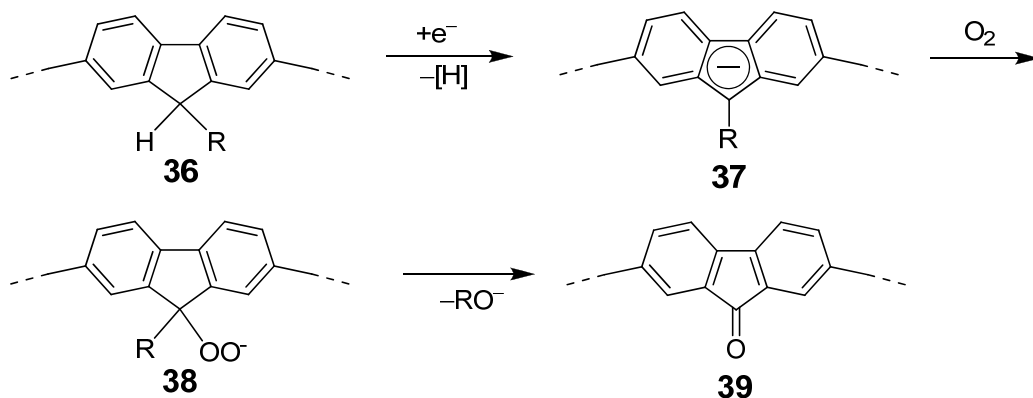
## 2.4. Optical and Electronic Properties of Polyfluorenes

Polyfluorenes display a rich and attractive variety of optical and electronic properties that are related to the intrachain order effects of the polymer backbone ( $\beta$ -phase formation) [28,51] as well as on those that are related to oxidative degradation of the material [52]. The latter is of special importance, since PFs have emerged as the most promising class of active, emissive materials for deep-blue OLEDs.

Over the last years, PFs have emerged as a promising class of conjugated polymers, which can be utilized as the blue light-emitting active layers in polymer light-emitting diodes (PLEDs), as the host material for internal color conversion techniques, or for PLEDs with polarized light emission, exploiting the liquid crystalline nature of most of the PFs [52]. Yet, despite the ongoing improvements in terms of stability and purity of PLEDs fabricated from PF type materials, most of these PLEDs suffer from a degradation of the device under operation documented in the formation of a low-energy emission band at 2.2-2.3 eV, which turns the desired blue emission color into an

undesired blue-green emission [28]. This band, which can also be found in photoluminescence (PL) emission upon photooxidation of the polymer, has been attributed to the formation of keto defects, which act as low-energy trapping sites for singlet excitons, being populated by an excitation energy transfer from the PF main chain [11,46].

The generation of the fluorenone defect sites can be explained by the following chemical reaction mechanism [28]: the highly active Ni(0) species used in the reductive coupling of the dibromo monomers reduce a certain amount of the 9-monoalkylated fluorene building blocks **36** to (aromatic) fluorenyl anions **37** (Scheme 11) under formation of hydrogen. These anions can form hydroperoxide anions **38** with atmospheric oxygen during the work-up of the reaction mixture. The hydroperoxide anions then undergo a final rearrangement to fluorenone moieties **39**.



**Scheme 11:** Proposed mechanism for the generation of keto defect sites.

It has been reported that a stable and efficient blue emission occurs at turn-on voltages for the 9,9-dialkylated PF-based EL devices (PLEDs). However, the color changes into a blue-greenish emission after more than 30 min of continuous operation in air [46]. This finding demonstrates that the formation of fluorenone defect sites also occurs during operation of PLEDs based on 9,9-dialkylated PF, especially under atmospheric conditions.

### 3. Objective of the Project Work

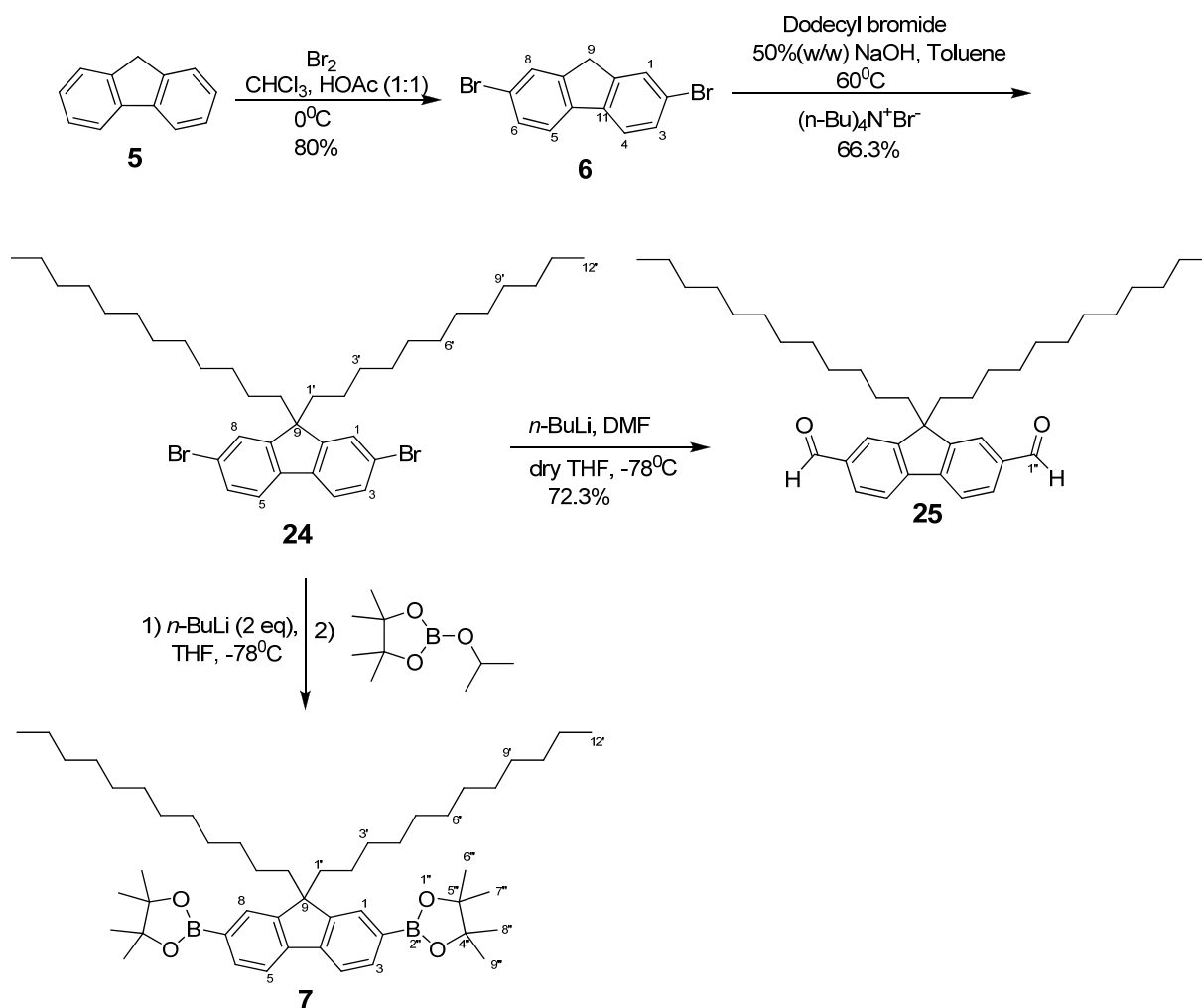
The aim of this graduate project is to synthesize some fluorene-based copolymers alternating with different kinds of aromatic sub-units. It generally involves the syntheses of the monomeric subunits such as 9,9-didodecyl-2,7-dibromofluorene (**24**), 9,9-didodecyl-9H-fluorene-2,7-dicarbaldehyde (**25**), 2,7-bis(4,4,5,5-tetramethyl-1,3,2-dioxaborolane)-9,9-didodecylfluorene (**7**), 1,4-bis(cyanomethyl)-2,5-bis(hexyloxy)-benzene (**31**) and 2,5-dihexyloxy-1,4-bis{2-(4'-bromothieryl)-2-cyanovinyl}-benzene (**32**) and subsequent polymerization of these monomers by Suzuki type polymerization reaction using palladium(0) catalyst and Knoevenagel polycondensation reaction. The intermediate compounds during the syntheses of monomeric sub-units will be characterized by NMR spectroscopy and the polymers will be characterized by <sup>1</sup>H-NMR spectroscopy, cyclic voltammetry (CV) and UV-Vis spectroscopy.

## 4. Results and Discussion

Four conjugated polymers based on substituted fluorene and aromatic sub-units were synthesized during this MSc project. The synthetic routes and structures of the polymers are shown in Schemes 15 and 16. Three of the conjugated copolymers, namely, poly[9,9-dioctyl-9H-fluorene-2,7-diyl-alt-2,5-dihexyloxy-1,4-bis(2-thienyl-2-cyanovinyl)benzene] (**40**), poly(9,9-didodecyl-9H-fluorene-2,7-diyl-alt-9,9-dibenzyl-9H-fluorene-2,7-diyl) (**41**) and poly[9,9-didodecyl-9H-fluorene-2,7-diyl-alt-2,5-dihexyloxy-1,4-bis(2-thienyl-2-cyanovinyl)-benzene] (**43**) (Scheme 15) were synthesized through palladium-catalyzed Suzuki coupling polymerization reaction and one of the polymers, namely, poly[(9,9-didodecyl-9H-fluorene-2,7-diyl)-(1-cyanoethene-1,2-diyl)-(2,5-bis(hexyloxy)phenylene)(2-cyanoethene-1,2-diyl)] (**42**), was synthesized by Knoevenagel condensation polymerization route. The polymers synthesized by Suzuki route were end-capped with bromobenzene and phenylboric acid. The syntheses began with preparation of the required monomeric sub-units for the copolymerization reactions as indicated in Schemes 12 and 14 and the monomers were subsequently polymerized.

### 4.1. Synthesis of Fluorene-Based Monomers

The general route for the synthesis of fluorene-based monomeric sub-units is indicated in Scheme 12. Initially, fluorene (**5**) was selectively brominated at the 2- and 7- positions with bromine in 1:1 mixture of chloroform and acetic acid. This reaction proceeded at 0°C and was followed by warming to room temperature. Higher reaction temperature would result in the undesirable bromination at other positions of compound **5**, which would be difficult to separate from the target molecule. Thin-layer chromatography was used to monitor the reaction progress to avoid the formation of byproduct compounds. The synthesis of 2,7-dibromofluorene (**6**) was then fairly easily accomplished in 80% yield as a white crystalline solid having a melting point of 154-156°C.



**Scheme 12:** Syntheses of fluorene-based monomers.

The  $^1\text{H-NMR}$  spectrum of compound **6** (Appendix 1) showed the presence of four different proton environments, of which three are in the aromatic region and one is in the aliphatic region. The singlet peak at  $\delta$ 3.80 is attributed to the two benzylic protons (H-9) of the fluorene moiety. The protons are deshielded as compared to the normal methylene protons ( $\delta$  ca.1.50 ppm) due to the electron withdrawing effects of the  $\text{SP}^2$  hybridized carbon atoms of the phenyl rings attached to the carbon bearing the benzylic protons. The doublet of doublet peak at  $\delta$ 7.49 ( $J = 8.1$  and  $1.6$  Hz) could only arise from the H-3 and H-6 protons, which are chemically equivalent. The two coupling constants are characteristic of *ortho* and *meta* couplings, respectively. The doublet signal at  $\delta$ 7.56 ( $J = 8.1$  Hz, which is characteristic of *ortho* coupling) can be attributed to the chemically

equivalent H-4 and H-5 protons. The broad doublet-like peak at  $\delta$ 7.64 ( $J = 1.0$  Hz) can be attributed to the two chemically equivalent H-1 and H-8 protons. The small coupling constant is due to the *meta* coupling of these protons with H-3 and H-6, respectively. Chemical shift values of H-1 and H-3 are shifted more towards the left than H-4. This is expected since the neighboring bromine substituent of H-1 and H-3 may deshield these protons more than H-4 as a result of the mutual repulsion of induced dipoles (dispersion forces) [20]. This van der Waals deshielding effect falls off very rapidly with increasing internuclear distance as its ability to repel electrons from the vicinity of the resonating atom decreases. The  $^1\text{H-NMR}$  spectral data for compound **6** is presented in Table 1.

**Table 1:**  $^1\text{H-NMR}$  (400MHz,  $\text{CDCl}_3$ ) data ( $\delta_{\text{ppm}}$ ) of compounds **6** and **24**.

<b>6</b>	<b>24</b>
7.64	7.54
(br d, $J = 1.0$ Hz, 2H, H-1, H-8)	(d, $J = 0.9$ Hz, 2H, H-1, H-8)
7.56	7.52
(d, $J = 8.1$ Hz, 2H, H-4, H-5)	(dd, $J = 8.4$ & $0.9$ Hz, 2H, H-3, H-6)
7.49	7.50
(dd, $J = 8.1$ & $1.6$ Hz, 2H, H-3, H-6)	(d, $J = 8.4$ Hz, 2H, H-4, H-5)
3.80	1.95
(s, 2H, H-9)	(t, 4H, 1')
	1.40-0.90
	(m, 40H, H-2'-11')
	0.80
	(t, 6H, H-12')

The  $^{13}\text{C-NMR}$  spectrum of compound **6** (Appendix 2) displayed six peaks in the aromatic region and only one signal in the aliphatic region. The DEPT-135 spectrum confirmed that three of the six carbon resonances in the aromatic region are due to quaternary carbon atoms since they disappeared in the spectrum and the remaining three carbon resonances are due to methine carbons since they appeared as upward signal in the spectrum. The substituted carbon atoms can also roughly be distinguished from the unsubstituted ones by inspection of their decreased peak intensities in the  $^{13}\text{C-NMR}$  spectrum. The common spin-lattice relaxation mechanism for  $^{13}\text{C}$  results from

dipole-dipole interaction with directly attached protons. Thus, non-protonated carbon atoms have longer relaxation times, which together with little or no Nuclear Overhauser Effect (NOE), results in small peaks. Of the quaternary carbon atoms, the two chemically equivalent carbon atoms, C-2 and C-7, can account for the most shielded peak of the aromatic region signals due to the heavy atom effect [50] of bromine atoms attached to them. The signals at  $\delta$ 139.7 can be attributed to C-11 and C-12 and the one at  $\delta$ 144.8 can be assigned to C-10 and C-13, which are chemically equivalent due to the symmetrical nature of the compound. C-11 and C-12 are expected to be more shielded than C-10 and C-13 due to higher electron density in the former carbons as a result of the  $\pi$ -electron delocalization through resonance. The  $^{13}\text{C}$  resonance in the aliphatic region can be accounted to the methylene carbon atom, which is also confirmed by its appearance as downward peak in the DEPT-135 spectrum. The  $^{13}\text{C}$ -NMR spectral data for compound **6** is presented in Table 2. Generally, both  $^1\text{H}$  and  $^{13}\text{C}$  NMR spectra are in good agreement with the structure of 2,7-dibromofluorene (**6**).

An important point concerning the application of PF-based materials in electronic devices is related to the presence (or absence) of defect states. One crucial point for avoiding defects is the use of completely 9,9-difunctionalized fluorene monomers. The presence of small amounts of non-alkylated or only mono-functionalized monomers (9-alkyl fluorene derivatives) yields preferred centers for photooxidative degradation. Such centers can already be oxidized during the coupling polymerization reaction or atmospheric work up under formation of fluorenone structural units. The complete absence of benzylic hydrogens in the 9-position of the fluorene moiety seems to be a key prerequisite for obtaining oxidatively stable, defect poor PFs. The synthesis of 9,9-didodecyl-2,7-dibromofluorene (**24**) was achieved in 66.3% yield as oily liquid from 2,7-dibromofluorene (**6**) using a two phase system composed of 50% (w/w) aqueous sodium hydroxide solution and toluene, in the presence of tetrabutylammonium bromide as a phase transfer catalyst. Initially mixtures of products were obtained which were then separated and purified by column chromatography giving the desired pure compound, **24**, as oily liquid and other byproducts.

The  $^1\text{H-NMR}$  spectrum of compound **24** (Appendix 4) showed three peaks, each integrating for a pair of chemically equivalent protons, in the aromatic region, and several other multiplet peaks in the aliphatic region of the spectrum (Table 1). The aromatic signals at  $\delta 7.50$ ,  $7.52$  and  $7.54$  arise from the protons of the fluorene moiety. The doublet of doublet peak at  $\delta 7.52$  ( $J = 8.41$  and  $0.91$  Hz) is due to H-3 and H-6, which are chemically equivalent and have an *ortho* coupling with H-4 and H-5, respectively, and *meta* coupling with H-1 and H-8 of the fluorene moiety. The doublet peak at  $\delta 7.50$  ( $J = 8.41$  Hz) can be attributed to H-4 and H-5, which are chemically equivalent and have an *ortho* coupling with H-3 and H-6, respectively. The doublet peak at  $\delta 7.54$  ( $J = 0.91$  Hz) can be attributed to H-1 and H-8, which are chemically equivalent and have a *meta* coupling with H-3 and H-6, respectively. The triplet peak at  $\delta 1.95$  and the multiplet peaks at  $\delta 1.40$ - $0.90$  are due to the methylene and the two terminal methyl protons of the two dodecyl side chains attached to the C-9 position of the fluorene moiety.

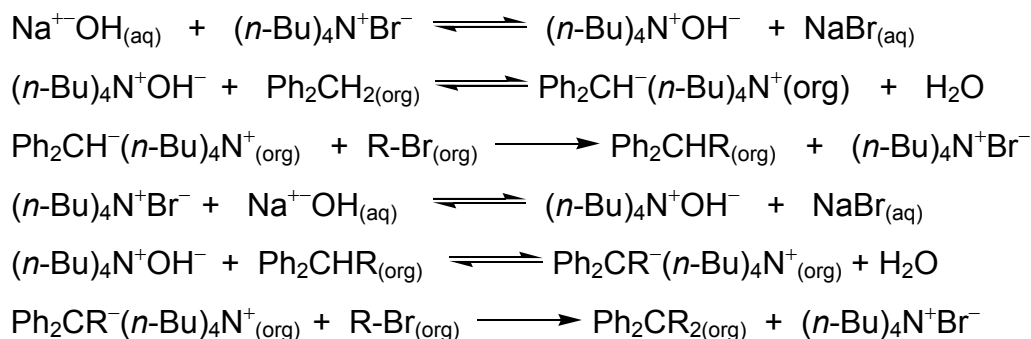
The  $^{13}\text{C-NMR}$  spectrum of compound **24** (Appendix 5) displayed a total of nineteen carbon signals, of which six appeared in the aromatic region and thirteen appeared in the aliphatic region (Table 2). The DEPT-135 spectrum revealed one methyl, eleven methylene and three methine carbon signals. The remaining four carbon signals can then be accounted for the quaternary carbon atoms, each peak representing a pair of chemically equivalent carbons. The peak at  $\delta 55.7$  can be attributed to the tetrahedrally substituted C-9 of the fluorene moiety which is further confirmed by the absence of the peak in the DEPT-135 spectrum. Its downfield shift relative to the other aliphatic carbon signals can also be described in terms of the  $\alpha$ -effect of the two phenyl rings and other two aliphatic methylene groups and the  $\beta$ -effect of the other two methylene groups which outweigh the shielding  $\gamma$ -effect of the two methylene groups. Among the chemical shifts of the carbons of the dodecyl side chain, the most down field position can be assigned for C-1' due to greater  $\alpha$ - and  $\beta$ -effects as compared to the opposing  $\gamma$ -effect, relative to the other carbons. The next most downfield signal can be due to C-10' since it has only one  $\gamma$ -effect, which has negative contribution to chemical shift values of alkanes, while the others encounter two  $\gamma$ -effects, the  $\alpha$ - and  $\beta$ - effects being the same.

**Table 2:**  $^{13}\text{C}$ -NMR (100.6 MHz,  $\text{CDCl}_3$ ) data ( $\delta_{\text{ppm}}$ ) for compounds **6**, **7**, **24** and **25**.

Carbon	<b>6</b>	<b>24</b>	<b>25</b>	<b>7</b>
1	130.1	130.2	130.3	133.7
2	120.9	121.1	136.5	133.6
3	121.2	121.5	123.4	128.9
4	128.3	126.2	121.3	119.4
5	128.3	126.2	121.3	119.4
6	121.2	121.5	123.4	128.9
7	120.9	121.1	136.5	133.6
8	130.1	130.2	130.3	133.7
9	36.6	55.7	55.6	55.2
10	144.8	152.6	152.9	150.4
11	139.7	139.1	145.6	143.9
12	139.7	139.1	145.6	143.9
13	144.8	152.6	152.9	150.4
1'		40.2	40.0	40.1
2'		28.8	23.8	23.7
3'		31.9	29.8	30.0
4'		29.9	29.6	29.7
5'		29.7	29.5	29.6
6'		29.6	29.4	29.4
7'		29.5	29.3	29.3
8'		29.4	29.2	26.9
9'		29.2	29.1	24.8
10'		33.9	31.9	31.9
11'		23.7	22.7	22.7
12'		14.2	14.1	14.2
1''			192.1	---
4''				83.7
5''				83.7
6''-9''				25.0

The third most downfield dodecyl carbon signal can be attributed to C-3' since it encounters greater  $\delta$ -effect, which contributes positively to chemical shift values of alkanes, than the others. The most up field signals can be due to the terminal methyl groups since it has the least number of  $\alpha$ - and  $\beta$ -carbons, which is also confirmed by the upward appearance of the signals in the DEPT-135 spectrum. The next most up field resonance is due to C-11' due to one less  $\beta$ -effect in it than the others. The third most up field signal can be attributed to C-2' since it encounters more number of the shielding  $\gamma$ -effect. The other signals with nearly equal chemical shift values can be assigned to carbons C4'-C9' which encounter almost similar  $\alpha$ -,  $\beta$ -,  $\gamma$ - and other branching effects. Generally, the  $^1\text{H-NMR}$  and  $^{13}\text{C-NMR}$  data discussed above agree very well with the structure of 9,9-didodecyl-2,7-dibromofluorene (**24**).

A difficulty that occasionally arises when carrying out nucleophilic substitution reactions is that the reactants do not mix. For the reaction to take place, the reacting molecules must collide. In this nucleophilic substitution reaction, the substrates, 2,7-dibromofluorene (**6**) and dodecyl bromide are soluble in toluene but insoluble in water, while the base ( $\text{Na}^+\text{OH}^-$ ) is soluble in water but not in the substrates and in toluene. Consequently, the uncatalyzed reaction does not take place because  $\text{OH}^-$  ions cannot cross the interface between the two phases. The reason is that the sodium ions are solvated by the water, and this solvation energy would not be present in the organic phase. The  $\text{OH}^-$  ions cannot cross without the sodium ions because that would destroy the electrical neutrality of each phase. The phase transfer catalyst, *tetrabutylammonium* bromide ( $\text{Bu}_4\text{NBr}$ ), is, therefore, used to carry the nucleophile ( $\text{HO}^-$ ) from the aqueous into the organic phase. In contrast to sodium ions, *tetrabutylammonium* ions are poorly solvated in water and prefer organic solvents. The sodium ions remain in the aqueous phase but *tetrabutylammonium* ions do cross the interface and carry  $\text{OH}^-$  anions with them to the organic phase. The  $\text{OH}^-$  deprotonates the benzylic protons of compound **6** to form the corresponding anion and water. The resulting 9-fluorenyl anion acts as a nucleophile and undergoes nucleophilic substitution reaction with dodecyl bromide producing the alkyl substituted fluorene with concomitant regeneration of the catalyst. The mechanism of the phase transfer reaction is depicted in Scheme 13.



**Scheme 13:** The mechanism of the phase transfer catalysis reaction

Two byproduct mixtures were identified as yellow solid for this reaction, in which no attempt was made to isolate them. The compounds identified are 2,7-dibromo-9-dodecyl-9-hydroperoxy-9H-fluorene (**26**) and 2,7-dibromo-9H-fluorene-9-one (**27**) (Figure 3). In the NMR spectra of the crude reaction product, *i.e.*, before separation and purification by column chromatography, no signal with the indication of the *mono*-alkylated material was observed. Some signals of the byproducts were observed after the crude material had passed through the column. The appearance of the  $^1\text{H}$ -NMR spectrum of the byproduct compound **26** is similar in many aspects to that of compound **24**. The marked difference exists due to the appearance of a singlet peak at  $\delta 2.55$  in the  $^1\text{H}$ -NMR spectrum of compound **26** which can be assigned to the proton of hydroperoxide attached at the C-9 position of the fluorene moiety. With respect to the  $^{13}\text{C}$  resonances, the existence of oxygenated carbon signal at  $\delta 82.5$  can confirm the formation of this byproduct compound. The formation of byproduct compound **27** was confirmed by the existence of carbonyl carbon resonance at  $\delta 190.9$  in the  $^{13}\text{C}$ -NMR spectrum which can be attributed to the ketone formed at the C-9 position of the fluorene moiety. The other  $^1\text{H}$  and  $^{13}\text{C}$  NMR signals of this compound are similar to that of 2,7-dibromofluorene (**6**) except for the presence of methylene carbon resonance for compound **6**.

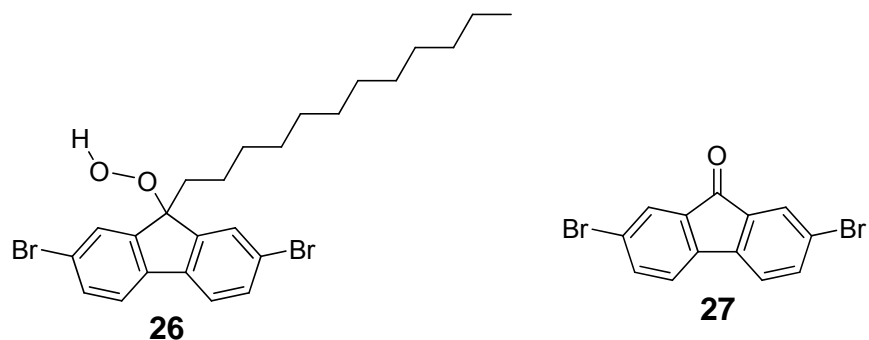


**Figure 3:** Structures of byproduct compounds identified during the alkylation of 2,7-dibromofluorene.

In the next step, 9,9-didodecyl-9H-fluorene-2,7-dicarbaldehyde (**25**) was synthesized by an adopted literature procedure [42]. Compound **25**, the crucial monomer in this approach, was synthesized by reacting compound **24** with two equivalents of *n*-BuLi and *subsequently* quenching with N,N-dimethylformamide (DMF) in dry THF. Careful preliminary drying of the solvent was necessary because this solvent can dissolve substantial quantities of water, which is incompatible with *n*-BuLi. THF was thus rigorously dried before use over sodium-benzophenone system under an inert atmosphere until the deep blue color of the ketyl radical anion persisted. The formylation reaction *via n*-BuLi/DMF mainly gave the desired compound **25**, but the product was contaminated with some impurities. The pure compound **25** was obtained as yellow crystalline solid (Mp. 47-49<sup>0</sup>C) with a yield of 72.3% after purification by column chromatography on silica gel using a solvent system of 10% solution of ethyl acetate in hexane.

The aromatic region of the <sup>1</sup>H-NMR spectrum of compound **25** is almost similar to that of compound **24** showing three peaks, each integrating for two protons. Several other peaks appeared in the aliphatic region of the spectrum (Appendix 7), but an additional signal at δ10.15 exists in the spectrum which is a characteristic peak for the aldehydic proton. The peaks in the aromatic region of the spectrum are shifted more towards the downfield position as compared to the <sup>1</sup>H-NMR spectrum of compounds **6** and **24**. This is expected since the shifts of protons *ortho*, *meta* and *para* to a substituent of an

aromatic ring are correlated with electron densities. In our case, replacement of the bromines by the more electron withdrawing carbonyl groups deshields the protons on the ring. The peaks at  $\delta$ 7.91, 7.94 and 7.96 of the aromatic region arise from the protons of the fluorene moiety. The doublet of doublet peak at  $\delta$ 7.94 ( $J = 3.4$  and  $1.0$  Hz) is due to H-3 and H-6, which are chemically equivalent and have an *ortho* coupling with H-4 and H-5, respectively, and a *meta* coupling with H-1 and H-8 of the fluorene moiety. The doublet peak at  $\delta$ 7.91 ( $J = 1.2$  Hz) is due to H-4 and H-5, which are chemically equivalent and have an *ortho* coupling with H-3 and H-6, respectively. The doublet peak at  $\delta$ 7.96 ( $J = 0.42$  Hz) is attributed to H-1 and H-8, which have *meta* coupling with H-3 and H-6, respectively. The protons *ortho* to the carbonyl are more deshielded than those *meta* to the carbonyl. This is not unexpected since electron delocalization with the carbonyl group makes the *ortho* positions more electron deficient than the *meta* position. The *meta* proton is shielded relative to that of the *ortho* protons because of the slightly higher electron density in the *meta* position that also accounts for the predominance of *meta* substitution by electrophilic reagents. The multiplet peaks at  $\delta$ 2.11 and  $\delta$ 1.30-0.80 which integrate to 50 protons are due to the protons of the dodecyl side chains attached to the C-9 position of the fluorene moiety and can be analyzed in the same way as was described for compound **24**.

The  $^{13}\text{C}$ -NMR spectrum of compound **25** (Table 2) showed a total of twenty carbon signals, of which seven appeared above  $\delta$ 100.0 and thirteen appeared below  $\delta$ 100.0. The peak at  $\delta$ 192.1 is a characteristic signal for the aldehydic carbon which is further confirmed by the upward appearance of the signal in the DEPT-135 spectrum. The peak is slightly shifted to the right as compared to the simple aldehydic signal presumably because charge delocalization by the aromatic ring makes the carbonyl carbon less electron deficient. The six carbon signals in the aromatic region can be attributed to the six aromatic carbons of the fluorene moiety, each peak representing two chemically equivalent carbons of the symmetrical molecule. Of the six peaks, three of the peaks are quaternary carbons as expected, which is further confirmed by the disappearance of the peaks in the DEPT spectrum and the remaining three represent the methine carbons of the fluorene moiety since they appeared as upward signal in the DEPT

spectrum. As compared to the  $^{13}\text{C}$ -NMR spectra of compounds **6** and **24**, the aromatic carbon attached directly to the carbonyl carbon is deshielded because the replacement of the bromine by the electron withdrawing carbonyl group makes it more electron deficient. The peak at  $\delta 55.6$  represents the *tetrasubstituted* benzylic carbon of the fluorene moiety which is further confirmed by the disappearance of the peak in the DEPT spectrum. The other signals in the chemical shift range of  $\delta 40.1$ - $14.1$  are attributed to the carbons of the dodecyl side chains and can be analyzed in similar manner as described for compound **24**. Generally, both the  $^1\text{H}$  and  $^{13}\text{C}$  signals match perfectly with the structure of compound **25**.

**Table 3:**  $^1\text{H}$ -NMR (400MHz,  $\text{CDCl}_3$ ) data ( $\delta_{\text{ppm}}$ ) of compounds **7** and **25**.

<b>7</b>	<b>25</b>
7.84 (dd, $J = 7.6$ and $0.8$ Hz, 2H, H-3, H-6)	10.1 (s, 2H, -CHO or H-1'')
7.78 (brs, 2H, H-1, H-8)	7.96 (d, $J = 0.4$ Hz, 2H, H-1, H-8)
7.75 (dd, $J = 7.6$ Hz, 2H, H-4, H-5)	7.94 (dd, $J = 3.4$ & $1.0$ Hz, 2H, H-3&6)
2.00 (m, 4H, H-1')	7.91 (d, $J = 1.2$ Hz, 2H, H-4, H-5)
1.30-0.85 (m, 40H, H-2'-11')	2.10 (t, 4H, H-1')
1.40 (s, 24H, H-6'' to H-9'')	1.30-0.90 (m, 40H, H-2'-11')
0.80 (t, 6H, H-12')	0.80 (t, 6H, H-12')

In separate reaction path, 2,7-dibromo-9,9-didodecylfluorene (**24**) was also converted to the corresponding diborolane **7** by halogen-metal exchange with *n*-butyllithium in anhydrous THF at  $-78^\circ\text{C}$  followed by the addition of 2-isopropoxy-4,4,5,5-tetramethyl-

1,3,2-dioxborolane according to the procedure reported by Ranger *et al.* [25]. The pure reaction product was obtained as yellow solid after purification of the crude oily product (which crystallized up on refrigeration) by chromatography on silica gel using 2% solution of ethyl acetate in hexane as eluent.

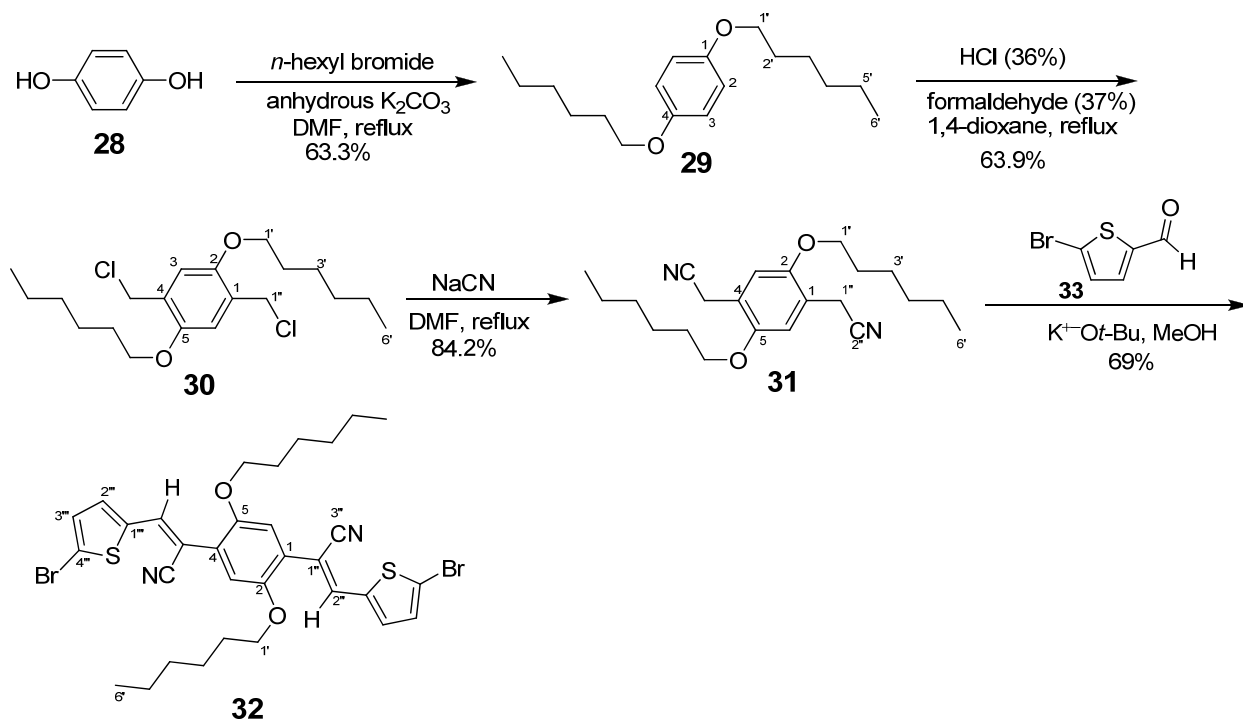
The  $^1\text{H-NMR}$  spectrum of the resulting compound **7** had very similar resonances in the aromatic region to that of compound **24**. The two-proton doublet of doublet at  $\delta$  7.83 ( $J = 7.6$  and  $0.8$  Hz) is due to H-3 and H-6, while the two-proton broad singlet at  $\delta$  7.77 is attributed to H-1 and H-8. The two-proton doublet peak at  $\delta$  7.75 ( $J = 7.6$  Hz) can be assigned to H-4 and H-5. In the aliphatic region of the spectrum, multiplet peaks appeared at  $\delta$  1.89, 1.71-0.90 and 0.45 which integrate for a total of 44 protons due to the methylene protons on the dodecyl side chains. The six-proton triplet at  $\delta$  0.85 can be assigned to the terminal methyl groups of the dodecyl side chain. The singlet signal at  $\delta$  1.40, which integrates for twenty-four protons is due to the protons on the four-methyl groups of the 4'',4'',5'',5''-tetramethyl-1,3,2-dioxborolane moieties on both sides of the symmetrical molecule.

The  $^{13}\text{C-NMR}$  and DEPT-135 spectra of compound **7** confirmed the presence of five methyl, eleven methylene and two quaternary carbon resonances in the aliphatic region. It also displayed the presence of three quaternary and three methine resonances in the aromatic region. Since the compound is symmetrical, only half of the carbon signals were observed in the  $^{13}\text{C-NMR}$  spectrum (Table 2). Both the  $^1\text{H-}$  and  $^{13}\text{C-NMR}$  data discussed above agree very well with the structure of the compound.

## 4.2. Synthesis of Alternating Monomeric Sub-units

As outlined in Scheme 14, the alternating aromatic monomeric subunits were easily prepared starting from hydroquinone (**28**). Initially, 1,4-bis(hexyloxy)benzene (**29**) was synthesized in 63.3% yield as crystalline solid (Mp.  $39-43^\circ\text{C}$ ) from hydroquinone (**28**)

and *n*-hexyl bromide by applying a modified Williamson ether synthetic strategy in the presence of potassium carbonate and DMF.



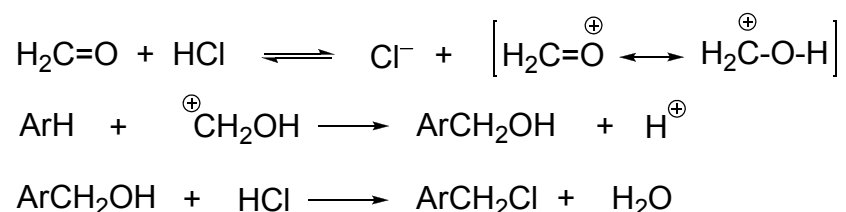
**Scheme 14:** Synthetic scheme for the alternating monomeric sub-units.

The  $^1\text{H-NMR}$  spectrum of compound **29** revealed a single proton resonance in the aromatic region and other multiplet peaks in the aliphatic region. The four hydrogen singlet peak at  $\delta 6.95$  can be attributed to the aromatic protons on the benzene ring, which are all chemically equivalent due to the symmetrical structure of the compound. The chemical shift value is shifted slightly to the right as compared to the normal phenylene protons of benzene. This is because resonance interaction of the ring with the ether oxygen increases the electron density on the ring, shielding the protons that are attached to the ring carbons  $\beta$ - to it. The triplet peak at  $\delta 3.95$ , which integrates for four chemically equivalent protons, is due to the methylene protons whose carbon is attached directly to the oxygen atom. The protons are deshielded as compared to the other methylene groups since electron withdrawing inductive effect of the directly attached oxygen atom, whose effect decreases up on increasing distance, makes them

electron deficient. The quintet peak at  $\delta$ 1.75, which is the next deshielded aliphatic resonance, can be assigned to the methylene protons  $\beta$ - to the oxygen atom, which have slight tendency to feel the inductive effect of the electronegative oxygen atom, and are adjacent to two different methylene groups which are responsible for the observed multiplicity. The other peaks in the range of  $\delta$ 1.60-1.20 can be assigned to the resonances of the remaining methylene protons of the *n*-hexyloxy side chains. The 6H triplet peak at  $\delta$ 0.90 is due to the terminal methyl protons of the *n*-hexyloxy groups, which are neighbored by methylene protons.

The  $^{13}\text{C}$ -NMR spectrum of compound **29** (Table 6) displayed the existence of eight carbon resonances, of which two are in the aromatic region and the remaining six are in the aliphatic region. The DEPT-135 spectrum showed one methine signal in the aromatic region, and five methylene carbon resonances and one methyl carbon peak in the aliphatic region. The most deshielded carbon resonance can be attributed to the aromatic carbons attached directly to the oxygen atoms since the electron withdrawing inductive effect of the oxygen atom makes them highly electron deficient. This is also further confirmed by the disappearance of the peak in the DEPT spectrum. The other signal in the aromatic region can be assigned to the methine protons of the aromatic ring, which are all chemically equivalent. This is also confirmed by the upward appearance of the signal in the DEPT spectrum. Their shielding, as compared to the normal carbon signals of benzene, is not unexpected since electron delocalization through resonance from the ether oxygen makes them less electron deficient. The peak at  $\delta$ 69.0 is due to the aliphatic methylene carbon attached directly to the oxygen whose deshielding is also the result of this neighboring atom. The other signals in the chemical shift range of  $\delta$ 40.0-20.0 are due to the remaining methylene carbon resonances of the *n*-hexyloxy side chains, which all appeared as downward peak on the DEPT spectrum. The most shielded resonance at  $\delta$ 14.1 is due to the terminal methyl carbon of the *n*-hexyl substituent, which is further confirmed by the upward appearance of the signal on the DEPT spectrum. Generally, the NMR results are in good agreement with the structure of compound **29**.

The next step in our synthetic plan was chloromethylation of compound **29**, which involves the replacement of a hydrogen atom in an aromatic compound by a chloromethyl (-CH<sub>2</sub>Cl) group in a single operation. The reaction consists essentially of the interaction of formaldehyde and hydrogen chloride with an aromatic system. The reaction is similar in some respect to that of Friedel-Crafts reaction and involves the hydroxymethyl cation as the electrophilic species. This reacts with the aromatic ring to give the benzylic alcohol which is then converted in to the chloromethyl derivative by hydrogen chloride.



In our case, 1,4-bis(hexyloxy)-2,5-bis(chloromethyl)benzene (**30**) was synthesized from compound **29** in 63.9% yield by treatment of **29** with excess 36% solution of hydrochloric acid and excess 37% solution of formaldehyde and refluxing in 1,4-dioxane for about three days.

The <sup>1</sup>H-NMR spectrum of the product showed a single peak in the aromatic region and several other peaks in the aliphatic region. The appearance of the spectrum is almost similar to the <sup>1</sup>H-NMR spectrum of compound **29** except for the presence of an additional proton peak at δ4.65 due to the protons of the newly introduced chloromethyl group. The singlet peak at δ6.95 can be assigned for the proton on the aromatic ring, which integrates for the two chemically equivalent protons of the symmetrical molecule. The four-proton singlet peak at δ4.65 can be attributed to the benzylic protons of the chloromethyl groups. Their being deshielded as compared to the normal benzylic protons of toluene is due to the attachment of the carbon bearing these protons to the electronegative chlorine atom. The four-proton triplet peak at δ4.05 is due to the methylene protons attached α-to the oxygen atom. The other signals can be analyzed in the same way as described for compound **29**.

The  $^{13}\text{C}$ -NMR spectrum of compound **30** (Table 6) displayed the existence of ten carbon resonances, of which three are in the aromatic region and the remaining seven are in the aliphatic region. The appearance of the spectrum is similar to that of the  $^{13}\text{C}$ -NMR spectrum of compound **29** with additional two carbon resonances, one in the aliphatic region at  $\delta$ 41.4 and the other in the aromatic region at  $\delta$ 127.1. The DEPT-135 spectrum has also similar appearance to that of compound **29** except for the presence of one methylene carbon peak at  $\delta$ 41.4. The peak at this position is the result of the methylene carbon of the newly introduced chloromethyl ( $-\text{CH}_2\text{Cl}$ ), which is also confirmed by the downward appearance of the peak on the DEPT spectrum. The signal at  $\delta$ 127.1 is due to the quaternary carbon atom of the ring at the *ortho* position to the hexyloxy substituent, which has been created as a result of the introduction of the chloromethyl group by the replacement of the ring hydrogen. This is further confirmed by the disappearance of the peak on the DEPT spectrum. The other  $^{13}\text{C}$  and DEPT resonances can be interpreted in the same way as was done for compound **29**. Generally, both  $^1\text{H}$  and  $^{13}\text{C}$  NMR spectral data agree very well with the structure of compound **30**.

In the subsequent step, 1,4-bis(cyanomethyl)-2,5-bis(hexyloxy)-benzene (**31**) was synthesized from compound **30** in 84.2% yield. Nucleophilic substitution of  $\text{Cl}^-$  by  $\text{CN}^-$  was effected by refluxing finely crushed sodium cyanide and **29** in anhydrous DMF to give white crystalline solid which precipitated out of the reaction mixture. Compound **31** was obtained in a pure form after recrystallization from hexane.

The  $^1\text{H}$ -NMR spectrum of compound **31** showed a single peak in the aromatic region and other singlet and multiplet peaks in the aliphatic region. The two-proton singlet peak at  $\delta$ 6.95 can be assigned for the two chemically equivalent protons of the aromatic ring. The four-proton triplet peak at  $\delta$ 4.00 can be attributed to the methylene protons of the *n*-hexyloxy side chain that are attached directly to the oxygen atoms and are neighbored by methylene groups, which are responsible for the resulting multiplicity. The four-proton singlet peak at  $\delta$ 3.74 is due to the methylene protons of the cyanomethyl ( $-\text{CH}_2\text{CN}$ ) group, which are slightly deshielded by the electron withdrawing cyano group.

The other multiplet peaks in the range of  $\delta$ 1.90-0.90 can be assigned for the remaining protons of the *n*-hexyloxy side chain in the same way as was done for compounds **29** and **30**.

The appearances of the  $^{13}\text{C}$ -NMR and DEPT-135 spectra for this compound are similar to that of compound **30** and the interpretation can be done in the same manner. The difference exists due to the appearance of a carbon resonance at  $\delta$ 117.8, which can be attributed to the non-protonated carbon of the newly added carbon of the cyano group. This is further confirmed by the disappearance of the signal in the DEPT-135 spectrum. Therefore, the existence of a good correlation between the spectral results and the structure of the compound proves the successful synthesis of compound **31**.

In the subsequent step, 2,5-dihexyloxy-1,4-bis{2-(4'-bromothieryl)-2-cyanovinyl}-benzene (**32**) was synthesized as a bright yellow solid (Mp 198-199 $^{\circ}$ C) by Knoevenagel condensation reaction. The compound was obtained with 69% yield after stirring the mixture of compound **31**, 5-bromothiophen-2-carbaldehyde and potassium *tert*-butoxide in methanol at reflux temperature. Washing the product with ice-cold methanol and recrystallization from 2-propanol gave compound **32**.

The  $^1\text{H}$  NMR spectrum of compound **32** revealed four signals in the aromatic region and six multiplet peaks in the aliphatic region, totally integrating for 34 protons. The signals in the aliphatic region can be assigned for the protons of the *n*-hexyloxy side chain in the same way as was done for compounds **29**, **30** and **31**. Of the aromatic proton resonances, the two doublet peaks are attributed to the neighboring protons of the thienyl group since they can couple with each other to bring about the resulting multiplicity. There are also two singlet proton peaks in the aromatic region at  $\delta$ 7.98 and 7.09, each integrating for two chemically equivalent protons.

The  $^{13}\text{C}$ -NMR spectrum of compound **32** (Appendix 20) revealed ten carbon resonances above  $\delta$ 100 and six carbon signals below  $\delta$ 100. Of the ten carbon signals in the aromatic region, four are methine carbons and the remaining six resonances represent

quaternary carbons as revealed by the DEPT-135 spectrum. The six carbon signals in the aliphatic region, of which five are methylene carbon peaks and one is methyl carbon peak, can be assigned for the carbons of the *n*-hexyloxy side chains.

2D-NMR spectroscopy was done to make appropriate assignment of each signal for each proton and carbon. The  $^1\text{H}$ - $^1\text{H}$  COSY NMR spectrum revealed that the proton signal at  $\delta 7.30$  shows strong correlation with the proton signal at  $\delta 7.13$  and weak correlation with the signal at  $\delta 7.98$ . But the proton signal at  $\delta 7.13$  shows only one strong correlation with the signal at  $\delta 7.30$ . Therefore the doublet signals at  $\delta 7.30$  and  $7.13$  can be assigned for H-2''' and H-3''' protons of the bromothieryl group. The assignment of the relatively more downfield position to H-2''' is also expected by looking at the structure of the compound. Electron delocalization with the cyano substituent, which forms a conjugated system with the double bonds of the thienyl group, makes the 2'''-position more electron deficient than the 3'''-position. The existence of long range  $^1\text{H}$ - $^1\text{H}$  correlation between H-2''' and the singlet proton signal at  $\delta 7.98$  also enables us to assign this singlet peak for the olefinic proton of the cyanovinylene moiety (H-2''), whose deshielding relative to simple olefinic protons is expected since electron delocalization with the conjugated cyano group can make it highly electron deficient. The remaining singlet proton peak at  $\delta 7.09$ , which shows only one weak correlation with the quartet proton signal at  $\delta 4.05$ , can then be attributed to the two chemically equivalent protons of the benzene ring *ortho* to the *n*-hexyloxy substituents. By relating these results with the HMQC spectrum, the methine carbon signals at  $\delta 138.2$ ,  $133.0$ ,  $130.6$  and  $114.1$  can be assigned, respectively, for C-2'', C-2''', C-3''' and C-3 carbons of compound **32**.

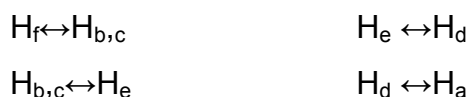
The HMBC spectrum revealed the existence of correlation between the proton signal at  $\delta 7.98$  (H-2'') and the carbon signals at  $\delta 139.7$ ,  $133.0$ ,  $123.8$ ,  $118.5$  and  $104.9$ . The proton signal at  $\delta 7.30$  also shows correlation with the carbon resonances at  $\delta 139.7$ ,  $130.6$  and  $118.3$ . From these two sets of data, the carbon signals at  $\delta 139.7$ ,  $123.8$ ,  $118.5$ ,  $118.3$  and  $104.9$  can be assigned for the carbons C-1''', C-1, C-3'', C-4''' and C-1'', respectively. The most deshielded carbon signal at  $\delta 150.6$  can, therefore, be

assigned for the two chemically equivalent oxygenated carbons of the benzene ring (C-2). The HMQC spectrum was used to make proper assignments of the proton and carbon resonances of the aliphatic region with their corresponding protons and carbons as depicted in Table 3.

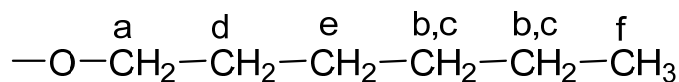
**Table 3:** HMQC data for compound **32**.

<sup>13</sup> C signals ( $\delta_{\text{ppm}}$ )	<sup>1</sup> H signals ( $\delta_{\text{ppm}}$ )	Remark
69.1	4.05 (H <sub>a</sub> )	CH <sub>2</sub>
31.6	1.45-1.25 (H <sub>b,c</sub> )	CH <sub>2</sub>
29.2	1.80 (H <sub>d</sub> )	CH <sub>2</sub>
25.9	1.52 (H <sub>e</sub> )	CH <sub>2</sub>
22.6	1.45-1.25 (H <sub>b,c</sub> )	CH <sub>2</sub>
14.1	0.95 (H <sub>f</sub> )	CH <sub>3</sub>

The six-proton triplet peak at  $\delta$ 0.95 can easily be assigned to the terminal methyl protons since it is the only methyl group and the corresponding <sup>13</sup>C signal of the terminal methyl carbon appears at  $\delta$ 14.1. The <sup>1</sup>H-<sup>1</sup>H COSY spectrum revealed the following correlation.



From this result, the following pattern can be predicted:



Therefore, the protons at  $\delta$ 4.05, 1.80, 1.52 and 1.45-1.25 can be assigned for H-1', H-2', H-3' and H-4',5', respectively and the carbon signals at  $\delta$ 69.7, 29.2 and 25.9 can be assigned for C-1', C-2' and c-3', respectively. The remaining to do is to distinguish the carbon signals at  $\delta$ 31.6 and 22.6 for C-4' and C-5'. HMBC spectral results enable us to do so. The proton signal at  $\delta$ 1.52 (H-3') shows strong correlation with the carbon signal at  $\delta$ 31.6 implying that C-4', the neighboring carbon to C-3', is responsible for the signal at  $\delta$ 31.6 and the remaining signal at  $\delta$ 22.6 is due to C-5'. Generally, the existence of a

perfect match between the spectral data and the structure of the compound indicates that the condensation reaction used to synthesize this desired compound was successful.

**Table 4:**  $^1\text{H-NMR}$  (400 MHz,  $\text{CDCl}_3$ ) data ( $\delta_{\text{ppm}}$ ) of compounds **29-32**.

<b>29</b>	<b>30</b>	<b>31</b>	<b>32</b>
6.95	6.95	6.95	7.98
(s, 4H, H-2,3,5,6)	(s, 2H, H-3, H-6)	(s, 2H, H-3,6)	(s, 2H, H-2'')
3.95	4.65	4.00	7.30
(t, 4H, H-1', H-5)	(s, 4H, H-1'')	(t, 4H, H-1')	(d, $J = 4.05$ Hz, 2H, H-2''')
1.75	4.05	3.74	7.13
(m, 4H, H-2')	(t, 4H, H-1')	(s, 4H, H-1'')	(d, $J = 3.95$ Hz, 2H, H-3''')
1.49	1.80	1.80	7.09
(m, 4H, H-3')	(m, 4H, 2')	(m, 4H, H-2')	(s, 2H, H-3,6)
1.45-1.25	1.55	1.52	4.05
(m, 8H, H-4', 5')	(m, 4H, H-3')	(m, 4H, H-3')	(t, 4H, H-1')
0.90	1.45-1.25	1.45-1.25	1.90
(t, 6H, H-6')	(m, 8H, H-4', 5')	(m, 8H, H-4',5')	(m, 4H, H-2')
	0.95	0.95	1.50
	(t, 6H, H-6')	(t, 6H, H-6')	(m, 4H, H-3')
			1.40-1.25
			(m, 8H, H-4',5')
			0.95
			(t, 6H, H-6')

**Table 5:**  $^{13}\text{C}$ -NMR (100.6 MHz,  $\text{CDCl}_3$ ) data ( $\delta_{\text{ppm}}$ ) for compounds **29-32**.

C	29	30	31	32
1	153.2	127.1	117.8	123.8
2	115.4	150.6	150.1	150.6
3	115.4	114.3	112.7	114.1
4	153.2	127.1	117.8	123.8
5	115.4	150.6	150.1	150.6
6	115.4	114.3	112.7	114.1
1'	68.6	69.1	69.0	69.7
2'	29.4	29.3	29.2	29.2
3'	25.8	25.7	25.7	25.8
4'	31.7	31.5	31.5	31.6
5'	22.7	22.6	22.6	22.6
6'	14.1	14.0	14.0	14.1
1''		41.4	18.6	104.9
2''			119.2	138.2
3''				118.5
1'''				139.7
2'''				133.0
3'''				130.6
4'''				118.3

### 4.3. Synthesis of Alternating Copolymers

Fluorene-based polymers were chosen for this project work, as they have often been used as the active material in organic optoelectronic devices because of their high efficiency and their deeply blue luminescence character [11, 12]. They are highly studied because of their exceptional electro-optical properties and their exceptional performance in light-emitting diodes. They are capable of emitting colors spanning the entire visible range with high efficiency and low operating voltage. Substitution of two

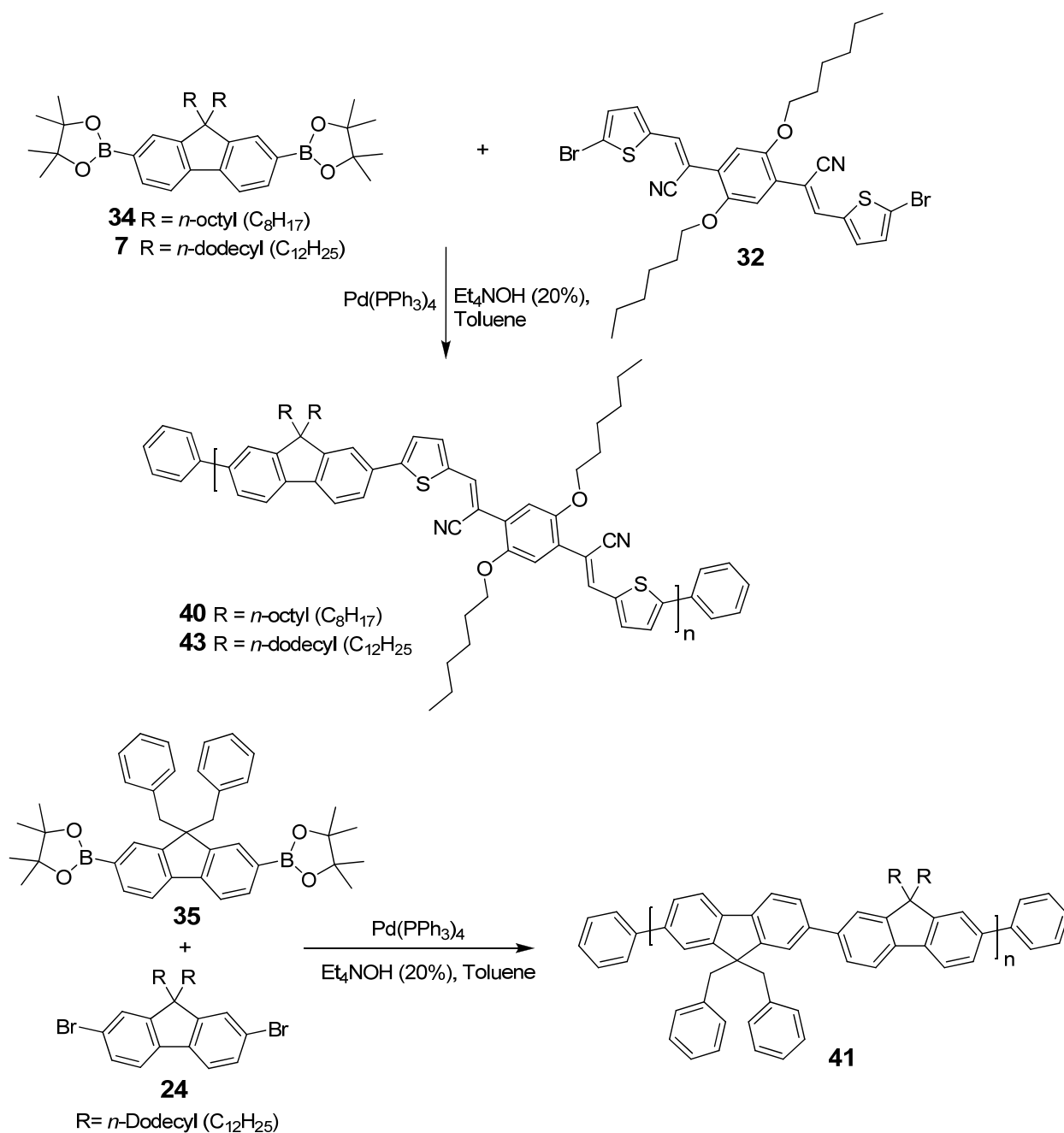
alkyl chains at the 9 and 9' positions has led to highly processable polymer derivatives, which also have well-defined structures due to regioregularity.

#### 4.3.1. Synthesis and Characterization

During this project work, four fluorene-based alternating copolymers, namely, poly[9,9-dioctyl-9H-fluorene-2,7-diyl-alt-2,5-dihexyloxy-1,4-bis(2-thienyl-2-cyanovinyl)-benzene] (**40**), poly(9,9-didodecyl-9H-fluorene-2,7-diyl-alt-9,9-dibenzyl-9H-fluorene-2,7-diyl) (**41**), poly[(9,9-didodecyl-9H-fluorene-2,7-diyl)-(1-cyanoethene-1,2-diyl)(2,5-bis(hexyloxy)-phenylene)-(2-cyanoethene-1,2-diyl)] (**42**) and poly[9,9-didodecyl-9H-fluorene-2,7-diyl-alt-2,5-dihexyloxy-1,4-bis(2-thienyl-2-cyanovinyl)-benzene] (**43**) were synthesized. The polymers described here were synthesized by two different polymerization routes: Knoevenagel polycondensation and a modified Suzuki polymerization reaction. Scheme 15 illustrates the synthesis of the polymers realized by palladium-catalyzed Suzuki type polymerization. These series of conjugated polymers were end-capped with benzene rings. Low molecular weight oligomers were removed by Soxhlet-extraction with diethyl ether and the chloroform-soluble materials were collected and the polymers were obtained in powder form after precipitation from methanol. The boronate esters **34** and **35** used in our synthesis were previously synthesized in our laboratory by Yadessa Melaku [18] and Zekarias Yacob [19], respectively.

The Suzuki polymerization is the most widely used synthesis of polyfluorene derivatives due to a simple conversion of the aryl dihalide comonomer to the boronic acid or ester (less toxic and more environmentally friendly than the tin reagents used in its analogue, the Stille reaction) [36].

Polymers **40** and **43** appeared as orange-red solid, **41** appeared as white solid but its chloroform solution was observed to be shimmering blue, and **42** appeared as yellowish-green solid. All of the synthesized polymers showed good solubility in chloroform. Solution processability for fabricating LED devices is one of the most attractive advantages of polymers over small organic molecule-based LEDs or inorganic LEDs.

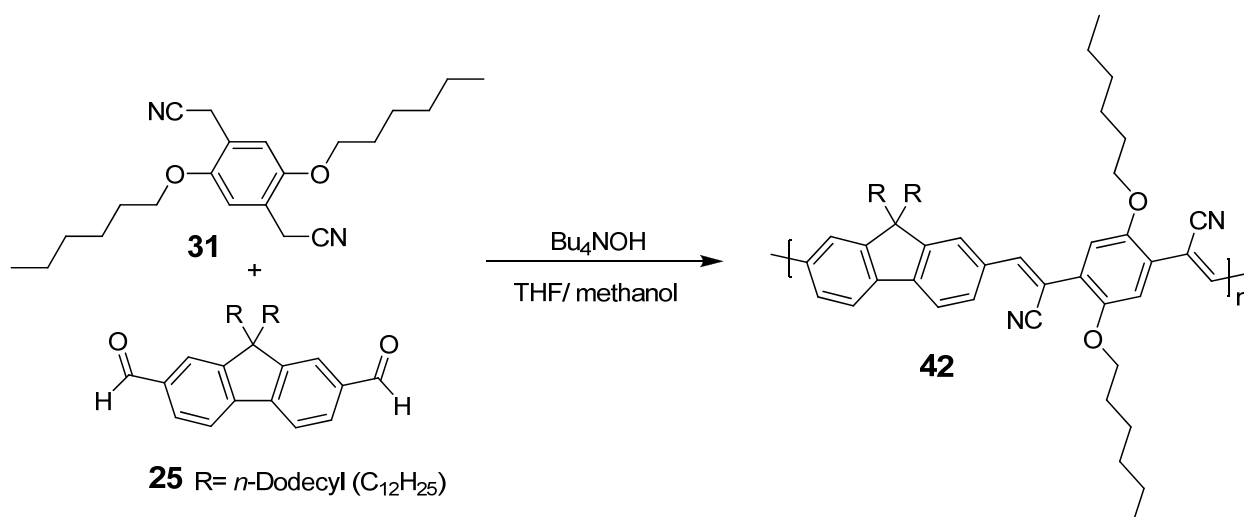


**Scheme 15:** Synthesis of **40**, **41** and **43** through a modified Suzuki polymerization reaction.

Cyanovinylene-based polymers are attractive targets because soluble high molecular weight polymers can be realized through a Knoevenagel polymerization to give regiosymmetric polymers with well-defined structures [4]. An advantage of the

Knoevenagel route is the robust nature of the reaction that gives polymers in the neutral form without the use of metal catalysts that could potentially be trapped in the polymer. Historically, overall synthetic yields for D-A monomers have often been hampered by the need to crosscouple two aromatic heterocycles with the concomitant loss in yield for the preparation of organo-tin, -ZnCl, or -boronate reagents and the coupling reactions used in Stille, Negishi, and Suzuki reactions [3]. The use of the Knoevenagel condensation for the preparation of the cyanovinylene acceptor core lessens some of the complications of combining premade D-A units and eliminates the need for expensive and toxic tin reagents completely. From an electronic point of view, such soluble polymers offer several strengths, which include air-stability (based on a low-lying HOMO), a narrow band gap (based on the donor-acceptor interaction), and a sufficiently electron-rich structure to allow them to function as donor materials in solar cells [4]. Relative to the variety of other low band gap polymers reported in the literature, this set of properties appears to make these polymers unique.

The basic strategy employed for the synthesis of **42** is based on Knoevenagel polycondensation between the dialdehyde **25** and the diacetonitrile **31** as the active methylene component in a mixture of THF and methanol by slowly adding Bu<sub>4</sub>NOH and methanol solution of potassium *tert*-butoxide. The synthetic route to this polymer is depicted in Scheme 16.



**Scheme 16:** Synthesis of **42** via Knoevenagel polycondensation route.

Carbonylmethylene condensation has been shown to proceed through three reaction steps shown in Equations 1-3 [55]. According to this mechanism, the equilibrium (1) may be displaced by mass-law action, and the reaction is retarded or even completely inhibited by added protonic acids and is accelerated by more or less strong bases (such as piperidine, sodium or quaternary ammonium hydroxides) or by the solvent effect. Knoevenagel condensation has been found kinetically controlled by reaction 1 and/or 2, reaction 3 being the faster of the sequence [55].



The chemical structures of the presented polymers were characterized by <sup>1</sup>H-NMR spectroscopy using very dilute CDCl<sub>3</sub> solutions of the polymers. Compared with the fine coupling peaks of the monomers, significant peak broadening of signal was observed for the polymers, which is attributed to the characteristics of high molecular weight polymers and is also indicative of the success in polymerization. Their band-gaps were also determined by cyclic voltammetry and UV-vis spectroscopy.

#### 4.3.2. Optical Properties

The optical properties of the conducting polymers are important to understand their basic electronic structure.  $\pi$ -Conjugation in the polymers is implied by their color and electronic spectra; thus spectroscopy is a powerful probe for characterizing the electronic processes.

UV-vis spectrum of copolymer **40** (Figure 4) in chloroform solution shows  $\pi$ - $\pi^*$  transitions of the polymer backbone occurring at 484 nm. This obvious relative spectral red shift, in both absorption and emission for this polymer, can be understood in terms of better conjugation as expected from the structural disparity and introduction of the

vinylene units in the backbone. The absorption spectrum of **40** in the film state shows an absorption maximum at 502 nm. The thin films were prepared by spin-coating a  $\text{CHCl}_3$  solution of the polymer on glass plates. In comparison with its solution, the absorption peak in the solid film is shifted by about 18 nm towards longer wavelength with a broadening peak shape. This suggests that the polymer chains are close enough in the film state to facilitate interchain energy transfer from fluorene segments to the lower band-gap co-monomer units. The solid state generally favors the formation of aggregates which benefits the polymer backbone in more planar conformation, which extends the conjugation length of the  $\pi$  electrons. Another possible reason is that in solution, the molecule can exist in the most stabilized state from the free rotation of the C-C bond, while in solid film the C-C bond cannot rotate freely. The broader peak means that there are more energy levels corresponding to the  $\pi$ - $\pi^*$  transitions. The more homogeneity of the polymer in the solution form leads to narrower absorption bands.

The normalized UV-vis absorption spectrum of polymer **41** in thin films prepared by spin-coating the polymer solutions in dichloromethane on glass plates is shown in Figure 5. The polymer exhibits absorption maximum at about 396 nm. This UV-vis absorption maximum is at a wavelength less than that of the copolymers **40** and **43**. This effect is due to the cyanovinylene linkage in the latter, which increases the conjugation length of the molecule, resulting in a red-shift in the absorption. The optical band-gap energies determined from the onsets of their absorptions are 2.0, 2.6 and 2.0 eV for copolymers **40**, **41** and **43**, respectively.

Figure 6 shows the UV-Vis absorption spectrum of polymer **43** in  $\text{CHCl}_3$  solution. In the absorption spectrum of **43** in  $\text{CHCl}_3$  solution, the  $\pi$ - $\pi^*$  transition maximum of the  $\pi$ -conjugated segments appear at 499 nm. The  $\lambda_{\text{max}}$  of **40** (484 nm) and **43** (499 nm) are higher than that of **41** (396 nm), resulting from the alternation of electron-rich and electron-deficient units, which is known to lower the optical band-gap for the copolymers **40** and **43**.

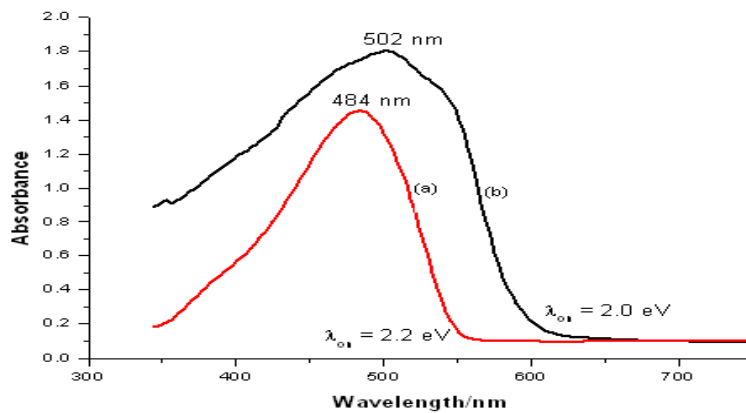


**Figure 4:** UV-vis absorption spectra of **40** in chloroform solution (a) and in thin films (b).

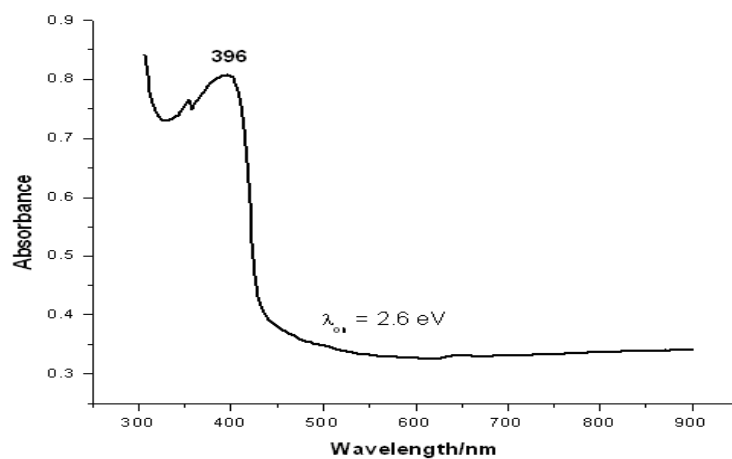


**Figure 5:** UV-vis absorption spectrum of **41** in thin films.

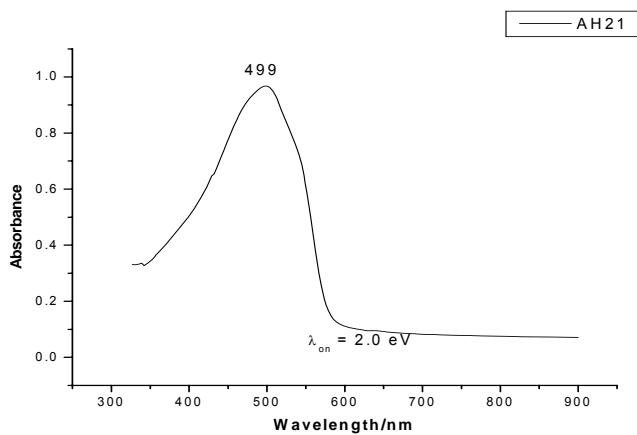


**Figure 6:** CHCl<sub>3</sub> solution UV-Vis absorption spectrum for **43**.

### 4.3.3. Electrochemical Properties

It is well known that the efficient injection and transporting balance of both holes and electrons are important parameters for the rational design of optimized OLEDs. In this regard, cyclic voltammetry (CV) has been employed and is considered to be an effective tool in investigating the electrochemical properties of conjugated compounds. The highest occupied molecular orbital (HOMO) and lowest unoccupied molecular orbital (LUMO) levels, which correspond to ionization potential ( $I_p$ ) and electron affinity ( $E_a$ ), can be estimated from the oxidation and reduction potentials revealed in cyclic voltammograms, respectively. The oxidation process corresponds to the removal of charge from the highest occupied molecular orbital (HOMO) band, whereas the reduction cycle corresponds to the filling of the energy state by electrons to the lowest unoccupied molecular orbital (LUMO) band. Therefore, the onset oxidation and reduction potentials were closely related to the energies of the HOMO and LUMO levels of an organic molecule and thus can provide important information regarding the magnitude of the energy gap. The onset potentials are determined from the intersection of the two tangents drawn at the rising current and baseline charging current of the CV traces. The polymer films coated on a glassy carbon working electrode, supported in 0.10 M *tetra-n*-butylammonium perchlorate ( $\text{Bu}_4\text{NClO}_4$ ) in anhydrous acetonitrile, were measured at a scanning rate of 100 mV/s. For polymer **40**, the onset of oxidation (*p*-doping) and reduction potentials (*n*-doping) are located at 1.21 V and -1.46 V (Figure 7); from these values the HOMO and LUMO energy levels are estimated to be 5.6 and 2.93 eV, respectively, according to the following empirical relationships proposed by Bredas [54].

$$I_p(\text{HOMO}) = -(E_{\text{onset,ox}} + 4.39) \text{ (eV)},$$

$$E_a(\text{LUMO}) = -(E_{\text{onset,red}} + 4.39) \text{ (eV)}$$

where  $E_{\text{onset,ox}}$  and  $E_{\text{onset,red}}$  are the onset potentials of oxidation and reduction, respectively.. The electrochemical band gap ( $E^{\text{el}}_g$ ) of the polymer is estimated from the HOMO and LUMO levels to be 2.6 eV, which is higher than the value obtained from the optical absorption spectra (2.0 eV). The difference may be caused by the interface barrier between the polymer film and the electrode surface. The electrochemical datum

may be the combination of the optical band gap and the interface barrier for charge injection, which makes it larger. However, the band gap obtained from the electrochemical method should be more meaningful as a reference for PLED device design due to similar configuration between the electrochemical system and practical PLED devices.

In the anodic scan, the onset of oxidation of polymer **41** (Figure 8) was estimated to be 1.3 V, which corresponds to HOMO energy level of 5.7 eV. The LUMO energy levels of the polymer can be calculated with the HOMO and optical band gap (2.6 eV) by assuming the optical and electrochemical band gaps to be approximately equal. The LUMO energy level of **41** was thus determined to be 3.1 eV.

The electrochemical response of polymer **43** was investigated by cyclic voltammetry (CV). As shown in Figure 9, the lowest unoccupied molecular orbital (LUMO) energy level of the polymer can be deduced as approximately 2.9 eV from the onset reduction potential of the voltammogram. A subsequent oxidative scanning gives a small anodic (or p-doping) peak at 1.30 V versus  $\text{Ag}^+/\text{Ag}$ . The highest occupied molecular orbital (HOMO) level of **43** is estimated at about 5.7 eV from the onset position of the p-doping peak. The electrochemically estimated band gap ( $E_g^{\text{el}} = 2.8$  eV) do not agree with that evaluated from the onset position of the UV-vis absorption peak (2.0 eV).

The variation in the band-gap energy level of the polymers is a result, not only of the introduction of cyano groups, but also as a function of effective conjugation length caused by the structural changes in the backbone.

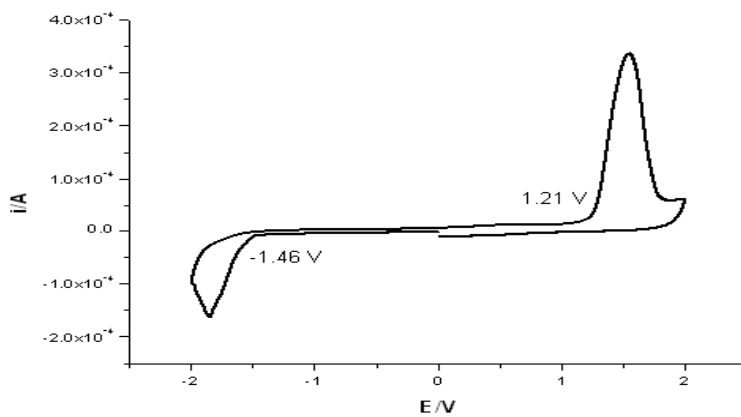


**Figure 7:** Cyclic voltammogram for copolymer 40.

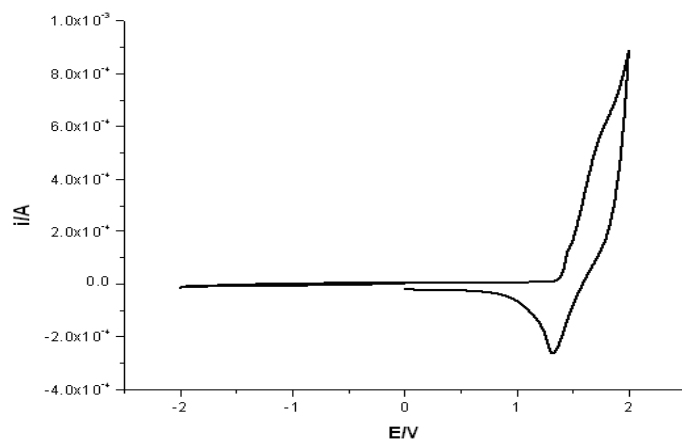


**Figure 8:** Cyclic voltammogram for copolymer 41.

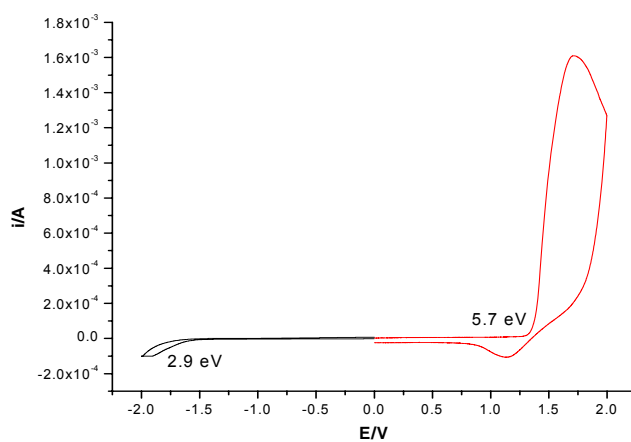


**Figure 9:** Cyclic voltammogram of copolymer 43 films on glassy carbon plates.

## 5. Conclusion

Fluorene as a monomer offers a number of advantages, the most significant being its ability to impart solubility while maintaining a high degree of delocalization. LED devices with fluorene-based polymers appear to have electrons as the majority carrier and their performance is markedly improved by incorporating electron deficient co-monomers such as cyano-substituted olefins into the polymer chain.

The modified Suzuki polymerization process can be used to synthesize homopolymers as well as alternating copolymers by simply using fluorene-2,7-diboronate as the building block to react with selected aromatic dibromide(s), the reaction uses catalytic amount of Pd(0) with sodium carbonate as a base. The reaction conditions are mild and the polymers synthesized are pure.

Cyanovinylene polymers based on PF derivatives are attractive targets because soluble polymers can be realized through Knoevenagel polymerization route to give regiosymmetric polymers. An advantage of the Knoevenagel route is that it gives polymers in the neutral form without the use of metal catalysts that could potentially be trapped in the polymer.

We have successfully prepared fluorene-based alternating copolymers that have luminescent properties from blue to red. The resulting polymers exhibited good solubility in chloroform. The UV-Vis absorption spectra of copolymers **40**, **41** and **43** showed absorption maxima at the wavelengths of 484, 396 and 499 nm, respectively. The optical band-gap onsets were also determined to be 2.0, 2.6 and 2.0 eV, for polymers **40** and **41**, respectively. Cyclic voltammetry was employed to estimate their HOMO and LUMO energy levels. The electrochemical energy band-gaps, which can be calculated from the HOMO/LUMO energy levels, for **40**, **41** and **43**, were found to be 2.6, 2.6 and 2.8 eV, respectively. Further studies on physical properties such as molecular weight determination, FTIR studies, thermal properties, etc., should be made to fully characterize the polymers.

## 6. Experimental Section

### 6.1. Materials and Methods

All of the monomers prepared in the course of the synthetic work were purified and characterized by NMR techniques and all of the polymers were characterized by CV, UV-Vis and NMR techniques.  $^1\text{H}$ -NMR and  $^{13}\text{C}$ -NMR spectra were recorded on a Bruker Avance 400 spectrometer at 400.13 and 100.6 MHz, respectively, with  $\text{CDCl}_3$  as a solvent.  $^1\text{H}$  and  $^{13}\text{C}$  chemical shifts are reported in ppm downfield from tetramethylsilane (TMS) reference using the residual protonated solvent resonance as an internal standard. The coupling constants are reported in hertz (Hz). Splitting patterns are designated as s (singlet), d (doublet), t (triplet), bs (broad singlet), bd (broad doublet), m (multiplet), and bm (broad multiplet). Analytical thin layer chromatography (TLC) was performed on Merck silica gel plates. Visualization was accomplished by an ultraviolet lamp (254 and 365 nm). Silica gel column chromatography was carried out with silica gel (230-400 mesh). All starting materials were purchased from commercial sources (Aldrich, BDH, Riedel de Haën) and were used without further purification. All the solvents used for column chromatography and extractions were distilled before use. Cyclic voltammograms (CVs) were recorded on a BASi Epsilon-EC potentiostat using platinum electrodes at a scan rate of  $100 \text{ mV}\cdot\text{s}^{-1}$  and a  $\text{Ag}/\text{Ag}^+$  (0.10 M of  $\text{AgNO}_3$  in acetonitrile) reference electrode in an anhydrous and argon-saturated solution of 0.1 M of tetrabutylammonium tetrachloroborate ( $\text{Bu}_4\text{NCl}_4$ ) in acetonitrile. UV-visible absorption spectra were taken using a Varian Cary 500 UV-VIS-NIR spectrophotometer. Melting points were measured using Mettler Toledo FP82HT hot stage with FP90 central processor and LEICA GALEN<sup>TM</sup> III microscope apparatus and are uncorrected.

### 6.2. Monomer Synthesis

#### 6.2.1. Synthesis of 2,7-dibromofluorene (6)

Fluorene (15 g, 0.09 moles) was dissolved in 1:1 mixture of chloroform and acetic acid (100mL). After complete dissolution, the solution was cooled in an ice-water bath and

bromine (23.15 mL, 72.19 g, 0.451 moles) was added from a pressure equalizing dropping funnel over a time of 20 minutes. The mixture was then stirred for additional one hour. The reaction was then quenched with a 10% solution of sodium metabisulfite. The resulting precipitate was filtered under suction and washed with isopropyl alcohol giving yellowish solid. The mother liquor was then taken and aqueous NaOH was added to it to neutralize the acetic acid. The isopropyl alcohol used for washing the precipitate was removed by using rotary evaporator. The remaining solution was extracted with chloroform and washed with brine and dried over anhydrous sodium sulphate. After filtration, the solvent was removed under vacuum and refrigerated to give some yellowish solid. The solid materials collected were then combined and recrystallized from isopropyl alcohol. 23.4 g (80%) yield was obtained after the recrystallization. Mp. 154-156<sup>o</sup>C; <sup>1</sup>H NMR (400 MHz, CDCl<sub>3</sub>) δ(ppm): 7.64 (bd, 2H, *J* = 1.0 Hz), 7.56 (d, 2H, *J* = 8.1 Hz), 7.49 (dd, 2H, *J* = 8.1 and 1.6 Hz), 3.80 (s, 2H); <sup>13</sup>C NMR (100.6 MHz, CDCl<sub>3</sub>) δ(ppm): 144.8, 139.7, 130.1, 128.3, 121.2, 120.9, and 36.6.

### 6.2.2. Synthesis of 2,7-dibromo-9,9-didodecylfluorene (24)

2,7-Dibromofluorene (10.0 g, 30.9 mmol) was dissolved in a two-phase system composed of toluene (100 mL) and sodium hydroxide (50%w/w) (100 mL) aqueous solution using tetrabutylammonium bromide (1.0 g, 2.70 mmol) as the phase transfer catalyst at 60 °C. 1-Bromododecane (15.37 g, 14.81 mL, 61.8 mmol) was added to the mixture from a pressure equalizing dropping funnel with in 10 minutes. The progress of the reaction was checked with TLC using 10% solution of ethyl acetate in hexane. After refluxing for 9 hours, the reaction mixture was diluted with ethyl acetate and the organic layer was extracted. The extract was washed with 2M aqueous HCl solution. The separated organic layer was dried over anhydrous sodium sulfate, and the solvent was evaporated by using rotary evaporator giving oily crude product. The attempt to purify the crude product by crystallization from methanol and further recrystallization from isopropyl alcohol was unsuccessful. The crude oil was then purified by column chromatography on silica gel using hexane:ethyl acetate (9:1) solvent system giving 13.5 g (66.3%) of the desired pure compound and two other byproducts. <sup>1</sup>H NMR (400

MHz, CDCl<sub>3</sub>)  $\delta$ (ppm): 7.54 (d, 2H,  $J$  = 0.91 Hz), 7.52(dd, 2H,  $J$  = 8.4 and 0.91 Hz), 7.50(d, 2H,  $J$  = 8.4 Hz), 1.95 (t, 4H), 1.40-0.90 (m, 36H), 0.80 (t, 6H), 0.65 (m, 4H); <sup>13</sup>C NMR (100.6 MHz, CDCl<sub>3</sub>)  $\delta$ (ppm): 152.6, 139.1, 130.2, 126.2, 121.5, 121.1, 55.7, 40.2, 33.9, 31.9, 29.9, 29.7, 29.6, 29.5, 29.4, 29.2, 28.8, 23.7, and 14.2.

### 6.2.3. Synthesis of 9,9-didodecylfluorene-2,7-dicarbaldehyde (25)

*n*-BuLi (8.72 mL, 2.5 M solution in hexane, 2.8 mmol) was added dropwise into dry THF solution containing 9,9-didodecyl-2,7-dibromofluorene (7.2 g, 10.9 mmol) at -78<sup>o</sup>C. After addition of *n*-BuLi was completed, DMF (1.594 g, 1.68 mL, 21.8 mmol) was added dropwise into the solution. The resulting mixture was stirred by gradually increasing the temperature to room temperature. After stirring for about 3 hours, about 100 mL of distilled water was poured into the reaction mixture and stirred. The ether layer was separated from the aqueous layer by using separatory funnel, washed twice with distilled water and the organic layer was then dried over anhydrous sodium sulphate. The ether was then removed by vacuum evaporation giving oily liquid as mixture of compounds. The resulting impure product was then purified by column chromatography over silica gel in 9:1 hexane:ethyl acetate solvent system to yield 4.4 g (72.3%) the desired pure compound. Mp. 47-49<sup>o</sup>C; <sup>1</sup>H NMR (400 MHz, CDCl<sub>3</sub>,  $\delta$ (ppm)): 10.10 (s, 2H, -CHO), 7.96 (d, 2H,  $J$  = 0.4 Hz), 7.94(dd, 2H,  $J$  = 3.4 and 1.0 Hz), 7.91(d, 2H,  $J$  = 1.2 Hz), 2.10 (t, 4H), 1.30-0.90 (m, 40H, R-CH<sub>2</sub>- of the hexyl group at the 9 position of fluorene), 0.80 (m, 6H, - CH<sub>3</sub>); <sup>13</sup>C NMR (100.6 MHz, CDCl<sub>3</sub>)  $\delta$ (ppm): 192.1, 152.9, 145.6, 136.5, 130.3, 123.4, 121.3, 55.6, 40.0, 31.9, 29.8, 29.6, 29.5, 29.4, 29.3, 29.2, 29.1, 23.8, 22.7, and 14.1.

### 6.2.4. Synthesis of 1,4-bis(hexyloxy)benzene (29)

Excess K<sub>2</sub>CO<sub>3</sub> (100 g, 0.724 mol) was added to the mixture of hydroquinone (20.0 g, 0.182 mol) and N,N-dimethylformamide (about 100 mL) in a three necked round-bottomed flask. The reaction mixture was stirred and 1-bromohexane (60.37 g, 51.33 mL, 0.37 mol) was added using a pressure equalizing dropping funnel when the

reaction temperature reached 100<sup>0</sup>C. The reaction mixture was heated for about 10 hours following the reaction progress by TLC using diethyl ether and hexane solvent composition in 3:2 ratio. The reaction mixture was then cooled to room temperature and filtered by suction to remove the excess (unreacted) potassium carbonate. The potassium carbonate residue was washed several times with diethyl ether. The solid compound which crystallized in the filtrate during filtration was then filtered by suction and collected. The remaining filtrate was acidified with 2M aq. HCl solution and then extracted with diethyl ether. The extract was washed with 2M aq. NaOH solution twice and then with brine (saturated NaCl solution) three times. The organic layer was again washed with distilled water and then dried over anhydrous sodium sulphate and filtered using fluted filter paper. The solvent was removed by rotary evaporator giving oily product which was converted to solid upon standing in a refrigerator for some time. The combined solid products were then recrystallized from small amount of isopropyl alcohol. 32.0 g (63.3%) of pure product was obtained after the recrystallization. Mp. 39-43<sup>0</sup>C; <sup>1</sup>H NMR (400 MHz, CDCl<sub>3</sub>) δ(ppm): 6.95 (s, 4H), 3.95 (m, 4H), 1.75 (m, 4H), 1.49 (m, 4H), 1.45-1.25 (m, 8H), 0.90 (t, 6H); <sup>13</sup>C NMR (100.6 MHz, CDCl<sub>3</sub>) δ(ppm): 153.2, 115.4, 68.6, 31.7, 29.4, 25.8, 22.7, and 14.1.

#### 6.2.5. Synthesis of 1,4-bis(chloromethyl)-2,5-bis(hexyloxy)benzene (30)

1,4-Bis(hexyloxy)benzene (**29**) (21.0 g, 0.075 mol) was added to excess HCl (36%) (about 100 mL) and excess 37% formaldehyde solution (about 100 mL) in 1,4-dioxane solvent (about 100 mL). The mixture was heated at 90<sup>0</sup>C for three days. The resulting mixture was cooled and the waxy solid residue was separated from the mother liquor by using suction filtration. The residue was washed with distilled water twice. About 100 mL of hexane was added to the waxy solid and heated under reflux until the residue had been dissolved. The hot solution was poured in to ice-cold methanol (about 200 mL) and the resulting white solid precipitate was filtered by suction. The residue was washed with methanol (about 50 mL) and then dried to afford 15.3 g of white solid. The mother liquor obtained during filtering the waxy residue was also extracted with ethyl acetate and the extract was washed with distilled water (3X). The solvent was then removed

under reduced pressure giving oily product which solidified upon standing in a refrigerator for some time. The resulting crude solid was dissolved in a small amount of hot hexane. The hot solution was then poured in ice-cold methanol and the resulting white solid was filtered under suction. 2.8 g of the desired pure compound was obtained from this step making the overall yield to be 18.1 g (63.9%). Mp. 58-61<sup>0</sup>C; <sup>1</sup>H NMR (400 MHz, CDCl<sub>3</sub>) δ(ppm): 6.95 (s, 2H), 4.65 (s, 4H), 4.05 (t, 4H), 1.80 (m, 4H), 1.55 (m, 4H), 1.45-1.25 (m, 8H), 0.95 (t, 6H); <sup>13</sup>C NMR (100.6 MHz, CDCl<sub>3</sub>) δ(ppm): 150.6, 127.1, 114.3, 69.1, 41.4, 31.5, 29.3, 25.7, 22.6, 14.0.

#### 6.2.6. Synthesis of 1,4-bis(cyanomethyl)-2,5-bis(hexyloxy)-benzene (31)

Finely crushed sodium cyanide (6.0 g, 0.123 mol) and 1,4-bis(chloromethyl)-2,5-bis(hexyloxy)benzene (**30**) (11.5 g, 0.031 mol) were dissolved in anhydrous DMF (80 mL). The mixture was heated at 110 °C for 2 h. After cooling, the mixture was poured into 200 mL of ice-water, upon which a brown solid precipitate was formed. The solid was collected by filtration and washed on the filter with hexane and ice water. 9.20 g (84.2%) yield of the desired compound was obtained as an off white solid after recrystallization from hexane. Mp. 96-97.5<sup>0</sup>C; <sup>1</sup>H NMR (400 MHz, CDCl<sub>3</sub>) δ(ppm): 6.95 (s, 2H), 4.00 (t, 4H), 3.74 (s, 4H), 1.80 (m, 4H), 1.52 (m, 4H), 1.45-1.25 (m, 8H), 0.95 (t, 6H); <sup>13</sup>C NMR (100.6 MHz, CDCl<sub>3</sub>) δ(ppm): 150.1, 119.2, 117.8, 112.7, 69.0, 31.5, 29.2, 25.7, 22.6, 18.6, 14.0.

#### 6.2.7. Synthesis of 2,5-dihexyloxy-1,4-bis{2-(4'-bromothiényl)-2-cyanovinyl}-benzene (32)

A mixture of 1,4-bis(cyanomethyl)-2,5-bis(hexyloxy)-benzene (**31**) (1.8 g, 5.06 mmol) and 2-bromothiophene-5-carboxaldehyde (1.93 g, 1.27 mL, 10.12 mmol) were dissolved in about 50 mL of MeOH. Potassium *tert*-butoxide (4.30 g, 48.30 mmol) was added as a solid, and the resulting mixture was stirred for 24 h at reflux temperature. The progress of the reaction was checked by TLC using dichloromethane and hexane solvent mixture

in 3:2 compositions. Upon cooling, a bright yellow solid precipitated, which was then filtered by suction and washed with cold methanol. 2.45 g (69% yield) of the desired compound was obtained after recrystallization from isopropyl alcohol. Mp: 155–157<sup>o</sup>C; <sup>1</sup>H NMR (CDCl<sub>3</sub>, 400 MHz) δ(ppm): 7.98 (s, 2H), 7.30 (s, 2H), 7.13 (d, 2H, *J* = 3.95 Hz), 7.09 (d, 2H, *J* = 4.05 Hz), 4.05 (t, 4H, *J* = 6.3 Hz), 1.90 (m, 4H), 1.50 (m, 4H), 1.40–1.25 (m, 8H), 0.95 (t, 6H, *J* = 6.84 Hz); <sup>13</sup>C NMR (100.6 MHz, CDCl<sub>3</sub>) δ(ppm): 150.6, 139.7, 138.2, 133.0, 130.6, 123.8, 118.5, 118.3, 114.1, 104.9, 69.7, 31.6, 29.2, 25.8, 22.6, and 14.1.

### 6.3.8. Synthesis of 2,7-bis (4,4,5,5-tetramethyl-1,3,2-dioxaborolane)-9,9-didodecyl fluorene (7)

To a solution of 2,7-dibromo-9,9-didodecyl fluorene (4.25 g, 6.44 mmol) in anhydrous THF (about 50 mL) at -78<sup>o</sup>C, *n*-BuLi (5.2 mL, 2.5 M solution in hexane, 1.30 mmol) was added by a syringe. The mixture was then stirred at -78<sup>o</sup>C for about 15 minutes. 2-Isopropoxy-4,4,5,5-tetramethyl-1,3,2-dioxaborolane (2.47 g, 1.30 mmol, 2.71 mL) was then added rapidly to the reaction mixture and the resulting solution was warmed to room temperature and then stirred for 24 h. About 25 mL of saturated ammonium chloride solution was added to the reaction mixture and stirred for some time. The resulting mixture was then extracted with diethyl ether. The organic extracts were washed with distilled water (3X), dried over anhydrous Na<sub>2</sub>SO<sub>4</sub> and filtered by gravity filtration to separate the solution from the sodium sulphate. After filtration, the solvent was removed by rotary evaporation to give a crude product contaminated with small amount of impurities as evidenced by analytical thin layer chromatography. The residue was then purified by column chromatography on silica gel using 2% solution of ethyl acetate in hexane to afford compound **7** (2.5 g, 51.5%) in pure form as a pale-yellow solid. Mp: 127-129<sup>o</sup>C; <sup>1</sup>H-NMR (CDCl<sub>3</sub>, 400 MHz) δ(ppm): 7.84 (dd, *J* = 7.6 and 0.8 Hz, 2H, H-3, H-6), 7.78 (brs, 2H, H-1, H-8), 7.75 (*d*, *J* = 7.6 Hz, 2H, H-4, H-5), 2.00 (m, 4H, H-1'), 1.40 (s, 24H, H-6'' to H-9''), 1.30-0.85 (m, 44H, H-2' to H-11'), 0.80 (*t*, 6H, H-12'); <sup>13</sup>C-NMR (CDCl<sub>3</sub>, 100.6 MHz) δ(ppm): 150.4, 143.9, 133.7, 128.9, 119.4, 83.7, 55.2, 40.1, 31.9, 30.0, 29.7, 29.6, 29.4, 29.3, 26.9, 25.0, 24.8, 23.7, 22.7, 14.2.

### 6.3. Polymer Synthesis

#### 6.3.1. Synthesis of poly[9,9-dioctyl-9H-fluorene-2,7-diyl-alt-2,5-dihexyloxy-1,4-bis(2-thienyl-2-cyanovinyl)benzene] (40)

2,5-Dihexyloxy-1,4-bis{2-(4'-bromothieryl)-2-cyanovinyl}benzene (**32**) (200 mg, 0.285 mmol), 2,7-bis(4,4,5,5,-tetramethyl-1,3,2-dioxaborolan-2-yl)-9,9-dioctylfluorene (**34**) (182.9 mg, 0.285 mmol) and tetrakis(triphenylphosphine)palladium [Pd(PPh<sub>3</sub>)<sub>4</sub>] (9.88 mg, 0.009 mmol) were dissolved in toluene (10 mL) and stirred under nitrogen atmosphere at a temperature of 110<sup>0</sup>C for about 15 minutes. A 20% aqueous solution of Et<sub>4</sub>NOH (0.86 mL) was then added to the mixture and the reflux was allowed to go on for additional 1 h and 45 min until gel formation was evidenced. By the end of the second hour, bromobenzene (0.05 mL) was added and refluxing was extended for a further of 1 h and phenylboric acid (48.0 mg) dissolved in toluene (1 mL) was added to the reaction mixture. The refluxing was then carried out for the final 1 h. The mixture was then allowed to cool down to room temperature and was poured into methanol to precipitate the polymer. The resulting solid was then filtered off by membrane filtration, dried, dissolved in chloroform, and washed with concentrated ammonia solution (3X) and distilled water (4X). After washing, the organic layer was separated and concentrated. The concentrated chloroform solution was slowly added into methanol and the precipitate was then separated from the mother liquor by membrane filtration, washed with methanol (3X), and then dried. The resulting solid was purified by Soxhlet extraction first with diethyl ether to isolate low molecular weight oligomers and then with chloroform to give the pure polymer of the desired degree of polymerization. The chloroform extract was then collected, concentrated, precipitated out by slowly adding into methanol. The precipitate was then filtered off, washed with methanol and dried. The yield of the resulting red polymer was 0.230 g (80%).

### 6.3.2. Synthesis of poly(9,9-didodecyl-9H-fluorene-2,7-diyl-alt-9,9-dibenzyl-9H-fluorene-2,7-diyl) (41)

Polymer **41** was synthesized using a similar procedure as described for the synthesis of **40**. Microgel formation was evidenced 45 minutes after the starting of the reaction. 9,9-Didodecyl-2,7-dibromofluorene (**24**) (231.6 mg, 0.351 mmol), 2,7-bis(4,4,5,5-tetramethyl-1,3,2-dioxaborolan-2-yl)-9,9-dibenzyl-9H-fluorene (**35**) (200 mg, 0.351 mmol), Pd(PPh<sub>3</sub>)<sub>4</sub> (12.17 mg, 0.011 mmol), a 20% aqueous solution of Et<sub>4</sub>NOH (1.06 mL), bromobenzene (0.06 mL) and phenylboric acid (59.2 mg) dissolved in toluene (1 mL) were used to finally obtain a white solid in 155 mg (54.2%) yield.

### 6.3.3. Synthesis of poly[(9,9-didodecyl-9H-fluorene-2,7-diyl)(1-cyanoethene-1,2-diyl)(2,5-bis(hexyloxy)phenylene)(2-cyanoethene-1,2-diyl)] (42)

To a stirred solution of 9,9-didodecylfluorene-2,7-dicarbaldehyde (**25**) (156.1 mg, 0.281 mmol) and 1,4-bis(cyanomethyl)-2,5-bis(hexyloxy)benzene (**10**) (100 mg, 0.281 mmol) in THF (20 mL) and MeOH (10 mL) at reflux (65 °C) under nitrogen was added a 40% aqueous solution of Bu<sub>4</sub>NOH (0.30 mL). After refluxing for about 12 h, 1M solution of potassium *tert*-butoxide in methanol was added to the mixture. After refluxing for additional 12h, the reaction mixture was treated with MeOH and distilled water mixture and refrigerated for a time of about 30min. The resulting solid obtained was then filtered off by membrane filtration technique.

### 6.3.4. Synthesis of poly[9,9-didodecyl-9H-fluorene-2,7-diyl-alt-2,5-dihexyloxy-1,4-bis(2-thienyl-2-cyanovinyl)benzene] (43)

Polymer **43** was synthesized using a similar procedure as described for the synthesis of **40** and **41**. Microgel formation was evidenced 1 h and 45 min after the addition of the base to the reaction mixture. 2,5-Dihexyloxy-1,4-bis{2-(4'-bromothieryl)-2-cyanovinyl}benzene (**32**) (200 mg, 0.285 mmol), 2,7-bis(4,4,5,5-tetramethyl-1,3,2-dioxaborolan-2-yl)-9,9-didodecyl-9H-fluorene (**35**) (215 mg, 0.285 mmol), Pd(PPh<sub>3</sub>)<sub>4</sub> (9.9 mg, 0.0086 mmol), a 20% aqueous solution of Et<sub>4</sub>NOH (0.86 mL), bromobenzene (0.05 mL) and phenylboric acid (48.0 mg) dissolved in toluene (1 mL) were used to finally obtain the title polymer in .....% yield.

## 7. References

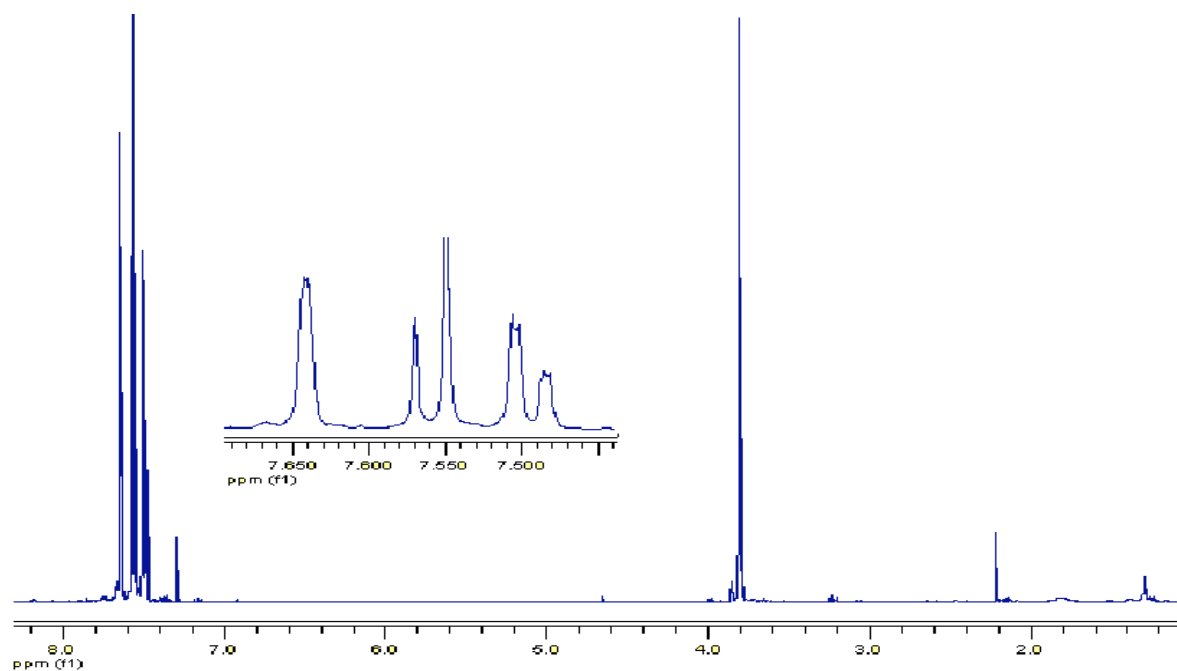
1. Patil, A. O.; Heeger, A. J.; Wudl, F. *Chem. Rev.* **1988**, *88*, 183.
2. Roncali, J. *Chem. Rev.* **1992**, *92*, 711.
3. Christopher, A.; Thomas; Kyukwan, Z.; Khalil, A.; Peter, J.; John, R. *J. Am. Chem. Soc.* **2004**, *126*, 16440.
4. Thompson, B. C.; Kim, Y.G.; McCarley, T.D.; Reynolds, J.R. *J. Am. Chem. Soc.* **2006**, *128*, 12714.
5. Potember, R. S.; Hoffman, R. C; Hu, H. S.; Cocchiaro. J. E.; Viands, C. A.; Murphy, R. A.; Poehler, T. O. *Polymer.* **1987**. *28*, 574..
6. Yoshino, K. *Synth. Met.* **1989**, *28*. 669.
7. Bernius, M.T.; Inbasekaran, M.; O'Brien, J.; Weishi, W. *Adv. Mater.* **2000**, *12*, 1737.
8. Mingliang, S.; Qiaoli, N.; Renqiang, Y.; Bin, D.; Ransheng, L.; Wei, Y.; Junbiao, P.; Yong, C. *Eur. Polym. J.* **2007**, *43*, 1916.
9. Taek, A.; Hong-Ku, S. *Macromol. Chem. Phys.* **2001**, *202*, 3180.
10. Bin, L.; Wang-Lin, Y.; Yee-Hing, L.; Wei, H. *Chem. Mater.* **2001**, *13*, 1984.
11. Arc, S.; Donal, D.C.; Marilu, A.; Mattijs, K.; Arris, A.; Martin, G. *Adv. Funct. Mater.* **2004**, 765.
12. Redecker, M.; Bradley, D.; Inbasekaran, M.; Wu, W.W.; Woo, E.P. *Adv. Mater.* **1999**, *11*, 241.
13. Heliotis, G.; Xias, R.;Turnbull, G.; Andrew, P.; Barnes, W.; Samuel, L.; Bradley, D. *Adv. Funct. Mater.* **2004**, *14*, 91.
14. Arno, K.; Andrew, C.; Grimsdale; Andrew, B. H. *Angew. Chem. Int. Ed.* **1998**, *37*, 402.
15. Taek, S. L.; Jongho, N.; Jin, K. L.; Won, H. P. *Opt. Mater.* **2002**, *21*, 429.
16. Silva, A.P.; Gunaratne, H.Q.N.; Gunnlaugsson, T.; Huxely, A.J.M.; McCoy, C.P.; Rademache, J.T.; Rice, T.E. *Chem. Rev.* **1997**, *97*, 1515.
17. Smith, M.B.; March, J. *March's Advanced Organic Chemistry* 6<sup>th</sup>ed., John Wiley and Sons, Inc., United States of America, **2007**, 63.
18. Yadessa Melaku , *MSc Project Paper*, Department of Chemistry, Addis Ababa

University, Ethiopia, **2007**.

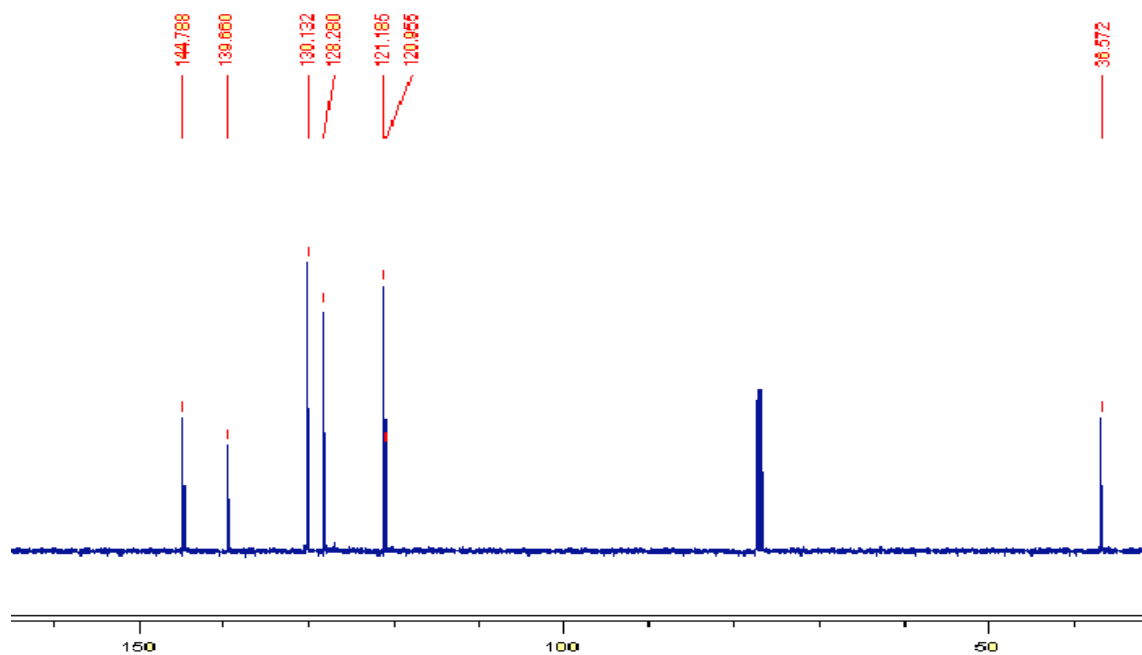
19. Zekarias Yacob, *Synthesis of some Fluorene co-polymers*, MSc Thesis, Addis Ababa University, Addis Ababa, Ethiopia, **2004**.
20. Lambert, J.B.; Shurvell, H.F.; Verbit, L.; Cooks, R.G.; Stout, G.H. *Organic Structural Analysis*, Macmillan Publishing Co., Inc., New York, **1976**, 33.
21. Andrew, C. G.; Khai, L. C.; Rainer, E. M.; Pawel, G.; Andrew, B. H. *Chem. Rev.* **2009**, *109*, 897.
22. Grell, M.; Bradley, D. D. C.; Ungar, G.; Hill, J.; Whitehead, K. S. *Macromolecules* **1999**, *32*, 5810.
23. Ranger, M.; Leclerc, M. *Can. J. Chem.* **1999**, *76*, 1571.
24. Sung-Hyun J.; Dong, Y.; Hyun-Nam, C.; Dong, H. *J. Polym. Sci. Part A: Polym. Chem.* **2006**, *44*, 1189.
25. Maxime, R.; Dany, R.; Mario, L. *Macromolecules* **1997**, *30*, 7686.
26. Chuanjun, X.; Rigoberto, C. A. *Macromolecules* **2001**, *34*, 5854.
27. Chang, S.W.; Hong, J.M.; Hong, J.W.; Choi, H.N. *Polym. Bull.* **2001**, *47*, 231.
28. Ullrich, S.; Emil, J.W.L. *Adv. Mater.* **2002**, *14*, 477.
29. Peng, C.; Guizhong, Y.; Tianxi, L.; Tingcheng, L.; Min, W.; Wei, H. *Polym. Int.* **2006**, *55*, 473.
30. Qibing, P.; Yang, Y. *J. Am. Chem. Soc.* **1996**, *118*, 7416.
31. Youngeup, J.; Jeongmin, J.; Jinwoo, K.; Sungeun, L.; Jin, Y.K.; Sung, H. P.; Sung-Ho, J.; Kwanghee, L.; Hongsuk, S. *Macromolecules* **2003**, *36*, 6970
32. Hemali, P.; Rathnayake, A. C.; Zeynep, D.; Pau, M. L.; Frank, E. K. *Adv. Funct. Mater.* **2007**, *17*, 115
33. Sung-Ho, J.; Seung-Yun, K.; Mi-Yeon, K.; Yoon, U. C. *Macromolecules* **2003**, *36*, 3841.
34. Nam, S.C.; Do-Hoon, H.; Jeong-Ik, L.; Byung-Jun, J.; Hong-Ku, S. *Macromolecules* **2002**, *35*, 1224.
35. Bernius, M.; Inbasekaran, M.; Woo, E.; Weishi, W.; Wujkowski, L. *J. Mater. Sci.: Materials in Electronics* **2000**, *11*, 111.
36. Ryan, M. W.; Robert, N. B.; Alice, M. S.; Eveline, M. van der Aa; John, R. R.; *Macromolecules* **2009**, *42*, 1445.

37. Mihaela, C.; Anna, E. J.; Itaru, O.; Richard, D. M. *Macromolecules* **2009**, *42*, 30.
38. Krasovskiy, A.; Knochel, P. *Angew. Chem., Int. Ed.* **2004**, *43*, 3333.
39. Inoue, A.; Kitagawa, K.; Shinokubo, H.; Oshima, K. *J. Org. Chem.* **2001**, *66*, 4333.
40. Iida, T.; Wada, T.; Tomimoto, K.; Mase, T. *Tet. Lett.* **2001**, *42*, 4841.
41. Liu, B.; Yu, W.; Lai, Y.; Huang, W. *Chem. Mater.* **2001**, *13*, 1984.
42. Zhonghua, P.; Ali, R.; Luping, Y. *J. Am. Chem. Soc.* **1997**, *119*, 4622.
43. Bunz, U. H.F. *Chem. Rev.* **2000**, *100*, 1605.
44. Prasad, T.; Mansour, A.; Ramanan, K.; Sukon, P.; Paralee, W.; Derek, P.; Timothy, F.; Rigoberto, A. *Macromolecules* **2006**, *39*, 3848.
45. Wu, F. I.; Shih, P. I.; Shu, C. F.; Tung, Y. L.; Chi, Y. *Macromolecules* **2005**, *38*, 9028.
46. Martin, G.; Emil, J. W. L.; Ullrich, S. *Macromolecules* **2003**, *36*, 4236.
47. Ding, L.; Karasz, F. E.; Lin, Z.; Zheng, M.; Liao, L.; Pang, Y. *Macromolecules* **2001**, *34*, 9183.
48. Xia, C.; Advincula, R. *Macromolecules* **2001**, *34*, 6922.
49. Chen, X. L.; Lovinger, A. J.; Bao, Z. N.; Sapjeta, J. *Chem. Mater.* **2001**, *13*, 1341.
50. Silverstein, R.M.; Webster, F.X. *Spectrometric Identification of Organic Compounds*, 6<sup>th</sup>ed., State University of New York, **1998**, 232.
51. Lu, H. H.; Liu, C. Y.; Chang, C. H. *Adv. Mater.* **2007**, *19*, 2574.
52. Emil, J. W. L.; Roland, G.; Patricia, S. F.; Ullrich, S. *Adv. Mater.* **2002**, *14*, 374.
53. Setyesh, S.; Grimsdale, A. C.; Weil, T.; Enkelmann, V.; Müllen, K.; Meghdadi, F.; List, E. J. W.; Leising, G. *J. Am. Chem. Soc.* **2001**, *123*, 946.
54. Chen, Z. K.; Huang, W.; Wang, L.H.; Kang, E. T.; Chen, B. J.; Lee, C. S.; Lee, S. T. *Macromolecules* **2000**, *33*, 9015.
55. Boucard, V; Ade, D; Siove, A. *Macromolecules* **1999**, *32*, 4729 and the references cited there in.

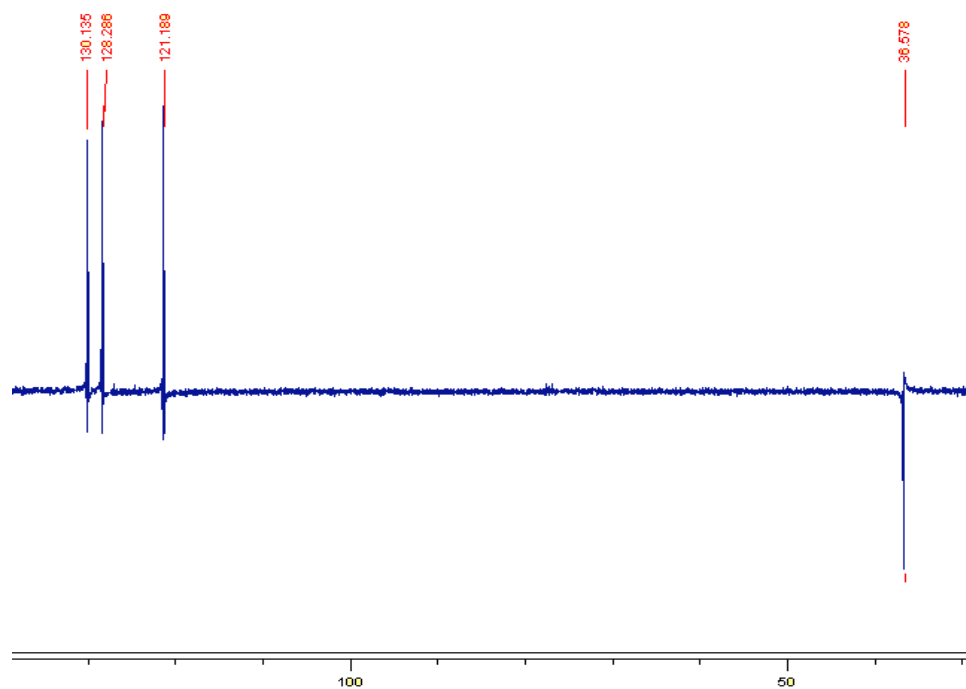
## 8. Appendices



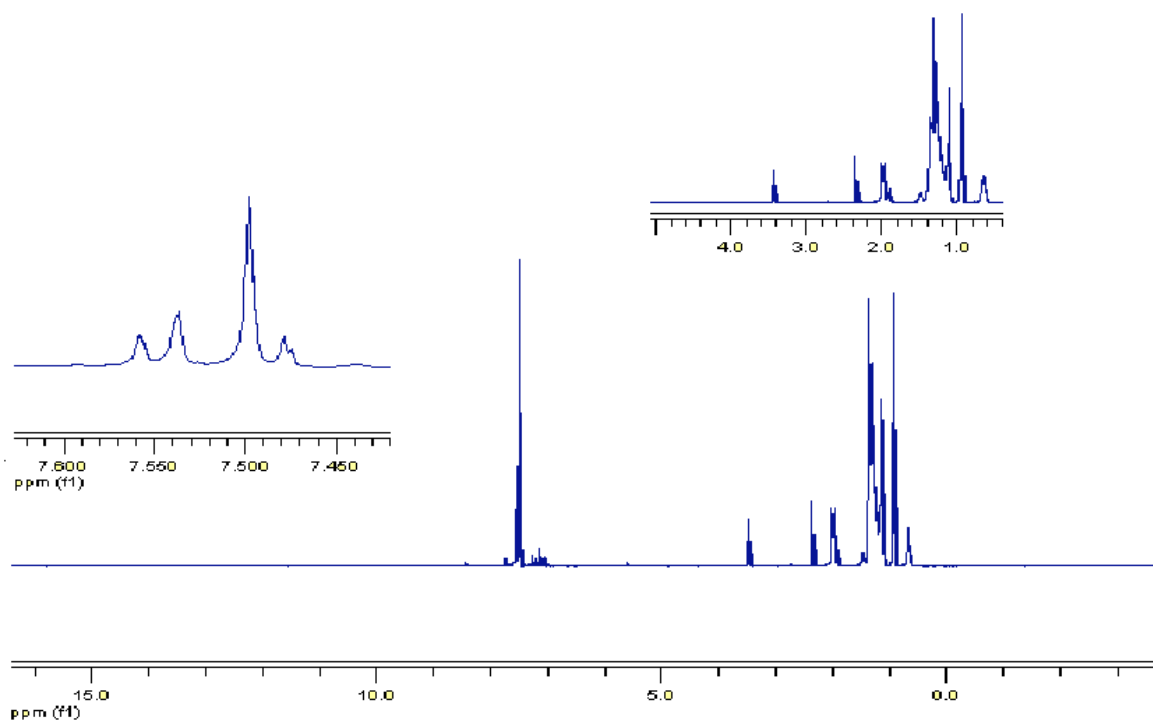
**Appendix 1:**  $^1\text{H-NMR}$  (400 MHz,  $\text{CDCl}_3$ ,  $\delta(\text{ppm})$ ) spectrum of 2,7-dibromofluorene (**6**).



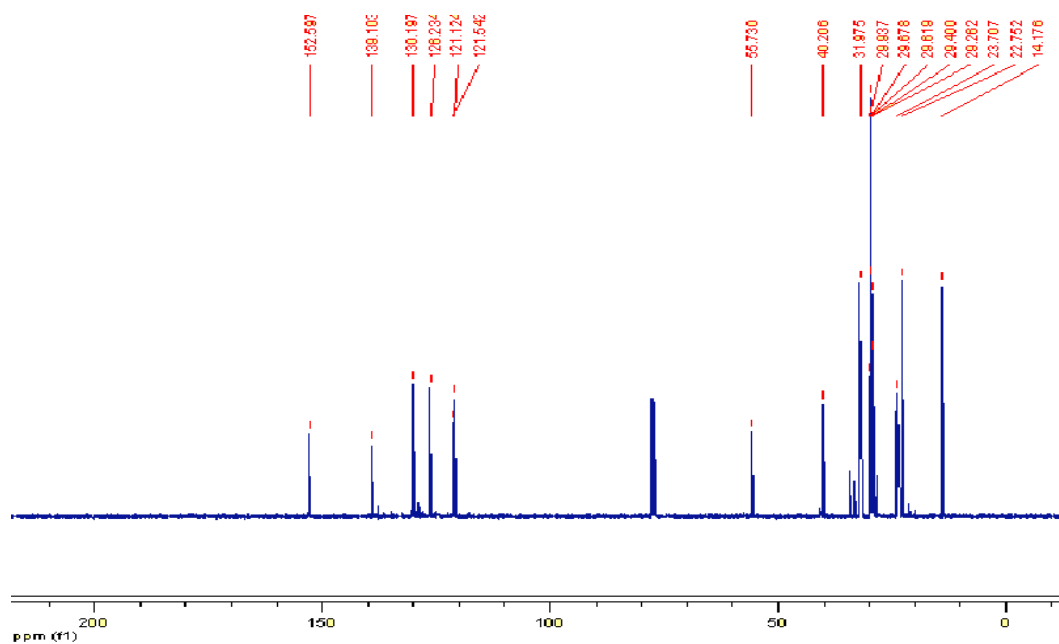
**Appendix 2:**  $^{13}\text{C-NMR}$  (100.6 MHz,  $\text{CDCl}_3$ ,  $\delta(\text{ppm})$ ) spectrum of 2,7-dibromofluorene (**6**).



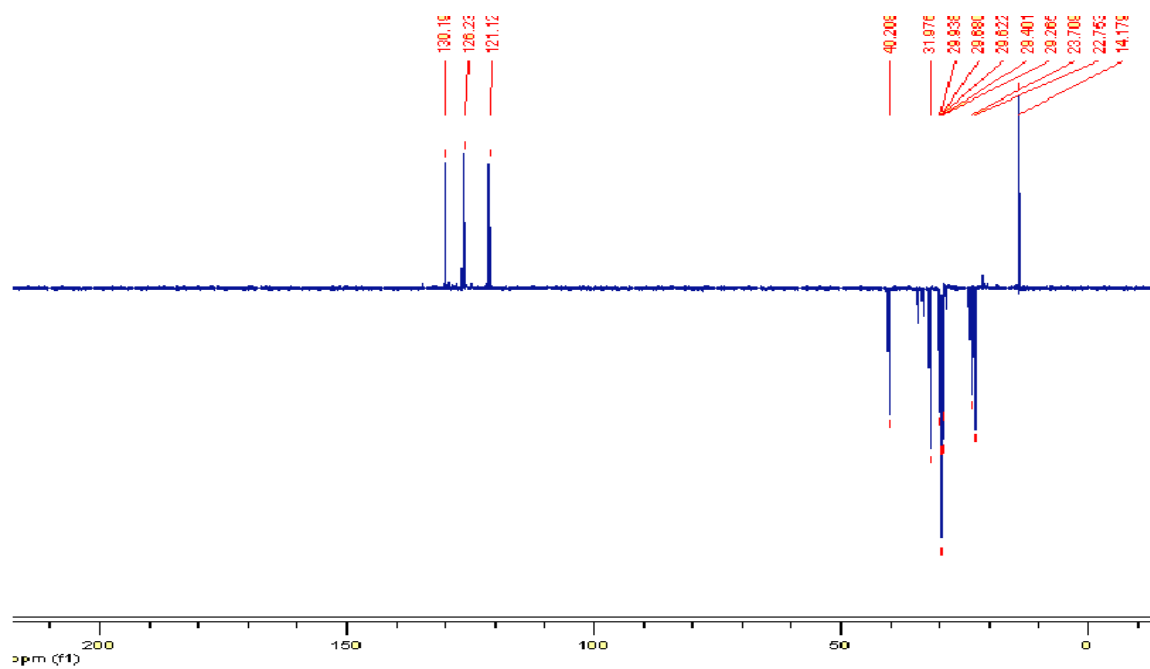
**Appendix 3:** DEPT-135 spectrum of 2,7-dibromofluorene (**6**).



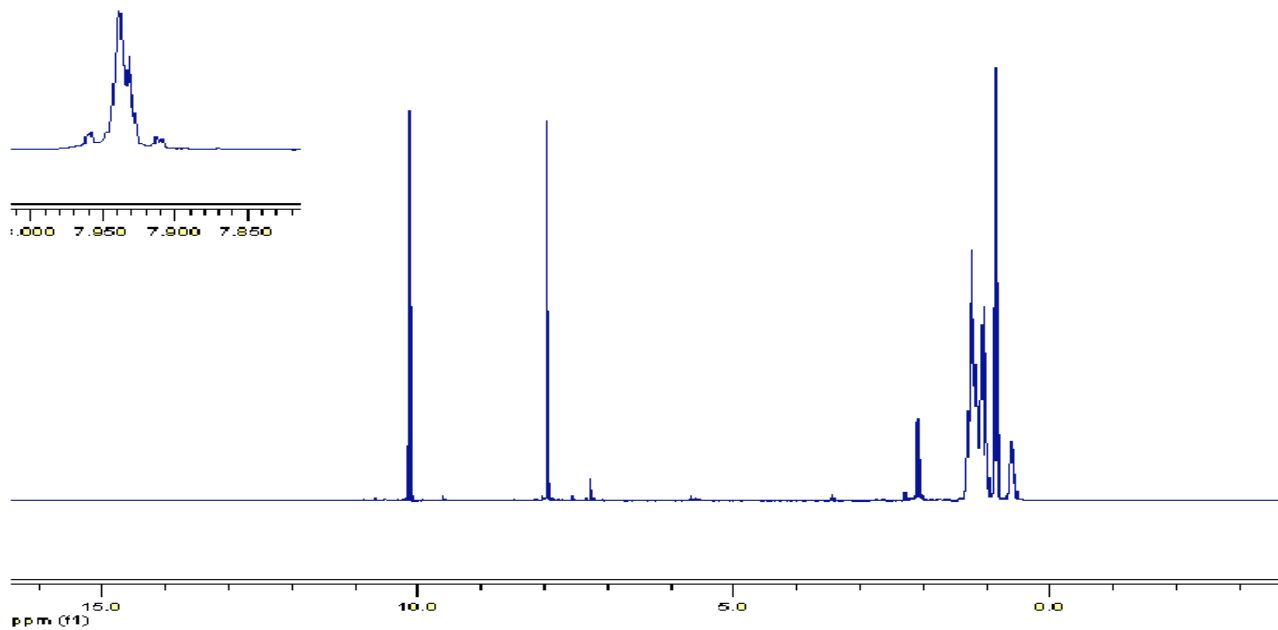
**Appendix 4:**  $^1\text{H-NMR}$  (400 MHz,  $\text{CDCl}_3$ ,  $\delta(\text{ppm})$ ) spectrum of 2,7-dibromo-9,9-didodecylfluorene (**24**).



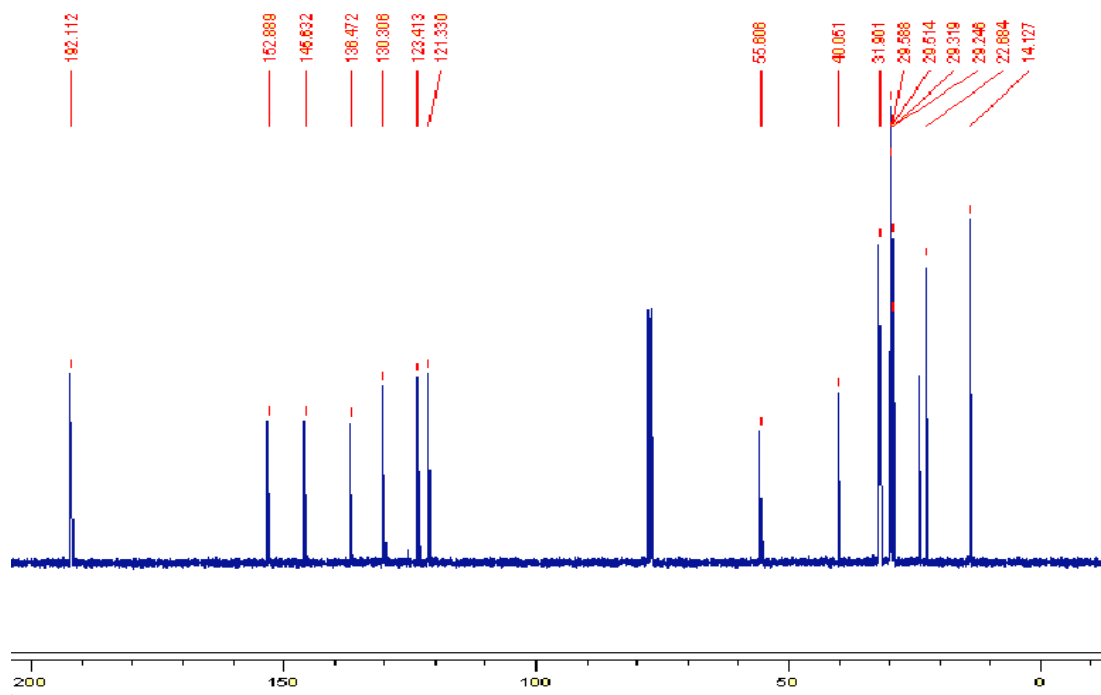
**Appendix 5:**  $^{13}\text{C}$ -NMR (100.6 MHz,  $\text{CDCl}_3$ ,  $\delta(\text{ppm})$ ) spectrum of 2,7-dibromo-9,9-didodecylfluorene (**24**).



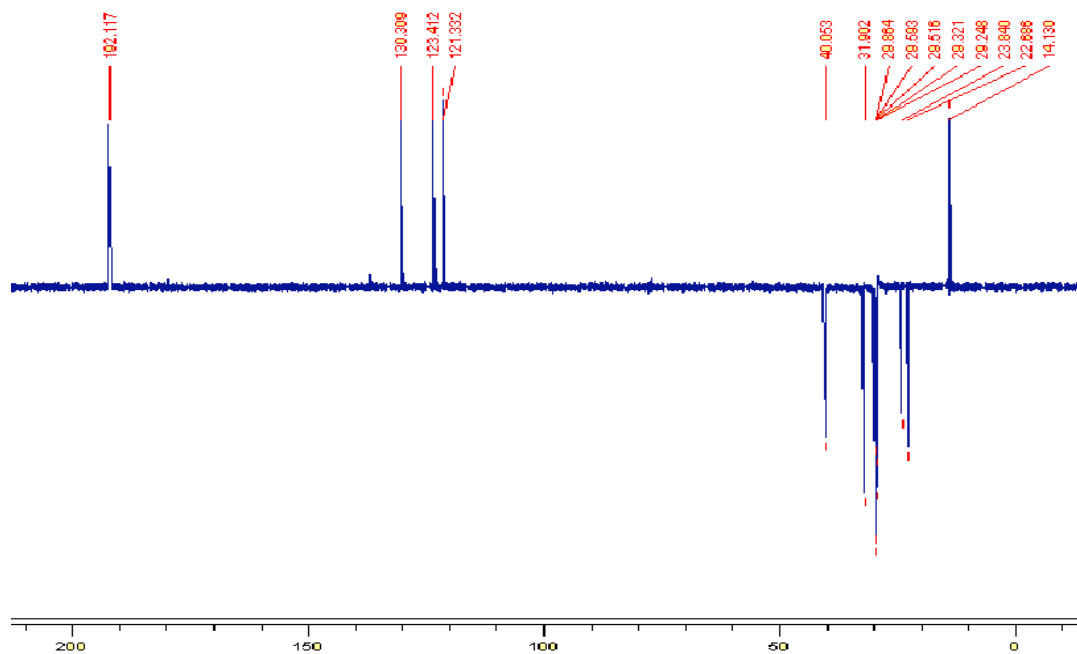
**Appendix 6:** DEPT-135 spectrum of 2,7-dibromo-9,9-didodecylfluorene (**24**).



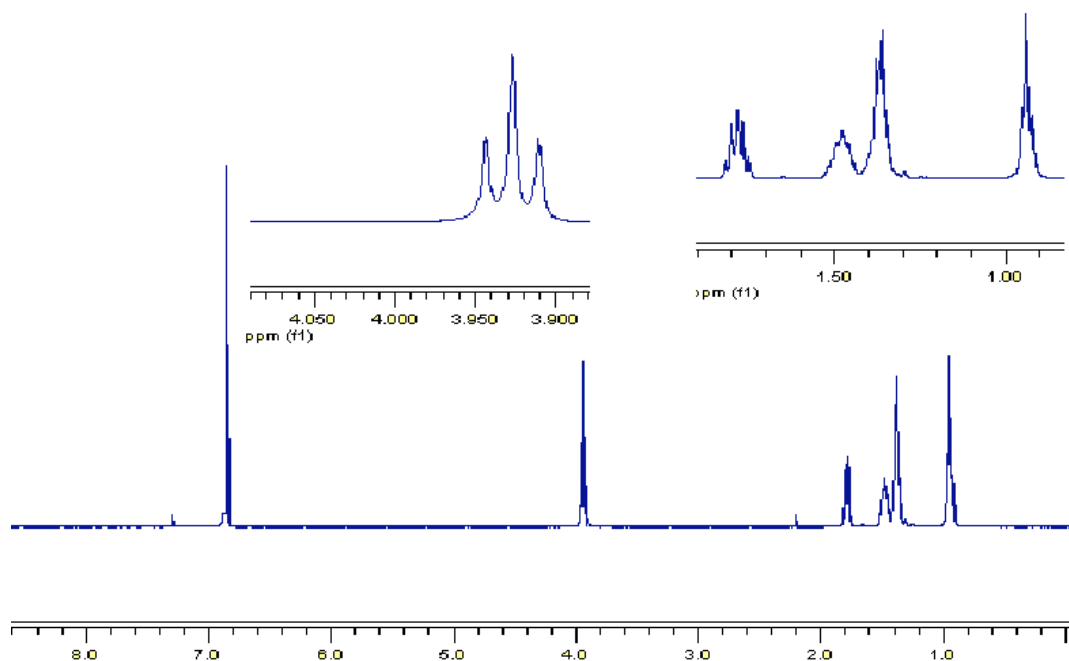
**Appendix 7:**  $^1\text{H-NMR}$  (400 MHz,  $\text{CDCl}_3$ ,  $\delta(\text{ppm})$ ) spectrum of 9,9-didodecylfluorene-2,7-dicarbaldehyde (**25**).



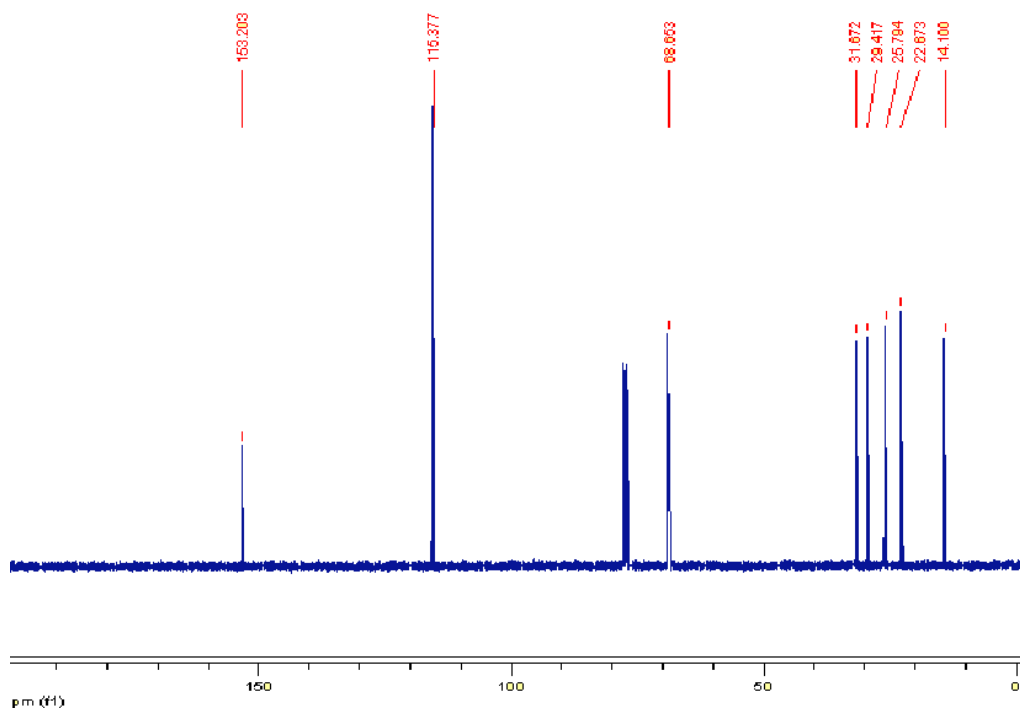
**Appendix 8:**  $^{13}\text{C-NMR}$  (100.6 MHz,  $\text{CDCl}_3$ ,  $\delta(\text{ppm})$ ) spectrum of 9,9-didodecylfluorene-2,7-dicarbaldehyde (**25**).



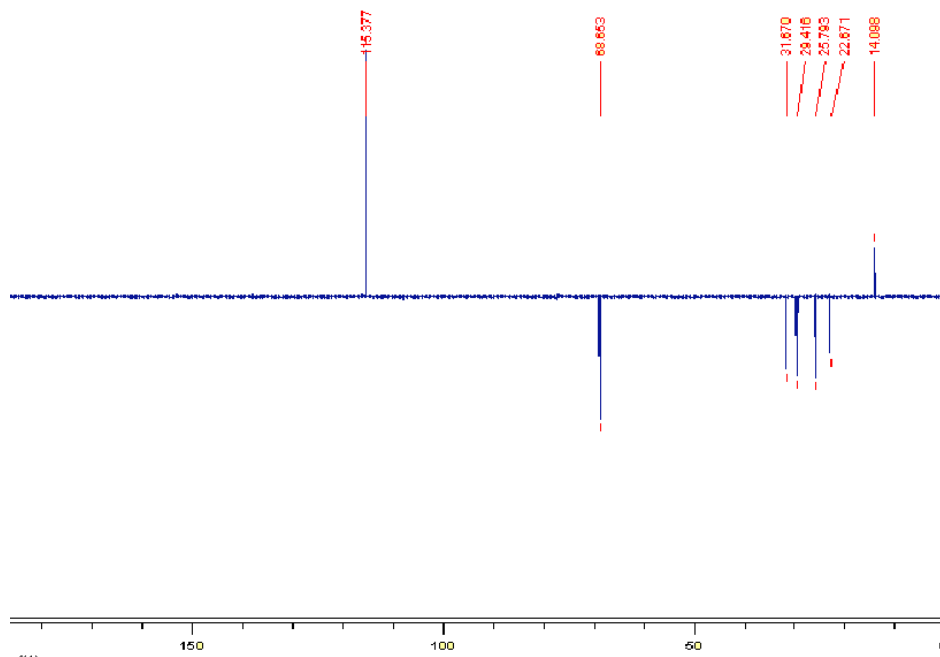
**Appendix 9:** DEPT-135 spectrum of 9,9-didodecylfluorene-2,7-dicarbaldehyde (**25**).



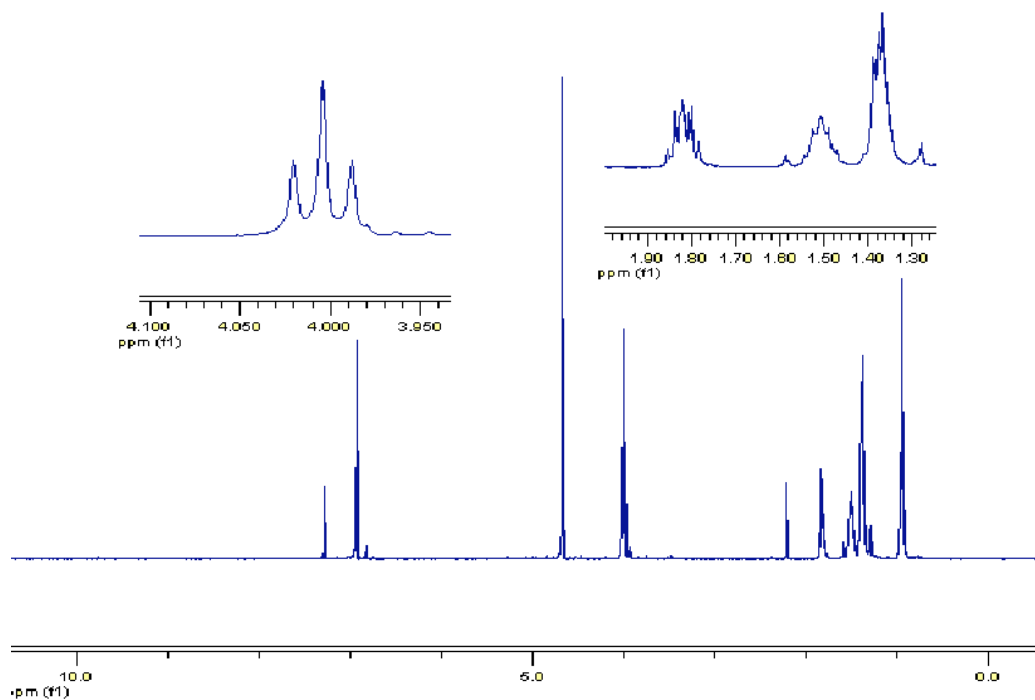
**Appendix 10:**  $^1\text{H-NMR}$  (400 MHz,  $\text{CDCl}_3$ ,  $\delta(\text{ppm})$ ) spectrum of 1,4-bis(hexyloxy)benzene (**29**).



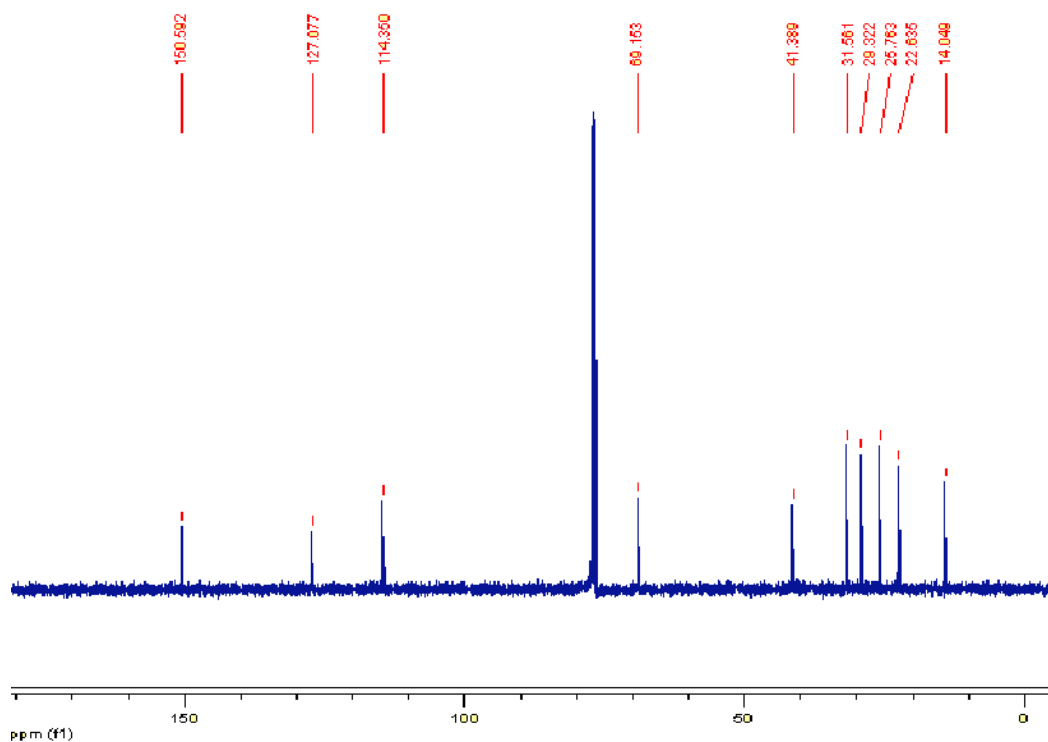
**Appendix 11:**  $^{13}\text{C}$ -NMR (100.6 MHz,  $\text{CDCl}_3$ ,  $\delta$ (ppm)) spectrum of 1,4-bis(hexyloxy)-benzene (**29**).



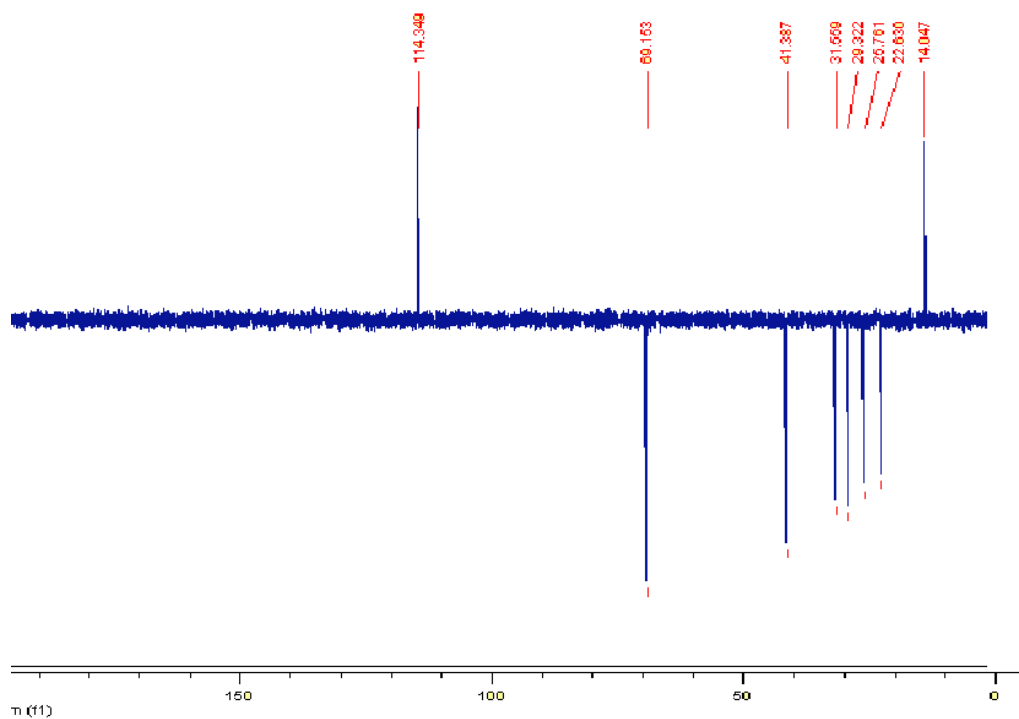
**Appendix 12:** DEPT-135 spectrum of 1,4-bis(hexyloxy)-benzene (**29**).



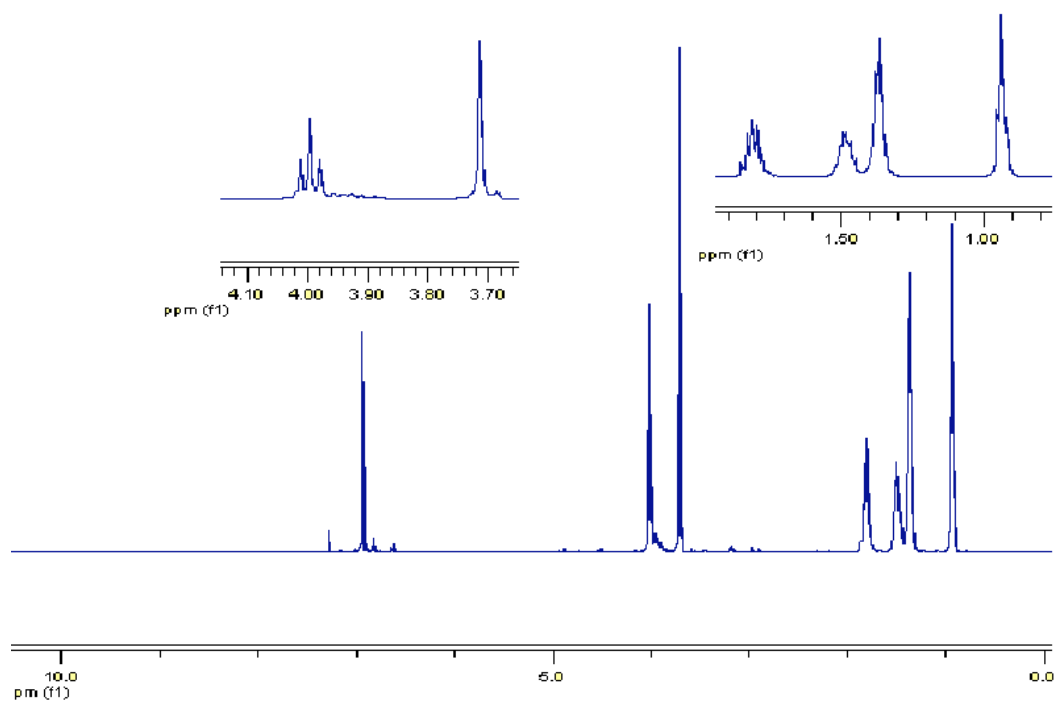
**Appendix 13:**  $^1\text{H-NMR}$  (400 MHz,  $\text{CDCl}_3$ ,  $\delta(\text{ppm})$ ) spectrum of 1,4-bis(chloromethyl)-2,5-bis(hexyloxy)benzene (**30**).



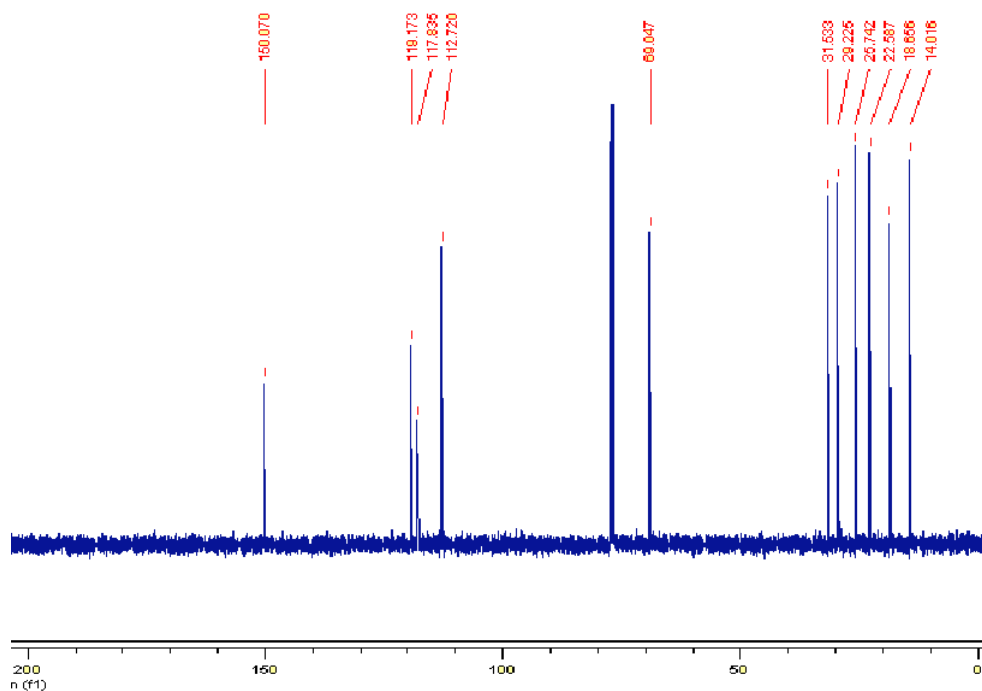
**Appendix 14:**  $^{13}\text{C-NMR}$  (100.6 MHz,  $\text{CDCl}_3$ ,  $\delta(\text{ppm})$ ) spectrum of 1,4-bis(chloromethyl)-2,5-bis(hexyloxy)benzene (**30**).



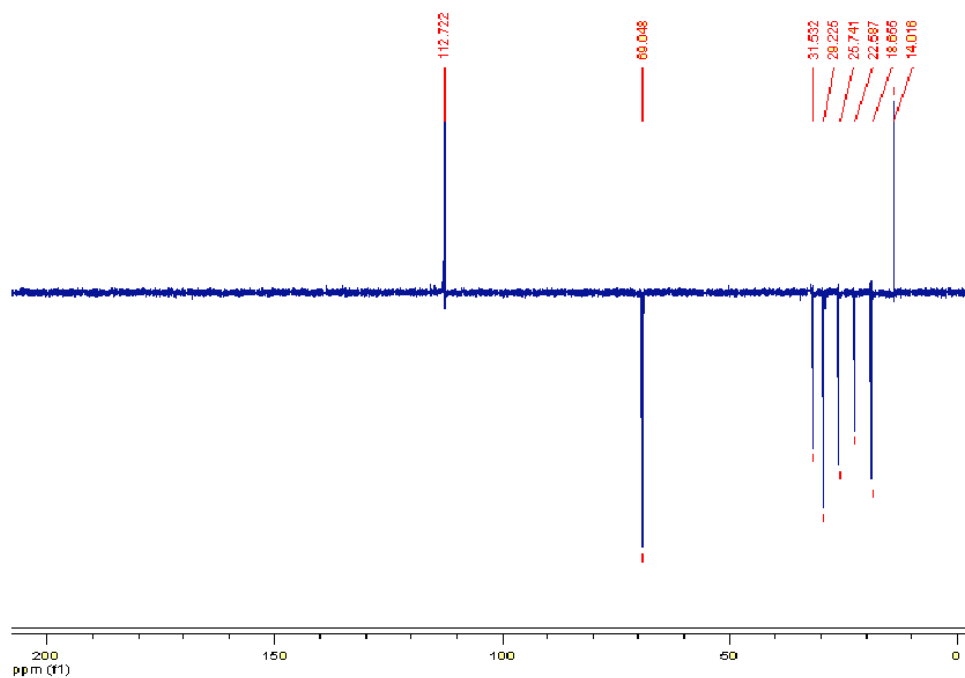
**Appendix 15:** DEPT-135 spectrum of 1,4-bis(chloromethyl)-2,5-bis(hexyloxy)benzene (30).



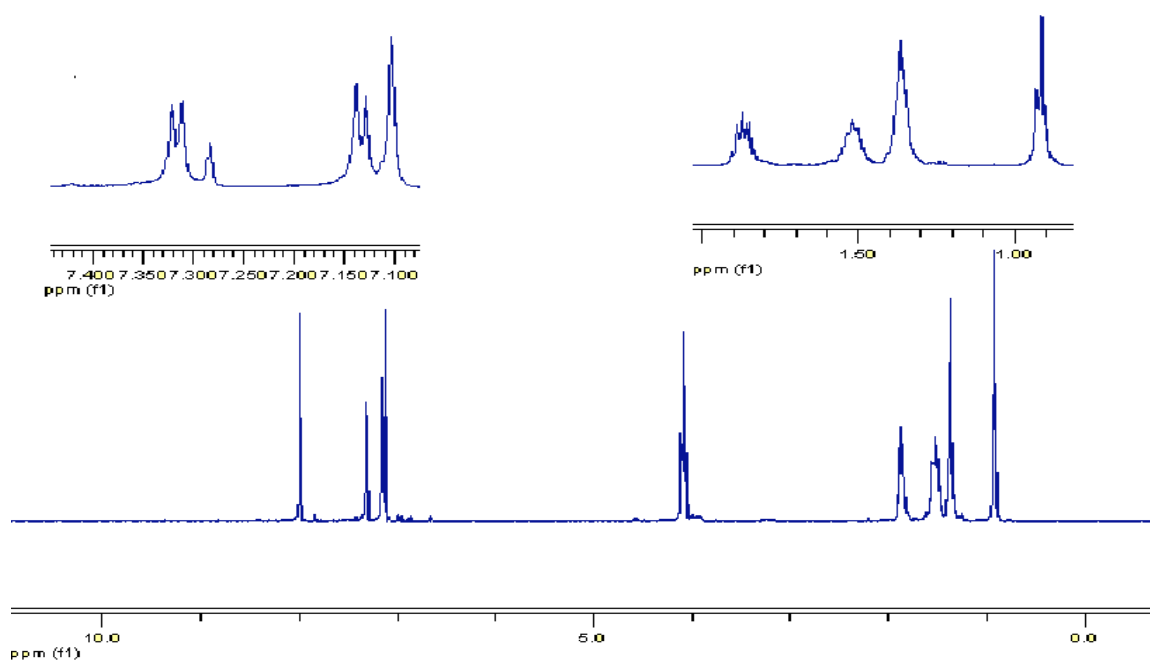
**Appendix 16:**  $^1\text{H-NMR}$  (400 MHz,  $\text{CDCl}_3$ ,  $\delta(\text{ppm})$ ) spectrum of 1,4-bis(cyanomethyl)-2,5-bis(hexyloxy)-benzene (31).



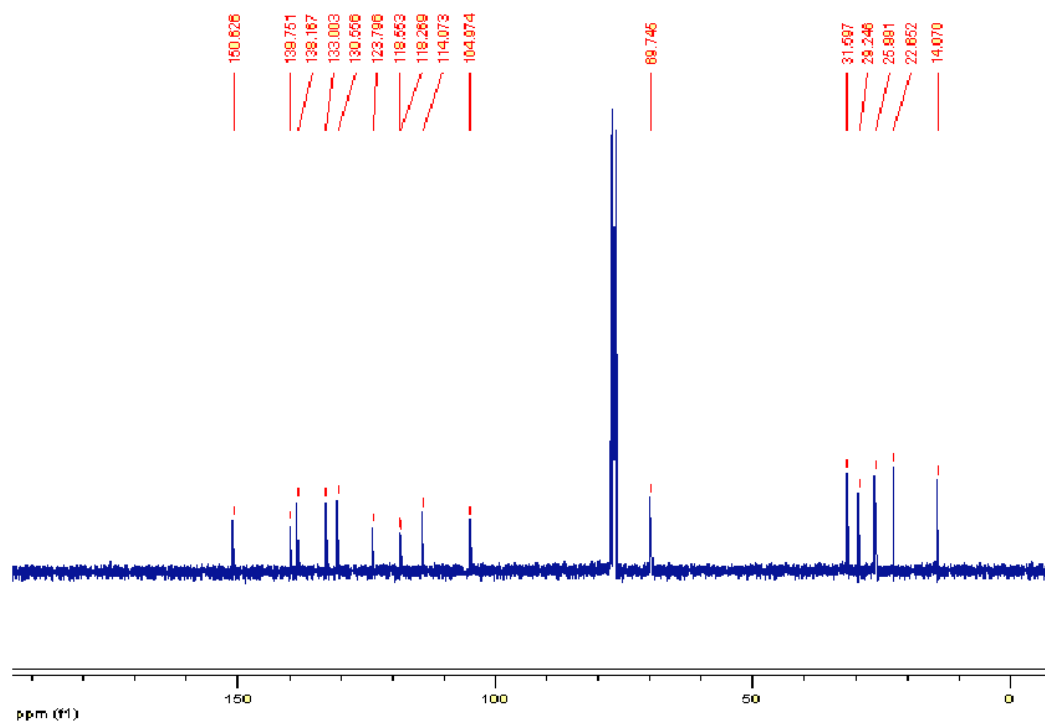
**Appendix 17:**  $^{13}\text{C}$ -NMR (100.6 MHz,  $\text{CDCl}_3$ ,  $\delta(\text{ppm})$ ) spectrum of 1,4-bis(cyanomethyl)-2,5-bis(hexyloxy)-benzene (**31**).



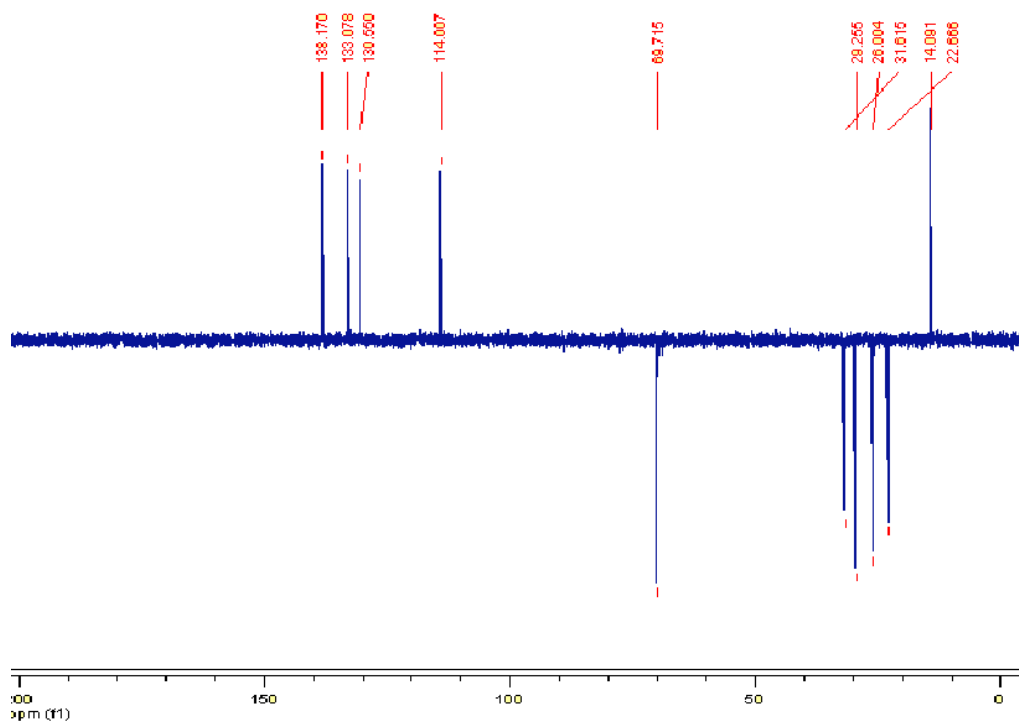
**Appendix 18:** DEPT-135 spectrum of 1,4-bis(cyanomethyl)-2,5-bis(hexyloxy)-benzene (**31**).



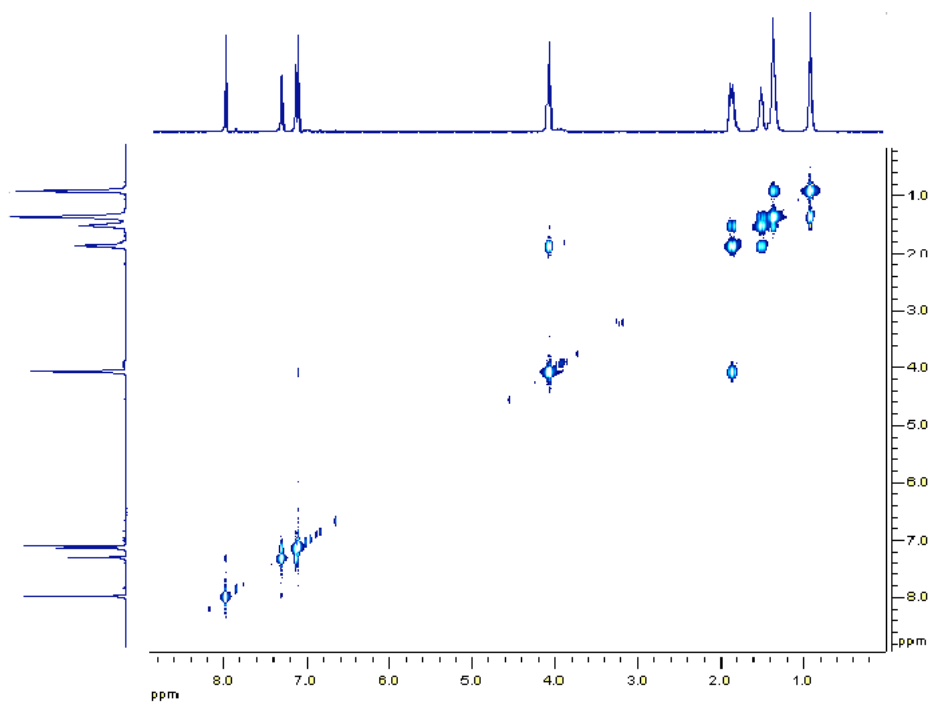
**Appendix 19:** <sup>1</sup>H-NMR (400 MHz, CDCl<sub>3</sub>, δ(ppm)) spectrum of 2,5-dihexyloxy-1,4-bis{2-(4'-bromothieryl)-2-cyanovinyl}benzene (**32**).



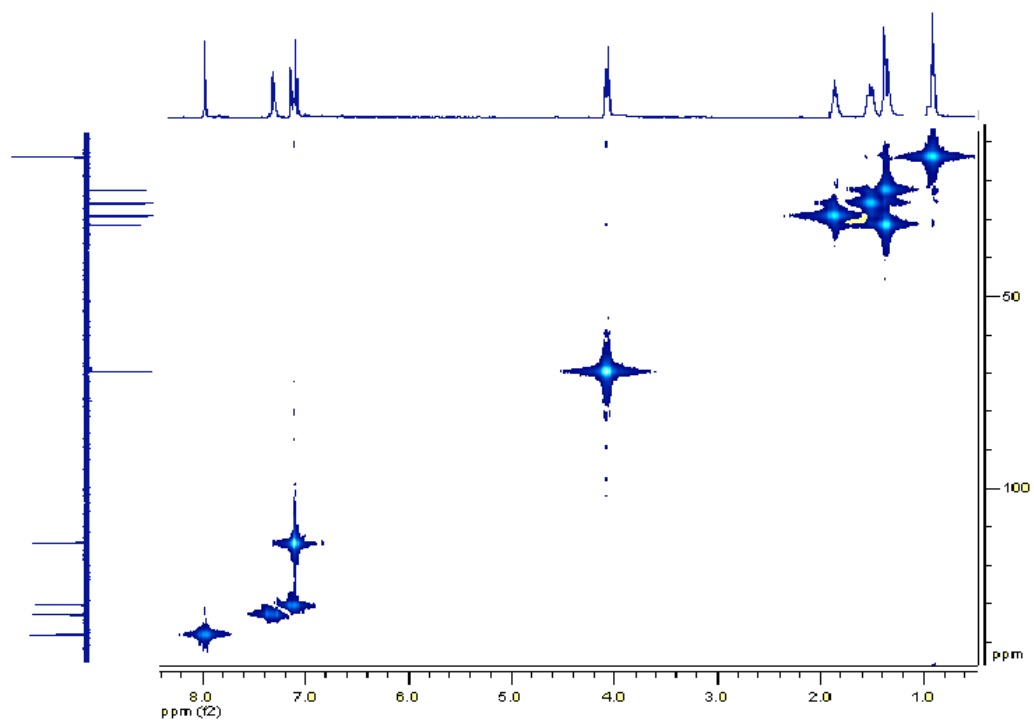
**Appendix 20:** <sup>13</sup>C-NMR (100.6 MHz, CDCl<sub>3</sub>, δ(ppm)) spectrum of 2,5-dihexyloxy-1,4-bis{2-(4'-bromothieryl)-2-cyanovinyl}benzene (**32**).



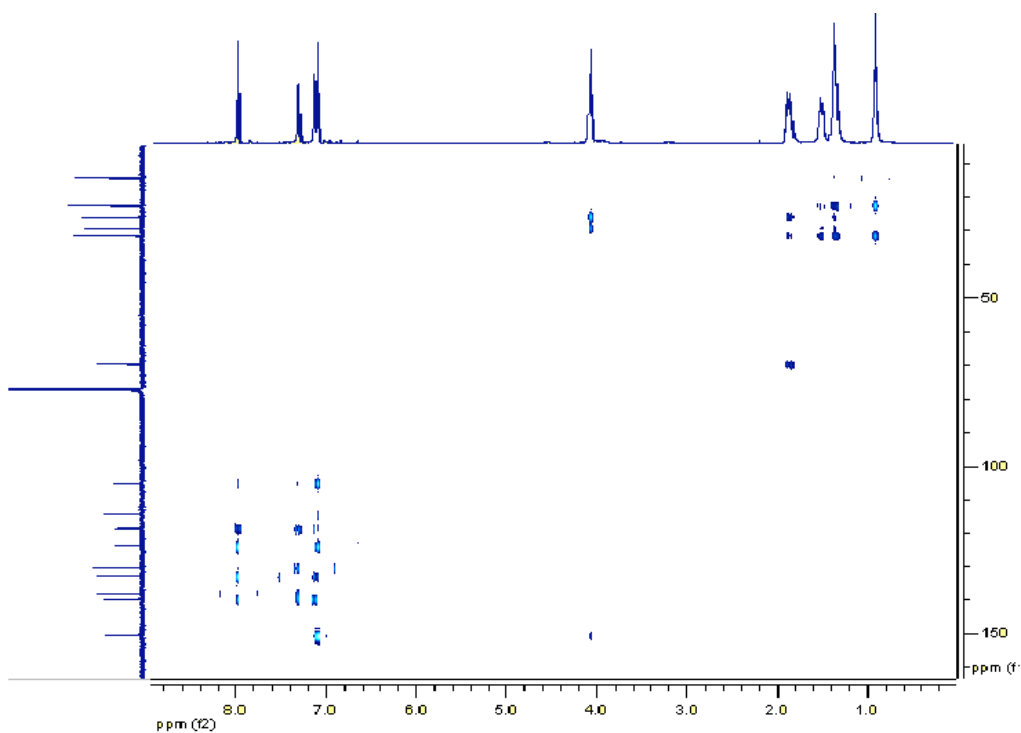
**Appendix 21:** DEPT-135 spectrum of 2,5-dihexyloxy-1,4-bis{2-(4'-bromothieryl)-2-cyanovinyl}benzene (**32**).



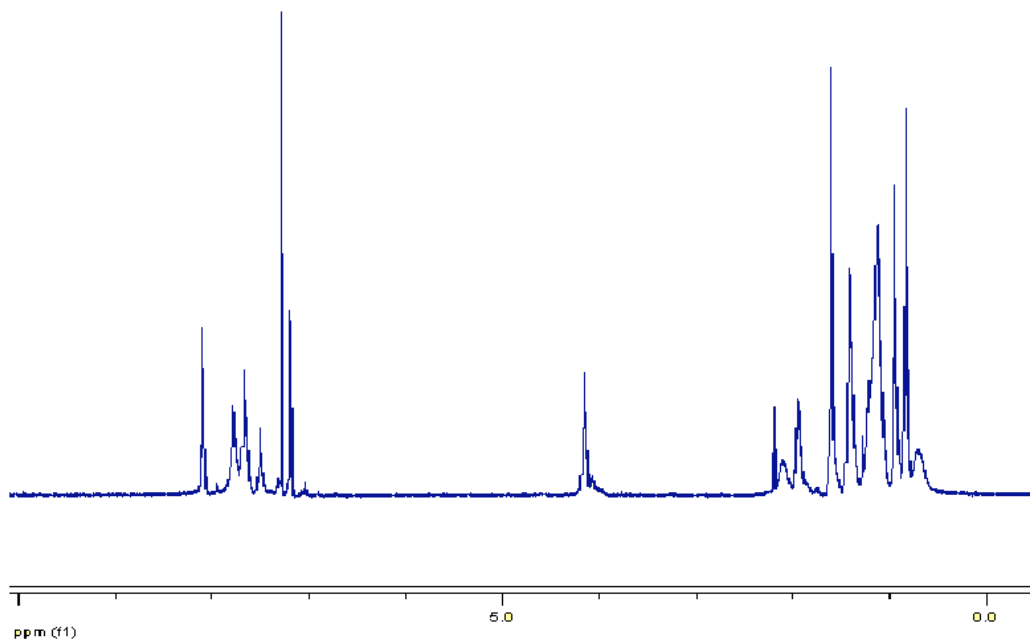
**Appendix 22:**  $^1\text{H}$ - $^1\text{H}$  COSY NMR spectrum of 2,5-dihexyloxy-1,4-bis{2-(4'-bromothieryl)-2-cyanovinyl}benzene (**32**).



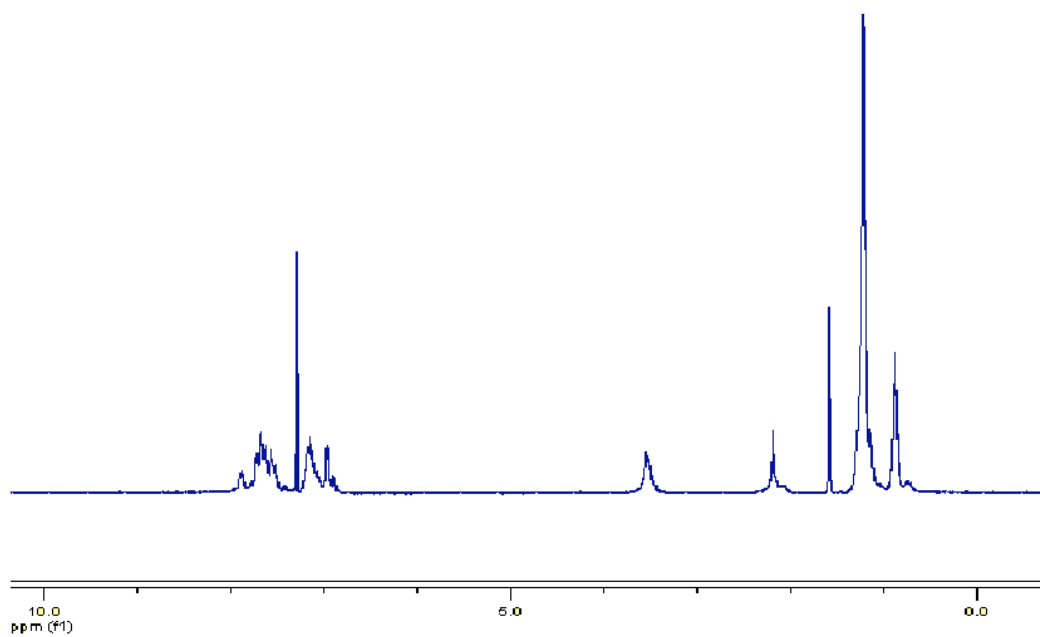
**Appendix 23:** HMQC spectrum of 2,5-dihexyloxy-1,4-bis{2-(4'-bromothieryl)-2-cyanovinyl}benzene (**32**).



**Appendix 24:** HMBC spectrum of 2,5-dihexyloxy-1,4-bis{2-(4'-bromothieryl)-2-cyanovinyl}benzene (**32**).



**Appendix 25:** <sup>1</sup>H-NMR (400 MHz, CDCl<sub>3</sub>, δ(ppm)) spectrum of polymer **40**.



**Appendix 26:** <sup>1</sup>H-NMR (400 MHz, CDCl<sub>3</sub>, δ(ppm)) spectrum of polymer **41**.